

2. SITE 407

Shipboard Scientific Party¹

SITE DATA

Date Occupied: 23 July, 1976

Date Departed: 27 July, 1976

Time on Hole: 3 days, 15.5 hours

Position: Latitude 63°56.32' N; Longitude 30°34.56' W

Water Depth (sea level): 2472 corrected meters, echo sounding

Water Depth (rig floor): 2482 corrected meters, echo sounding

Bottom Felt at: 2492.5 meters, drill pipe

Penetration: 458.5 meters

Number of Holes: 1

Number of Cores: 47

Total Length of Cored Section: 458.5 meters

Total Core Recovered: 183.31 meters

Percentage Core Recovered: 40 per cent

Oldest Sediment Cored:

Depth sub-bottom: 405 meters

Nature: Sandy calcareous mud

Chronostratigraphic unit: Lower-upper Oligocene

Basement:

Depth sub-bottom: 304² meters

Nature: Basalt

Velocity range: 3.8-5.6 km/s

Principal Results: Site 407 is on the western flank of the Reykjanes Ridge and lies on magnetic anomaly 13 (35 to 36 m.y.). The hole was cored continuously from the mud line.

Approximately 46 meters of Pleistocene glacial marine sediment, with occasional erratics and some layers of volcanic ash, overlies a unit of upper Miocene to Pliocene nannofossil ooze and chalk, which extends to 161 meters sub-bottom. A unit of siliceous nannofossil chalk, containing one thick middle Miocene ash band, continues to 272 meters. The fourth

sedimentary unit is upper Oligocene to lower Miocene nannofossil chalk which contains increasing amounts of very angular black basalt clasts toward the first basalt lavas at 300 meters.

The lava sequence consists of flows and pillow lavas interbedded with nannofossil chalk, some of which was recovered. Thin sections of the basalts show a uniform aphyric or nearly aphyric texture, with phenocrysts of olivine (fresh only in glass rinds), plagioclase, and sometimes augite. Zeolite facies alteration is present throughout the section. Geochemistry enabled us to separate the lavas into four distinct chemical lithostratigraphic units.

BACKGROUND AND OBJECTIVES

Hole 407 lies on magnetic anomaly 13 (indicating a basement age of 35.26 to 35.86 m.y.; LaBrecque et al., 1977), on the west flank of the Reykjanes Ridge. The JOIDES Ocean Crust Panel decided to locate the hole on this anomaly on the grounds that crust of this age forms the deepest sea-bed along the Iceland-Greenland Ridge, and is conjectured to have formed at a time when volcanic activity in Iceland was at a minimum [perhaps a measure of the rate of discharge of the Icelandic plume, if Schilling's (1973) picture is followed]. However, crust formed by spreading, whether of Icelandic type or normal oceanic type, subsides as it ages, and closer to continents it becomes covered by thick sediment. The axis of maximum depth at anomaly 13 may thus represent no more than an interplay of these two effects, just as do the lateral basins in the Gulf of Aden, on a smaller scale.

The position of Hole 407 along anomaly 13 was governed by a desire to put the three Reykjanes Ridge holes along a plate-mantle flow line away from the point on the ridge crest where the transition from Icelandic to ocean-floor geochemistry is halfway complete. After the area for this hole had been broadly delineated by JOIDES, the German survey ship *Meteor* (cruise 42B) conducted a magnetic and seismic reflection survey in February, 1976.

We hoped to be able to position our hole in the positively magnetized crust which generated anomaly 13 (Figure 1). The magnetostratigraphy would be crucial in resolving flow units, because we did not have an XRF facility available on board. We therefore sought to avoid positioning near crustal magnetization transitions where very low magnetic inclinations might limit the resolution of the magnetic stratigraphy. Synthetic models were calculated to determine the position of the magnetized crust causing the anomaly. These indicated, depending on the nature of the assumptions made, a variable but distinct offsetting of the anomalies southeast of the magnetized blocks that generate them. Because of uncertainty about these assumptions, a position down about one-third of the anomaly amplitude northwest

¹Bruce P. Luyendyk (Co-Chief Scientist), University of California, Santa Barbara, Santa Barbara, California; Joe R. Cann (Co-Chief Scientist), University of East Anglia, Norwich, England; George Sharman, Scripps Institution of Oceanography, La Jolla, California; William P. Roberts, Madison College, Harrisonburg, Virginia; Alexander N. Shor, Woods Hole Oceanographic Institution, Woods Hole, Massachusetts; Wendell A. Duffield, U.S. Geological Survey, Menlo Park, California; Jacques Varet, Dt. Géothermie, B.R.G.M., Orleans, France; Boris P. Zolotarev, Geological Institute of the USSR Academy of Sciences, Moscow, USSR; Richard Z. Poore, U.S. Geological Survey, Menlo Park, California; John C. Steinmetz, University of Miami, Miami, Florida; Angela M. Faller, Leeds University, Leeds, England; Kazuo Kobayashi, University of Tokyo, Nakano, Tokyo, Japan; Walter Vennum, California State College, Sonoma, Rohnert Park, California; David A. Wood, University of London, London, England; and Maureen Steiner, University of Wyoming, Laramie, Wyoming.

²From drilling log.

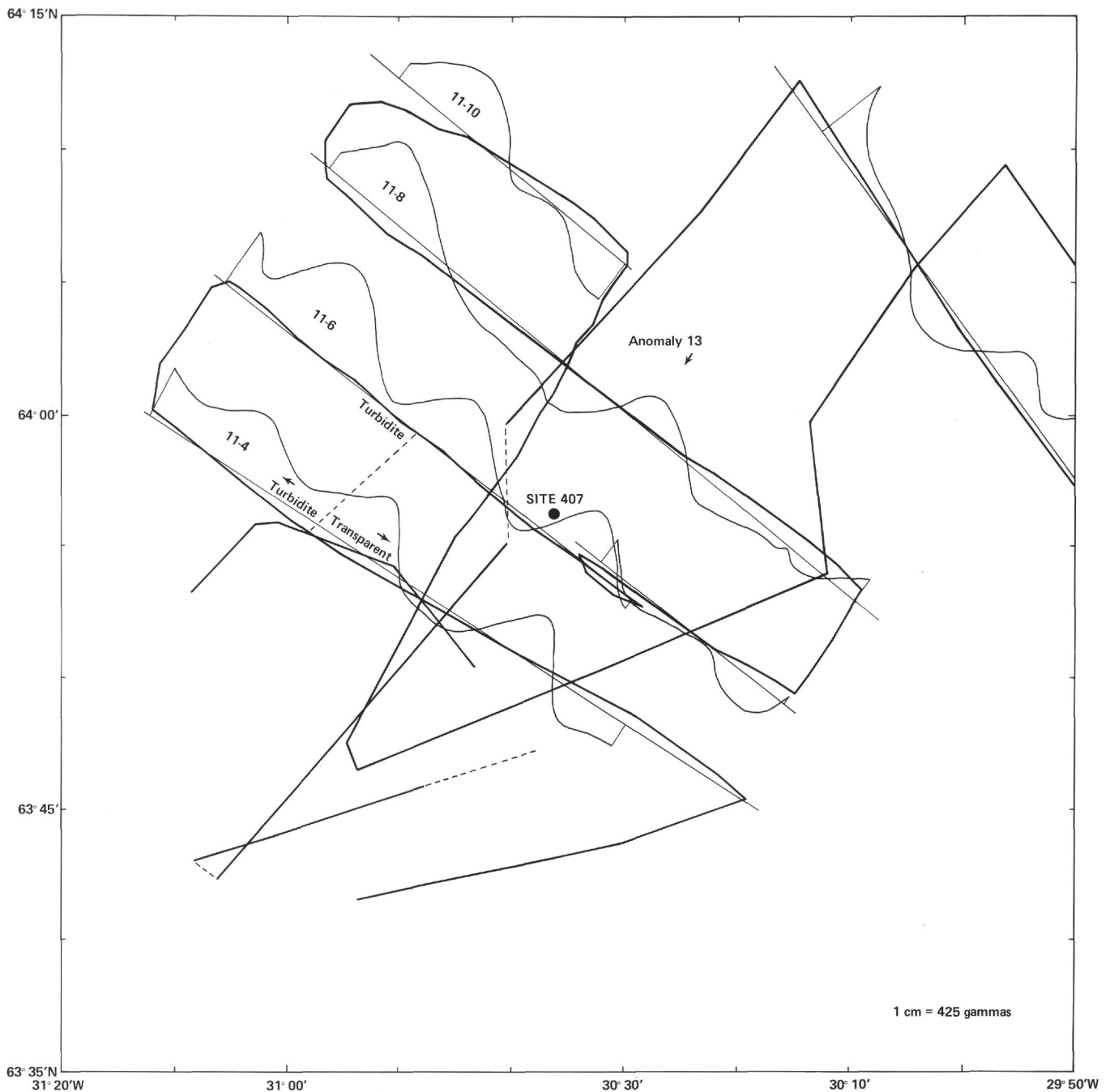


Figure 1. Magnetic anomalies measured along the track of the R/S Meteor.

of its peak was selected as giving the best assurance that we would find uniformly magnetized crust with steep magnetic inclinations. The three *Meteor* seismic profiles crossing anomaly 13 were then searched at the appropriate place, and one profile was selected as having no interfering basement ridges or other apparent complicating factors (Figures 2 and 3).

The sedimentary blanket is about 300 to 500 meters thick. A cover of turbidites fills the central part of the Denmark Strait, a few miles to the northwest. The blanket seems to be composite in form, with piles (ridges?) of relatively

transparent sediment overlapped by a filling of more clearly laminated material, which itself has an irregular surface. The hole was positioned to intersect first the basin fill and then the transparent sediment.

The objectives of drilling Hole 407 can be summarized more specifically as follows:

a) The petrography and geochemistry of the lava from the bottom of the hole should indicate the history of volcanic activity of the Reykjanes Ridge. In particular, augite phenocrysts are relatively common in Icelandic basalts, but rather rare in ocean-floor basalts.

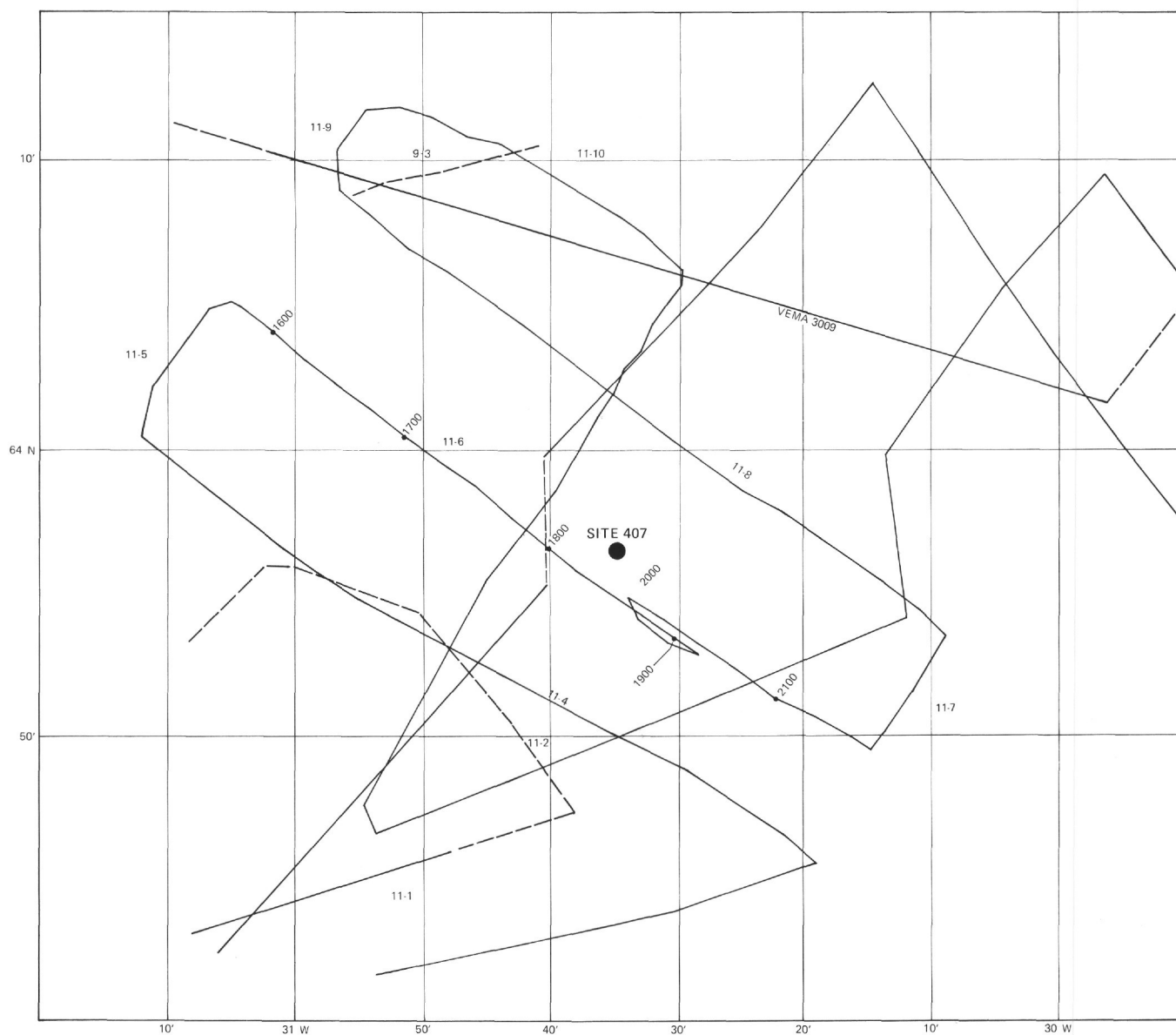


Figure 2. Track chart for the R/S Meteor (Cruise 42B), pre-site survey.

b) Because this was only the second IPOD-DSDP leg to have drilled seriously into basement, the basement rocks also are of interest from this point of view.

c) The sedimentary history of the western side of the Reykjanes Ridge is poorly understood. Studies of grain size, composition, sedimentary structure, and fauna and flora should enable some of the complex environmental history of this region to be determined.

OPERATIONS

At Site 407 we drilled one hole for a total penetration of 458.5 meters, and recovered 183.31 meters (40%) through continuous coring (Table 1).

We approached the site at half-speed from the southeast on course 305°T. We used 5- and 10-in.³ airguns in tandem to produce a high-frequency source spectrum. This was to increase resolution of the sea floor and acoustic basement. We monitored the magnetic record and dropped the beacon

at 0916Z, 23 July, while traversing down the northwest side of the anomaly, 100 gammas below the peak (Figures 4 and 5). We then realized that we might have dropped too far to the northwest, and therefore positioned the ship 1500 feet southeast of the beacon, on bearing 126°T. At 1100Z, 23 July, we began running in the hole. Spud-in was at 2100Z, 12 hours after beacon drop. Bottom was felt at 2492.5 meters, compared with our depth recorder estimate of 2482 meters from the rig floor.

We conducted continuous coring down to Core 41, which was in basalt basement. Recovery was low at this point, and we believed the bit to be in a zone of basalt rubble and/or thin flows. Also, we were being pressed for time: the ship's doctor informed us that because of a crew member's medical problem, we might have to abandon the site and sail for Reykjavik, Iceland. Consequently, we overcored for two cores, 42 and 43, coring down 19 meters then pulling in the barrel. This saved us one sand line round trip and

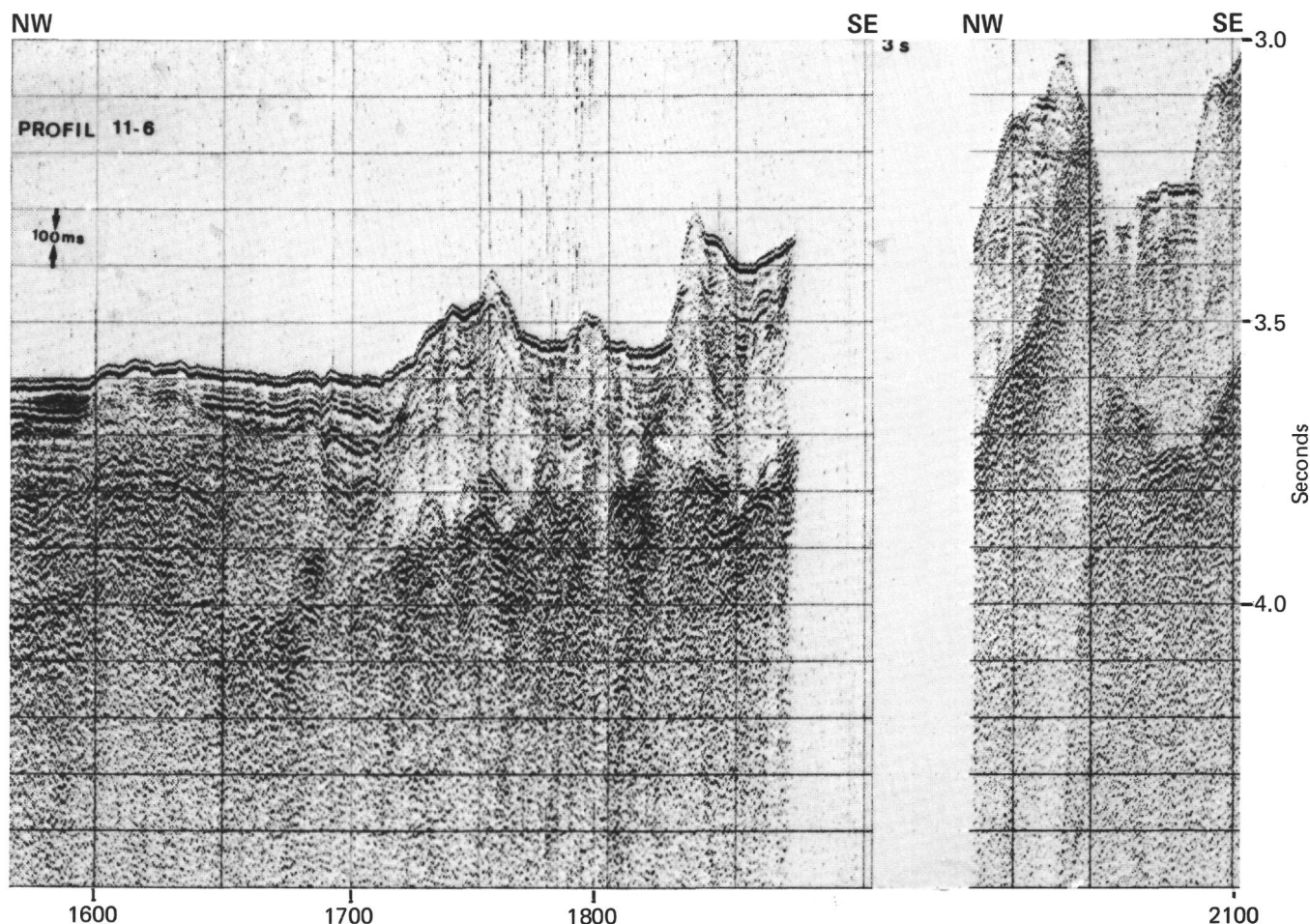


Figure 3. Seismic reflection profile 11-6 (Figure 2) taken by the R/S Meteor just south of Site 407.

yielded the same recovery percentage as a 9.5-meter core. We returned to the 9.5-meter coring program after the medical problem apparently passed. We then cored down to 458.5 meters sub-bottom, at which point the gauge of the basalt cores was so narrow that we believed the bit was destroyed.

Total time for coring, pumping the barrel down, cutting core, and retrieving, was about an hour in the sediment section and 3 to 3-1/3 hours in basalt. Cores could be cut in about 10 minutes in the sediment and two hours or more in the basalt. The coring time per 9.5-meter barrel is shown in Figure 6. This shows the clear contrast in sediment and basalt coring times. Hard layers in Cores 16 and 21 may correspond to intermediate reflectors in the on-site CSP profile. The first significant basalt drilling was in Core 37; this was followed by sediment layers and more massive basalt in Core 45.

At the termination of drilling, an inclinometer survey found the bottom of the hole to be 2.5° off vertical. The last core was on deck at 2055Z on 26 July, and the bit was retrieved at 0215Z on 27 July, giving a total out-of-hole time of 5 hours. After the rig floor was secured, we steamed to the west-southwest on course 266°T while streaming gear. We then came about and profiled over the site at half

speed, obtaining an airgun and magnetic profile on course 086°T (Figure 4).

SEDIMENT LITHOSTRATIGRAPHY

Introduction

We have distinguished four units on the basis of lithologic characteristics (Figure 7) (depths quoted are recovery depths not correlated with drilling logs). Three additional thin zones of interlayered sediment occur within the basalt.

Unit 1 (0 to 46.3 m): Pleistocene calcareous sandy mud with intervals of calcareous and marly calcareous ooze of variable volcanic ash content (up to 20%).

Unit 2 (46.3 to 160.7 m): Pliocene to upper Miocene nannofossil ooze (46.3 to 124.0 m) and nannofossil chalk (124.0 to 160.7 m).

Unit 3 (160.7 to 272.0 m): middle to lower Miocene siliceous nannofossil chalk with an interbedded chalk-volcanic ash zone between 215 and 224.5 meters.

Unit 4 (272.0 to 300.5 m): lower Miocene nannofossil chalk (272.0 to 280.0 m) and lower Miocene to upper Oligocene nannofossil chalk basalt pebble gravel.

TABLE 1
Coring Summary, Site 407

Core	Date (July 1976)	Time	Depth From Drill Floor (m)	Depth Below Sea Floor (m)	Length Cored (m)	Length Recovered (m)	Recovery (%)
1	23	2235	2492.5-2498.5	0.0- 6.0	6.0	6.0	100
2	23	2323	2498.5-2508.0	6.0- 15.5	9.5	9.1	96
3	24	0023	2508.0-2517.5	15.5- 25.0	9.5	5.4	57
4	24	0111	2517.5-2527.0	25.0- 34.5	9.5	6.0	63
5	24	0158	2527.0-2536.5	34.5- 44.0	9.5	3.9	41
6	24	0247	2536.5-2546.0	44.0- 53.5	9.5	4.4	46
7	24	0332	2546.0-2555.5	53.5- 63.0	9.5	3.07	32
8	24	0420	2555.5-2565.0	63.0- 72.5	9.5	3.5	37
9	24	0505	2565.0-2574.5	72.5- 82.0	9.5	0.55	6
10	24	0612	2574.5-2584.0	82.0- 91.5	9.5	5.55	58
11	24	0745	2584.0-2593.5	91.5-101.0	9.5	6.0	63
12	24	0845	2593.5-2603.0	101.0-110.5	9.5	4.84	51
13	24	0940	2603.0-2612.5	110.5-120.0	9.5	8.48	89
14	24	1107	2612.5-2622.0	120.0-129.5	9.5	5.28	56
15	24	1205	2622.0-2631.5	129.5-139.0	9.5	0.00	0
16	24	1320	2631.5-2641.0	139.0-148.5	9.5	4.84	51
17	24	1415	2641.0-2650.5	148.5-158.0	9.5	4.15	44
18	24	1515	2650.5-2660.0	158.0-167.5	9.5	7.4	78
19	24	1605	2660.0-2669.5	167.5-177.0	9.5	7.4	78
20	24	1700	2669.5-2679.0	177.0-186.5	9.5	2.18	23
21	24	1810	2679.0-2688.5	186.5-196.0	9.5	0.45	5
22	24	2015	2688.5-2698.0	196.0-205.5	9.5	4.07	43
23	24	2115	2698.0-2707.5	205.5-215.0	9.5	4.34	46
24	24	2210	2707.5-2717.0	215.0-224.5	9.5	9.62	101
25	24	2310	2717.0-2726.5	224.5-234.0	9.5	0.58	6
26	25	0010	2726.5-2736.0	234.0-243.5	9.5	0.44	5
27	25	0210	2736.0-2745.5	243.5-253.0	9.5	0.0	0
28	25	0315	2745.5-2755.0	253.0-262.5	9.5	7.22	76
29	25	0421	2755.0-2764.5	262.5-272.0	9.5	9.1	96
30	25	0530	2764.5-2774.0	272.0-281.5	9.5	8.43	89
31	25	0636	2774.0-2783.5	281.5-291.0	9.5	9.2	97
32	25	0845	2783.5-2793.0	291.0-300.5	9.5	1.02	11
33	25	0951	2793.0-2802.5	300.5-310.0	9.5	cc	0
34	25	1122	2802.5-2812.0	310.0-319.5	9.5	cc	0
35	25	1320	2812.0-2821.5	319.5-329.0	9.5	1.5	16
36	25	1505	2821.5-2831.0	329.0-338.5	9.5	3.7	39
37	25	1730	2831.0-2840.5	338.5-348.0	9.5	2.5	26
38	25	2010	2840.5-2850.0	348.0-357.5	9.5	3.0	32
39	25	2340	2850.0-2859.5	357.5-367.0	9.5	3.5	37
40	26	0311	2859.5-2869.0	367.0-376.5	9.5	0.47	5
41	26	0510	2869.0-2878.5	376.5-386.0	9.5	0.65	7
42	26	0800	2878.5-2897.5	386.0-405.0	19.0	2.13	11
43	26	0936	2897.5-2916.5	405.0-424.0	19.0	cc	0
44	26	1131	2916.5-2926.0	424.0-433.5	9.5	0.85	9
45	26	1405	2926.0-2935.5	433.5-443.0	9.5	3.0	32
46	26	1735	2935.5-2945.0	443.0-452.5	9.5	5.0	53
47	26	2155	2945.0-2951.0	452.5-458.5	6.0	4.5	75
Totals					458.5	183.31	40

Interlayered sediments: upper Oligocene foraminiferal nannofossil chalk (320.3 to 321.3 m), upper Oligocene foraminiferal nannofossil chalk (329.4 to 331.2 m), and "mid-" Oligocene sandy calcareous mud (405 to 405.4 m).

Description of Lithologic Units

Unit 1 (Cores 1 to 6, 0 to 46.3 m)

The first 15 cm of Core 1 is a pale brown nannofossil ooze which probably represents deposition during Holocene time. Below this level, the sediments are predominantly calcareous sandy muds with ice-rafted grains (mainly

basalt) which range in size from sand to gravel. Thin (40 to 130 cm) interbeds of nannofossil and nannofossil/foraminiferal ooze occur in this interval. The calcareous sandy mud consists of 65 to 85 per cent detrital minerals, of which 45 to 80 per cent is terrigenous clay. The coarse silt- and sand-size minerals are predominantly ash (up to 20% in Cores 4 to 6), quartz, feldspar (5 to 15% combined). Nannofossils and "unspecified carbonate" are the dominant carbonate components, and typically make up less than 30 per cent of the samples.

Interbedded and calcareous ooze and marly calcareous ooze contains 30 to 90 per cent calcium carbonate in smear

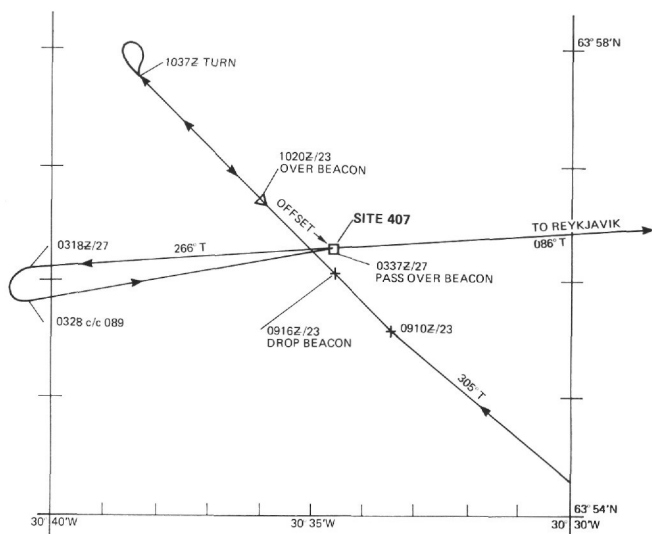


Figure 4. Track chart of Glomar Challenger approaching and leaving Site 407.

slides. Detrital quartz, feldspar, and heavy minerals total less than 5 per cent in these sediments; terrigenous clay-size detritus is the principal minor component.

The color changes in Unit 1 reflect fluctuations in carbonate content. The sandy muds with less than 15 per cent carbonate are brown or pale yellowish brown, the calcareous sandy muds are generally olive-gray, and the carbonate oozes are grayish brown to light gray.

The soft sediments of Unit 1 were deformed by drilling, and contain only rare thin, distorted laminae. Thus, although we found only one graded unit near the base of this unit (Core 5; 36.2 to 37.8 m sub-bottom), turbidity currents must be considered a possible depositional mechanism.

Ice-rafted basalt pebbles are scattered throughout the unit, and there is a rhyolite pebble.

Unit 2 (Cores 6 to 18, 46.3 to 160.7 m)

At 2.3 meters below the top of Core 6 (46.3 m sub-bottom), the sediment changes abruptly from ash-rich calcareous mud to a very soft nannofossil ooze. This lithologic boundary coincides with the Pliocene/Pleistocene boundary. The lack of glacial detritus in the Pliocene deposits below this level indicates an unconformity (see Biostratigraphy).

The lithology of Unit 2 is very uniform; it consists of 60 per cent or more nannofossils, a few per cent of foraminifers, and volcanic glass, zeolites, quartz, feldspars, and sponge spicules (typically totaling less than 2 per cent). CaCO_3 is fairly uniform, and ranges from 75 to 95 per cent. Core 10 (82 to 89 m) contains four thin (5 to 10 cm) layers of unaltered volcanic ash (> 90% ash). In Core 13 (115 m sub-bottom), the ooze abruptly becomes firm enough to be classified as chalk. Except for 4 meters of ooze in Core 17 (148.5 to 152.5 m) and soupy zones up to 10 cm thick at the tops of some cores, the unit remains firm to its base, in Core 18, at a depth of 160.7 meters.

The color remains uniformly light gray to white throughout most of Unit 2, so it is difficult to detect evidence of bioturbation. Bioturbation is indicated, however, at depths below 149.5 meters, where scattered silt- to sand-size, dusky green, partially lithified particles occur which are interpreted from their shape as possible burrow fill (probably glauconite) or fragments of reworked current-winnowed sand/silt laminations.

Unit 3 (Cores 18 through 29, 160.7 to 272.0 m)

In Core 18 (160.7 m), the nannofossil chalk changes abruptly to a siliceous nannofossil chalk containing 5 to 15

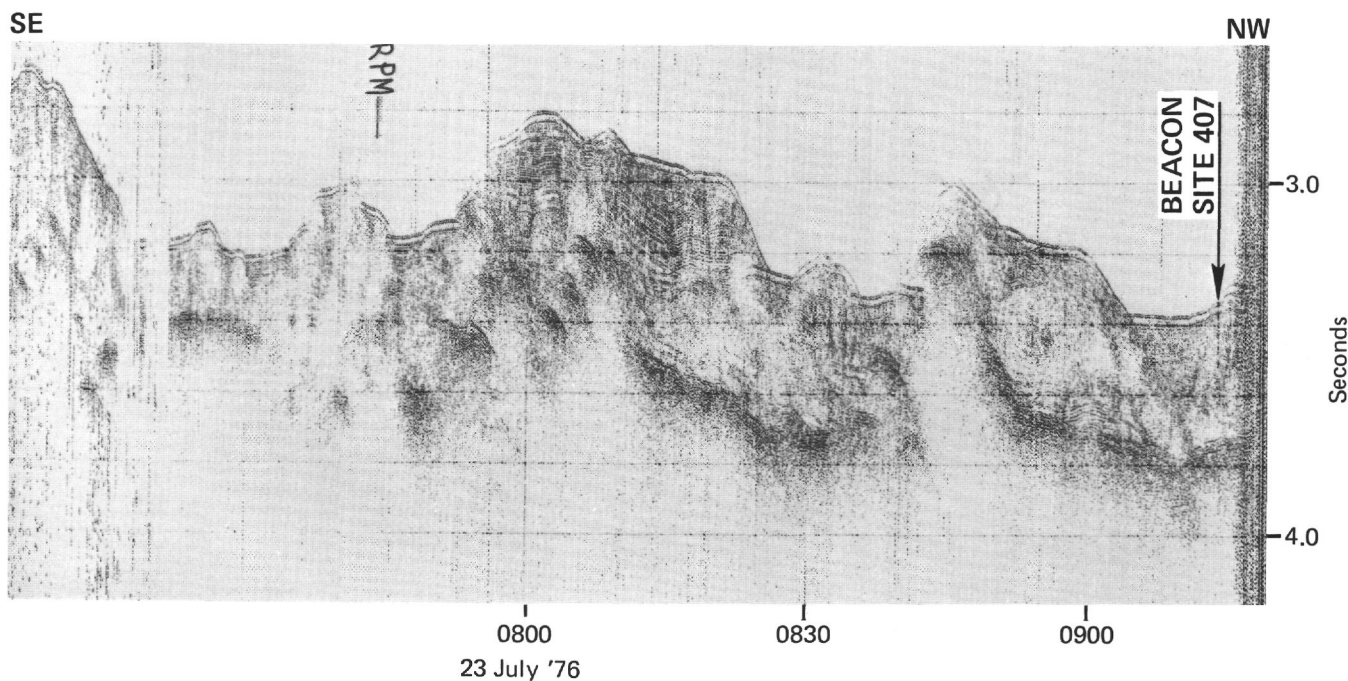


Figure 5. Seismic reflection profile taken from Glomar Challenger on approaching Site 407.

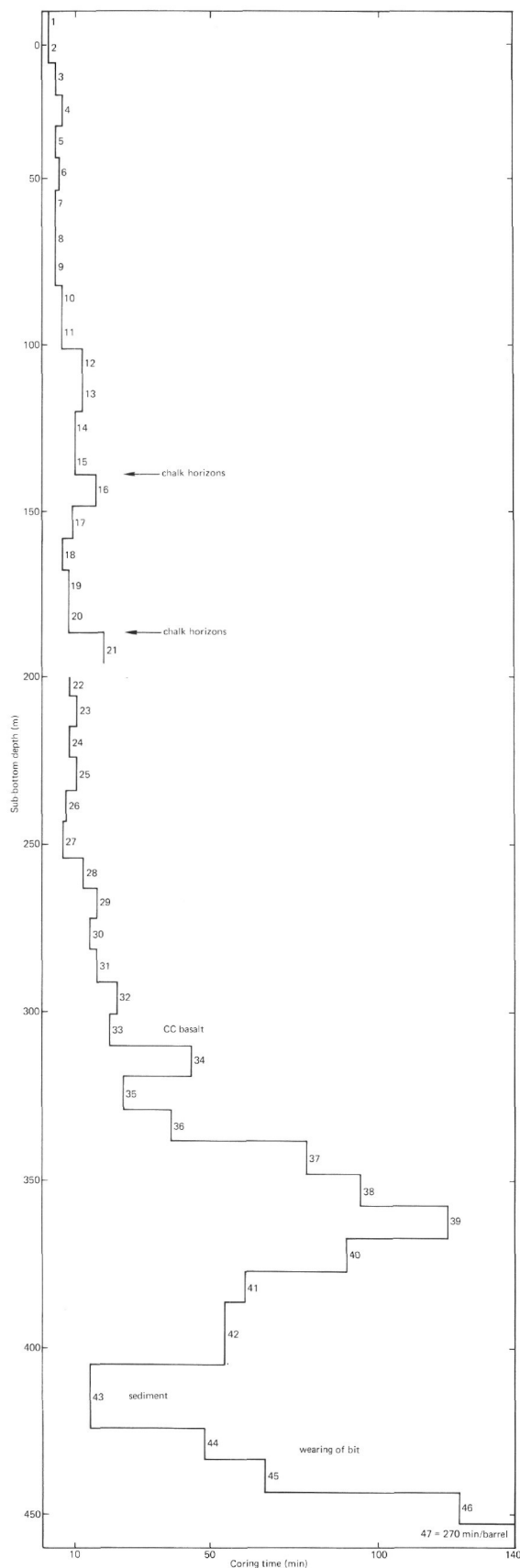


Figure 6. Coring time in minutes per core at Hole 407.

per cent siliceous material (Figure 7). The dominant siliceous components are fine (silt-size) spines, probably radiolarian spines, and larger (sand-size) sponge spicules with central tubes. Diatoms and radiolarians are also present. This lithologic change corresponds closely to the upper Miocene/middle Miocene boundary, and appears to represent a hiatus. The volcanic ash content also increases relative to Unit 2, to over 5 per cent in many samples. Near the middle of Unit 3 (Core 24, 215 to 224.5 m) is a zone of interbedded volcanic ash and ash-rich siliceous nannofossil chalk. The ash layers in this core are from 60 to 230 cm thick, and contain 75 to 90 per cent volcanic glass; the remainder is mostly sponge spicules. Except for the ash zone in Core 24 and two thin zones of nannofossil ooze in Cores 24 and 25, most of Unit 3 is light gray to greenish gray siliceous nannofossil chalk in which sponge spicules constitute the principal siliceous component. Carbonate drops from an average value of about 75 per cent at the top of Unit 3 to about 50 per cent near the base. A single ash layer occurs in Core 23 (205.7 m; 15 cm thick), and fine black laminae (millimeter-thick ash deposits) are in undisturbed sections throughout Unit 3. Detrital quartz, feldspar, and heavy mineral grains constitute less than 5 per cent of most smear slide samples. Foraminifers are present in most samples in quantities less than 10 per cent. Bioturbation is common throughout the unit, as shown by moderate to intense mottling.

Unit 4 (Cores 30 through 32, 272 to 300.5 m)

Unit 4 begins with a marked decrease in sponge spicule content to 2 to 3 per cent, and a decrease in volcanic ash content in most samples to below 5 per cent. The sediment in Core 30 between 272 and 280 meters is white to light gray nannofossil chalk, composed of 50 to 60 per cent carbonate (principally nannofossils) and 2 to 3 per cent quartz and heavy minerals, in addition to the volcanic ash and sponge spicules (about 10% combined). There is discrepancy between the carbonate analyses (50 to 60% CaCO_3) and visual estimates of carbonate (80 to 90%). This may be the result of an increase in clay-size basalt fragments below Core 29.

From the bottom of Core 30 (280 m) through Core 32 (300.5 m), angular basalt particles of sand to gravel size, with distinct conchoidal fracture, make up about 25 to 50 per cent of the sediment, classified as nannofossil chalk basalt pebble gravel. Carbonate content decreases from 55 per cent near the top of Core 31 (281.5 m) to 30 per cent in Core 32 (292 m).

Pebble-size ash clasts with millimeter-thick laminae occur throughout the lower part of Core 31 (286 to 290 m).

Deformation is intense throughout Unit 4, but mottling caused by bioturbation can be distinguished in most of the cores. On the basis of drilling log data, the base of this unit is near 304 meters sub-bottom. There is no sediment between Sample 32, CC (292 m) and basalt in Core 33 (300.5 to 310 m).

Sediments Interlayered With Massive Basalts

We recovered massive basalts below Core 32. Thin zones of sediments occur within the basalts in Cores 35 (320.3 to

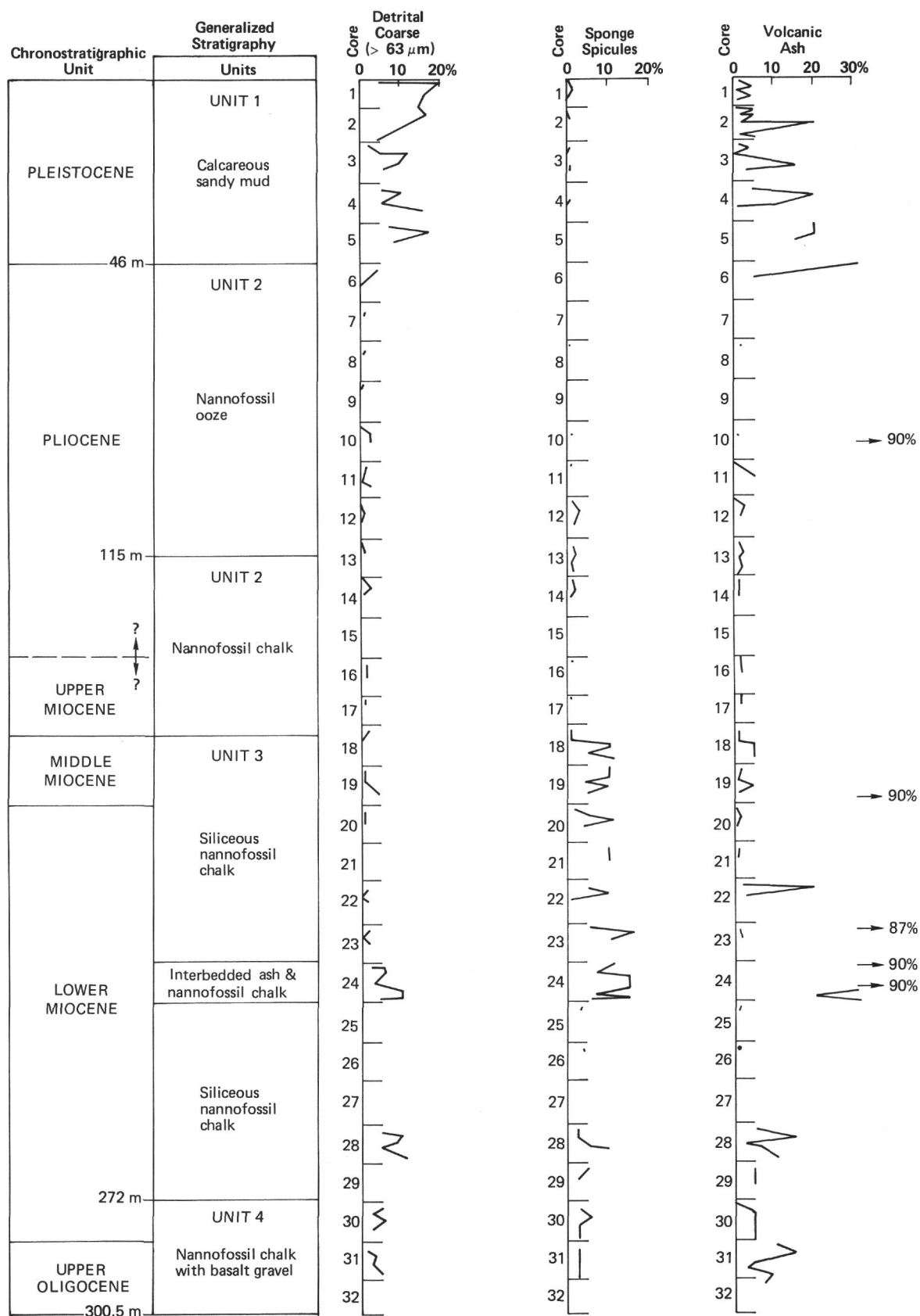


Figure 7. Generalized stratigraphy and sedimentology from Hole 407.

321.3 m), 36 (329.4 to 331.2 m), and 43 (two core-catcher sections between 405 and 405.4 m). The sediment in Core 35 is upper Oligocene greenish gray to olive-gray nannofossil-foraminiferal chalk; Core 36 contains gray ash-rich nannofossil chalk of the same age. Smear slides of Core 35 are composed almost entirely of microfossils; a sample from Core 36 contains 10 per cent ash and 3 per cent zeolites in a nannofossil ooze matrix. These units are somewhat firmer than the sedimentary units above; this may indicate some baking. From the drilling log, the sediment recovered may represent soft material from 323.5 to 328.5 meters and 337 to 339 meters sub-bottom.

The two core-catcher samples from Core 43 contain yellowish green calcareous sandy mud with about 60 per cent clay, 25 per cent nannofossils, and minor amounts (1 to 5%) of volcanic glass, heavy minerals, and quartz. A thin (2 mm) streak of pale yellowish orange calcareous zeolitic mud in the middle of Sample 43, CC-2 contains 40 per cent zeolite minerals in addition to about equal amounts of clay and nannofossils. Core 43 (405 to 424 m sub-bottom) contains Oligocene (approximately 30 to 32 m.y.) assemblages of nannofossils and foraminifers. The drilling log indicates that this unit may extend from 404 to 428 meters sub-bottom.

BIOSTRATIGRAPHY

We recovered Quaternary to Oligocene sediments at Site 407 (Table 2).

The upper 46 meters of the sedimentary section represents a Pliocene (?)–Pleistocene glacial sequence with abundant ice-rafted mineral grains and occasional large basalt erratics. Although control points are presently limited, it appears that the base of the glacial sequence occurs very near the Pliocene/Pleistocene boundary, as delineated by examination of core-catcher samples. This interpretation conflicts with the results of DSDP Leg 12 (Laughton, Berggren, et al., 1972), where the base of the glacial sequence in the North Atlantic was seen to have been deposited in the late Pliocene, at about 3.0 m.y. ago. Thus it is possible that a portion of the upper Pliocene to lower Pleistocene is absent or highly condensed at Site 407.

A thick (80 m) Pliocene section, consisting of light gray to white nannofossil ooze, occurs below the glacial section. The Miocene/Pliocene boundary occurs within an alternating sequence of nannofossil ooze and chalk between 129.5 and 158 meters sub-bottom (between Samples 14, CC and 17, CC), but recovery in this interval was extremely poor and placement of the boundary is uncertain.

A marked lithologic change from nannofossil ooze and chalk to siliceous nannofossil chalk occurs at or near the upper Miocene/middle Miocene boundary. This lithologic change and the apparent absence of at least foraminiferal Zone N 15 suggest a condensed or missing section near the boundary. Middle Miocene sediments grade downward from greenish yellow siliceous nannofossil chalk to nannofossil ooze and chalk. Samples from Cores 18 and 19 are middle Miocene, whereas Sample 23, CC (210 m sub-bottom) is lower Miocene. Our limited data from Samples 20, CC through 22, CC, however, are not definite as to age, and we have arbitrarily placed the lower encountered below 300.5 meters sub-bottom (Core 33). The

Oligocene/Miocene boundary occurs between Samples 30, CC (280.5 m sub-bottom) and 31, CC (291 m sub-bottom).

Greenish gray to gray nannofossil chalk interlayered with basalt was recovered in Cores 35 and 36. Nannofossils from these cores are uppermost Oligocene; foraminifers from these cores are also upper Oligocene.

Sandy calcareous mud from Sample 43, CC, (approximately 100 m below the first basalt) contains nannofossils and planktonic foraminifers indicating the “mid-” Oligocene.

Planktonic Foraminifers

With few exceptions, what follows is based on shipboard examination of core-catcher samples.

Samples 1, CC to 5, CC yield assemblages dominated by *Neoglobobadrina pachyderma* (sinistral). Other taxa present include *Globigerina bulloides*, *Globorotalia scitula*, *G. inflata*, and *Turborotalita quinqueloba*. The occurrence of *Neoglobobadrina atlantica* (sinistral) in Sample 6, CC is significant in that previous studies in the North Atlantic (e.g., Berggren, 1972a) suggest that the last occurrence of *N. atlantica* approximates the Pliocene/Pleistocene boundary. Thus, we place the Pliocene/Pleistocene boundary between Cores 5 and 6 (38.5 m to 48.5 m sub-bottom).

Neoglobobadrina atlantica (sinistral) is abundant in samples from Cores 6 to 14, and in some cases (i.e., Cores 8, 9, and 11) it completely dominates the planktonic assemblage. The presence of *Globorotalia puncticulata* in Samples 7, CC through 10, CC and the sporadic occurrence of *Neoglobobadrina acostaensis* below Sample 9, CC, suggest Zone 19. Therefore, Cores 9 to 14 are lower Pliocene and Samples 7, CC and 8, CC are lower Pliocene, according to foraminifer evidence.

The assemblage in Sample 16, CC consists almost entirely of *Globigerina bulloides*, with rare *Globorotalia scitula*, *Orbulina universa*, and *Turborotalita quinqueloba*. Although the planktonic foraminifer assemblage is not particularly age-diagnostic, the associated nannofossil assemblage suggests that Sample 16, CC is upper Miocene. Moreover, *Neoglobobadrina atlantica* (dextral) is abundant in Sample 17, CC. Berggren (1972) has shown that in the North Atlantic, right-coiling *N. atlantica* is restricted to the upper Miocene, whereas left-coiling *N. atlantica* is characteristic of the Pliocene. Thus, the Miocene/Pliocene boundary occurs between Samples 17, CC (158 m sub-bottom) and 14, CC (129.5 m sub-bottom).

Samples 18, CC through 19, CC contain *Globorotalia mayeri* and several other middle Miocene taxa, such as *Globigerina druryi* (Sample 18, CC) and *Globorotalia* aff. *G. miozea* (Sample 19, CC). In general, the abundance of planktonic foraminifers decreases with depth below Sample 18, CC. This trend culminates in Samples 22, CC to 28, CC, which contain relatively few planktonic foraminifers; most of those present are non-diagnostic juvenile forms. However, the first occurrence (downward) of *Catapsydrax dissimilis* (s.l.), in Sample 23, CC, indicates the lower Miocene. Samples 22, CC through 20, CC did not yield stratigraphically diagnostic taxa and, for the present, the Miocene/middle Miocene boundary at the top of Core 20 (177.0 m sub-bottom).

TABLE 2
Paleo/Biostratigraphic Summary of Core-Catcher Samples (CC), Leg 49, Site 407

Core	Depth (m)	Chronostratigraphic Unit	Planktonic Foraminifers	Zone	Calcareous Nannofossils	Zone
1	6.0	Pleistocene	<i>Neogloboquadrina pachyderma</i> (S) <i>Globigerina bulloides</i> <i>Globorotalia scitula</i> <i>G. inflata</i> <i>Turborotalita quinqueloba</i>	N 22/ N 23	<i>Coccolithus pelagicus</i> <i>Gephyrocapsa aperta</i> <i>G. caribbeanica</i> <i>G. oceanica</i> <i>Helicopontosphaera kamptneri</i>	NN 20
2	15.5	Pleistocene	As above		<i>C. pelagicus</i> <i>G. caribbeanica</i> <i>G. oceanica</i> <i>H. kamptneri</i> <i>Cyclococcolithina leptopora</i>	NN 20
3	21.0	Pleistocene	<i>N. pachyderma</i> (S) <i>T. quinqueloba</i>		<i>G. caribbeanica</i> <i>G. doricoides</i> <i>G. oceanica</i> <i>C. pelagicus</i>	
4	30.5	Lower Pleistocene	As above	N 22	<i>G. pelagicus</i> <i>H. kamptneri</i> <i>Emiliania annula</i> <i>C. leptopora</i> <i>G. oceanica</i> <i>G. aperta</i>	NN 19/ NN 20
5	38.5	Lower Pleistocene	<i>N. pachyderma</i> (S) <i>Globigerina bulloides</i> <i>Globorotalia inflata</i> <i>G. scitula</i>		<i>C. pelagicus</i> <i>C. leptopora</i> <i>E. annula</i> <i>H. kamptneri</i>	NN 19
6	48.5	Upper(?) Pliocene	<i>Neogloboquadrina atlantica</i> (S) <i>N. pachyderma</i> <i>Globorotalia inflata</i> <i>G. scitula</i> <i>Turborotalita quinqueloba</i>		<i>C. pelagicus</i> <i>G. caribbeanica</i> <i>G. doricoides</i> <i>C. leptopora</i> <i>E. annula</i>	NN 18
7	56.5	Upper Pliocene	<i>Globigerina bulloides</i> <i>Neogloboquadrina atlantica</i> (S) <i>N. pachyderma</i> <i>Globorotalia scitula</i> <i>G. aff. G. puncticulata</i>		<i>C. pelagicus</i> <i>G. caribbeanica</i> <i>G. doricoides</i> <i>H. sellii</i> <i>D. brouweri</i>	NN 18
8	66.5	Lower Pliocene	As above		<i>C. pelagicus</i> <i>G. caribbeanica</i> <i>G. doricoides</i> <i>H. sellii</i> <i>E. annula</i> <i>Reticulofenestra pseudumbilica</i> <i>D. brouweri</i>	NN 18
9	73.0	Lower Pliocene	As above		<i>C. pelagicus</i> <i>G. doricoides</i> <i>H. sellii</i> <i>R. pseudumbilica</i>	NN 15/18
10	87.5	Lower Pliocene	<i>Globigerina bulloides</i> <i>Neogloboquadrina atlantica</i> (S) <i>N. pachyderma</i> s.l. <i>Globorotalia puncticulata</i> <i>G. scitula</i> <i>Orbulina</i> <i>Turborotalita quinqueloba</i>		As above	NN 15/18
11	97.5	Lower Pliocene	<i>Globigerina bulloides</i> <i>Neogloboquadrina atlantica</i> (S) <i>Orbulina</i> <i>Turborotalita quinqueloba</i> <i>Globigerinita</i> spp.		<i>C. pelagicus</i> <i>H. kamptneri</i> <i>H. sellii</i> <i>R. pseudumbilica</i> <i>C. leptopora</i>	NN 15/18
12	105.5	Lower Pliocene	<i>Globigerina bulloides</i> <i>Neogloboquadrina atlantica</i> (S) <i>N. humerosa</i> <i>N. pachyderma</i> s.l. <i>Globorotalia scitula</i>		<i>C. pelagicus</i> <i>C. leptopora</i> <i>R. pseudumbilica</i> <i>D. pentaradiatus</i>	NN 15/17

TABLE 2 – Continued

Core	Depth (m)	Chronostratigraphic Unit	Planktonic Foraminifers	Zone	Calcareous Nannofossils	Zone
13	119.0	Lower Pliocene	<i>Globigerina bulloides</i> <i>Neogloboquadrina atlantica</i> (S) <i>N. humerosa</i> <i>N. acostaensis</i> <i>Globorotalia scitula</i>		<i>C. pelagicus</i> <i>H. kamptneri</i> <i>C. leptopora</i> <i>R. pseudoumbilica</i> <i>D. variabilis</i>	NN 15/16
14	125.5	Lower Pliocene	<i>Globigerina bulloides</i> <i>Neogloboquadrina atlantica</i> (S) <i>N. humerosa</i> <i>N. pachyderma</i> s.1 <i>Turborotalita quinqueloba</i>		<i>C. pelagicus</i> <i>H. kamptneri</i> <i>H. sellii</i> <i>R. pseudoumbilica</i>	NN 13/15
15			Void		Void	
16	144.0	Upper Miocene (?)	<i>Globigerina bulloides</i> <i>Turborotalita quinqueloba</i> <i>Globigerinita</i> spp. <i>Orbulina</i> <i>Globorotalia scitula</i>		<i>C. pelagicus</i> <i>H. kamptneri</i> <i>H. sellii</i> <i>R. pseudoumbilica</i> <i>D. brouweri</i> <i>D. exilis</i> <i>D. bollii</i>	NN 9/11
17	152.5	Upper Miocene	<i>Neogloboquadrina atlantica</i> (D) <i>N. humerosa</i> <i>N. acostaensis</i> <i>Globorotalia scitula</i> <i>Globigerina bulloides</i>		As above	NN 9/11
18	165.5	Middle Miocene	<i>Globoquadrina dehiscens</i> <i>Globorotalia mayeri</i> <i>Globigerina woodi</i> <i>G. praebulloides</i> <i>G. druryi</i>		<i>C. pelagicus</i> <i>H. kamptneri</i> <i>R. pseudoumbilica</i> <i>Sphenolithus abies</i> <i>D. deflandrei</i> <i>Coronocyclus</i> sp. <i>Cyclicargolithus floridanus</i>	NN 5/7
19	175.0	Middle Miocene	<i>Globoquadrina dehiscens</i> <i>Globorotalia mayeri</i> <i>Globigerina woodi</i> <i>G. praebulloides</i> <i>G. aff. G. druryi</i> <i>Globorotalia</i> aff. <i>G. miozea</i>		<i>C. pelagicus</i> <i>H. kamptneri</i> <i>C. floridanus</i> <i>R. pseudoumbilica</i> <i>D. challengerii</i> <i>D. deflandrei</i>	NN 7
20	179.0	Lower Miocene	<i>Globoquadrina dehiscens</i> <i>Globorotalia</i> cf. <i>G. mayeri</i> <i>G. woodi</i> <i>G. praebulloides</i> <i>Globigerinita</i> spp.		<i>C. pelagicus</i> <i>R. pseudoumbilica</i> <i>C. floridanus</i> <i>D. deflandrei</i> <i>D. saundersi</i> <i>D. kugleri</i> <i>D. obtusus</i>	NN 5/7
21	187.0	Lower Miocene (?)	<i>Globigerina woodi</i> <i>G. pseudociperoensis</i> <i>G. praebulloides</i> <i>Globorotalia</i> aff. <i>G. continuosa</i> <i>Globorotaloides</i> sp.		<i>C. pelagicus</i> <i>R. pseudoumbilica</i> <i>D. druggi</i> <i>D. saundersi</i> <i>D. bollii</i> <i>D. deflandrei</i> <i>C. floridanus</i> <i>S. abies</i>	NN 4
22	200.0	Lower Miocene (?)	<i>Globigerina woodi</i> <i>G. pseudociperoensis</i> <i>G. praebulloides</i> <i>Globoquadrina venezuelana</i> <i>Globorotalia</i> sp.		<i>C. pelagicus</i> <i>H. intermedia</i> <i>R. pseudoumbilica</i> <i>R. scrippsae</i> <i>C. floridanus</i> <i>D. deflandrei</i> <i>S. abies</i>	
23	210.0	Lower Miocene	<i>Globoquadrina venezuelana</i> <i>Globigerinita</i> spp. <i>Catapsydrax dissimilis</i> <i>Globorotaloides suteri</i> (?)		<i>C. pelagicus</i> <i>R. pseudoumbilica</i> <i>S. abies</i> <i>D. deflandrei</i> <i>C. floridanus</i> <i>D. adamanteus</i> <i>D. obtusus</i>	NN 3

TABLE 2 – Continued

Core	Depth (m)	Chronostratigraphic Unit	Planktonic Foraminifers	Zone	Calcareous Nannofossils	Zone
24	224.5	Lower Miocene	<i>Globoquadrina venezuelana</i> <i>Globigerinita</i> spp. <i>Globigerina woodi</i> <i>G. praebuloides</i> <i>Globorotaloides suteri</i>		<i>C. pelagicus</i> <i>R. pseudoumbilica</i> <i>R. scrippsae</i> <i>C. floridanus</i> <i>S. moriformis</i>	NN 2/3
25	225.0	Lower Miocene	<i>Globoquadrina venezuelana</i> <i>Globigerinita</i> spp. <i>Globigerina praebuloides</i> <i>Globorotalia continuosa</i> <i>G. sp.</i>		Not examined	
26	234.5	Lower Miocene	<i>Globoquadrina venezuelana</i> <i>Globigerina praebuloides</i> <i>Globigerinita</i> spp. <i>Globorotalia continuosa</i>		<i>C. pelagicus</i> <i>R. pseudoumbilica</i> <i>R. scrippsae</i> <i>S. abies</i> <i>C. floridanus</i> <i>H. obliqua</i> <i>Chiasmolithus altus</i>	NN 2/3
27			Void		Void	
28	260.0	Lower Miocene	<i>Globoquadrina dehiscens</i> <i>Globigerina praebuloides</i> <i>Globigerinita</i> spp. <i>Globorotalia continuosa</i>		<i>C. pelagicus</i> <i>D. druggi</i> <i>D. deflandrei</i> <i>C. floridanus</i> <i>R. bisecta</i> <i>H. euphratis</i> <i>Discolithina vigintiforatae</i> <i>Zygrhablithus bijugatus</i>	NN 1/2
29	271.0	Lower Miocene	<i>Globorotalia kugleri</i> <i>Globoquadrina dehiscens</i> <i>G. praedeheiscens</i> <i>Catapsydrax dissimilis</i> <i>Globigerina praebuloides</i>		<i>C. pelagicus</i> <i>H. intermedia</i> <i>H. euphratis</i> <i>D. vigintiforatae</i> <i>C. floridanus</i> <i>R. bisecta</i> <i>Z. bijugatus</i>	NN 1
30	280.5	Lower Miocene	<i>Globorotalia kugleri</i> <i>Globoquadrina praedeheiscens</i> <i>Catapsydrax dissimilis</i> <i>C. unicava</i> <i>Globigerina praebuloides</i> <i>Globigerinoides primordius</i> (one specimen)		<i>C. pelagicus</i> <i>C. altus</i> <i>Discolithina anisotrema</i> <i>D. vigintiforatae</i> <i>C. floridanus</i> <i>R. bisecta</i> <i>Orthorhabdus servatus</i> <i>Triquetrorhabdulus carinatus</i> <i>Z. bijugatus</i>	NN 1
31	291.0	Upper Oligocene	<i>Globoquadrina praedeheiscens</i> <i>Globigerina praebuloides</i> <i>G. ciperoensis</i> <i>Globorotalia</i> sp.		<i>C. pelagicus</i> <i>C. floridanus</i> <i>R. bisecta</i> <i>O. serratus</i> <i>Z. bijugatus</i> <i>D. vigintiforata</i>	NP 25
32	292.0	Upper Oligocene	<i>Catapsydrax dissimilis</i> <i>Globorotalia</i> aff. <i>G. opima</i> <i>Globoquadrina</i> sp. <i>Globorotaloides suteri</i> <i>Globigerina praebuloides</i>		As above	NP 25
35	321.5	Oligocene	35-1, 400-102 cm <i>Globorotalia opima</i> <i>Globigerina praebuloides</i> <i>G. ciperoensis</i> <i>G. juvenilis</i> <i>Catapsydrax dissimilis</i>		No Sample	
36	331.0	Oligocene	36-2, 52-54 cm <i>Globorotalia opima</i> <i>Globigerina praebuloides</i> <i>G. ciperoensis</i> <i>G. juvenilis</i> <i>Catapsydrax dissimilis</i>		36-2, 39-40 cm <i>C. pelagicus</i> <i>C. floridanus</i> <i>S. moriformis</i> <i>R. bisecta</i> <i>O. serratus</i> <i>Z. bijugatus</i>	NP 25

TABLE 2— Continued

Core	Depth (m)	Chronostratigraphic Unit	Planktonic Foraminifers	Zone	Calcareous Nannofossils	Zone
43	405.5	Oligocene	<i>Catapsydrax dissimilis</i> s.l. <i>C. unicava</i> <i>C. gortanii</i> <i>Globigerina angiporoides</i> <i>Chiloguembelina cubensis</i> <i>Globorotalia</i> aff. <i>G. munda</i>		<i>Isthmolithus recurvus</i> <i>Chiasmolithus oamaruensis</i> <i>Reticulofenestra hillae</i> <i>Z. bijugatus</i> <i>H. cf. H. recta</i>	NP 22/23

Lower Miocene to upper Oligocene nannofossil chalks and siliceous nannofossil chalks overlie basalt, which was lower Miocene/middle Miocene boundary is placed at the top of Core 20 (177.0 m sub-bottom), that is, below the last assemblage assignable to the middle Miocene.

Planktonic foraminifers become more common in Cores 29 through 32, but again most specimens are small, and most cannot be identified with certainty. *Globorotalia kugleri* and *Globoquadrina praedehiscens* are present in 29, CC to 31, CC, and one specimen tentatively identified as *Globigerinoides primordius* occurs in Sample 30, CC (280.5 m sub-bottom). Thus, the Oligocene/Miocene boundary is placed between Samples 30, CC and 31, CC.

Sample 32, CC, which overlies basalt, contains *Catapsydrax dissimilis*, *Globigerina angustumilicata*, *Globorotalia* aff. *G. opima*, *Globoquadrina* sp., and *Globorotaloides suteri*, and is considered to be upper Oligocene.

Samples 35-1, 100-102 cm, 36-2, 52-54 cm, and 43, CC are of interest because they are from nannofossil chalk and calcareous mud interlayered with basalt. The assemblages from Cores 35 and 36 contain abundant and extremely variable representatives of the *Globigerina praebuloides* group, as well as *Globorotaloides suteri*, *Catapsydrax unicava*, *C. dissimilis* (s.l.), *Globigerina ciperoensis*, *G. juvenilis*, and *Globorotalia opima*. These assemblages are considered to represent Zones P20 to P21. Calcareous mud recovered about 100 meters below basalt (Sample 43, CC) contains abundant but poorly preserved planktonic foraminifers. Taxa recorded include *Catapsydrax dissimilis* (s.l.), *G. unicava*, *C. gortanii*, *Globigerina praebuloides*, *G. angiporoides*, and *Chiloguembelina cubensis*. This association probably represents "mid-" Oligocene Zones P19 to P20.

Nannofossils

Upper Pleistocene to (?) lower Oligocene coccolith assemblages occur in samples recovered at Site 407. The sediments are generally rich in well-preserved nannofossils, but because of low assemblage diversity and the lack of reliable markers, many age assignments are not to be considered too rigorous. All observations reported here refer to core-catcher (CC) samples unless otherwise noted.

Pleistocene sediments were recovered in the first five cores. Present and common in Samples 1, CC to 3, CC are *Cyclococcolithina leptopora*, *Gephyrocapsa aperta*, *G. caribbeanica*, *G. doronicoides*, and *G. oceanica*, suggesting the *Gephyrocapsa oceanica* Zone (NN 20).

Coccolithus pelagicus is present throughout the entire section at Site 407, and predominates in all assemblages examined. Sample 4, CC is probably transitional between Zones NN 19 and NN 20, because it contains the assemblage above plus common occurrences of *Emiliania annula*. Sample 5, CC is assigned to the *Emiliania annula* Zone (NN 19) on the basis of absence of *G. oceanica* and the presence of *E. annula*.

The Pliocene/Pleistocene boundary, as established with nannofossils, is between Samples 5, CC and 6, CC, although the last occurrence of *Discoaster brouweri* is in Sample 7, CC. Samples 7, CC and 8, CC are placed in the upper Pliocene *Discoaster brouweri* Zone (NN 18) because of the rare occurrences of *D. brouweri* in both. Also present are *Helicopontosphaera sellii*, *P. lacunosa*, *G. doronicoides*, and *G. leptopor*. Cores 9 through 14 contain mixed assemblages of lower and upper Pliocene nannofossils. *Reticulofenestra pseudumbilica* and *Helicopontosphaera kamptneri* occur in common abundance. *Discoaster pentaradiatus* is present in Sample 12, CC and *D. variabilis* occurs in Sample 13, CC; highest occurrences of each are NN 17 and NN 16, respectively. *G. caribbeanica* is anomalously present in common abundance in Samples 9, CC, 10, CC, 12, CC, and 13, CC. This suggests downhole contamination. No sediment was recovered in Core 15.

Samples 16, CC and 17, CC contain nannofossils indicating the upper Miocene (Zones NN 9 to NN 11): *H. kamptneri*, *H. sellii*, *R. pseudumbilica*, *Discoaster bollii*, *D. brouweri*, *D. exilis*, and *D. variabilis*.

A hiatus exists between Samples 17, CC and 18, CC, because Samples 18, CC and 19, CC are assigned to the upper middle Miocene *Discoaster kugleri* Zone (NN 7). *R. pseudumbilica* occurs in great abundance, together with *Discoaster adamanteus*, *D. challengerii*, *D. deflandrei*, *Coronocylus* sp., *Cyclicargolithus floridanus*, *Sphenolithus abies*, and *Triquetrorhabdulus rugosus*. The assemblage in Sample 20, CC is rather mixed and indicative of those in Zones NN 5 to NN 7, middle Miocene.

Lower Miocene nannofossil assemblages occur in Samples 21, CC to 30, CC. Sample 21, CC contains *D. adamanteus*, *D. bollii*, *D. deflandrei*, *D. druggi*, *D. obtusus*, *D. saundersi*, *C. floridanus*, *R. pseudumbilica*, and *S. abies*. It is assigned to the upper lower Miocene *Helicopontosphaera ampliaperta* Zone (NN 4). Sample 22, CC contains a mixed lower Miocene assemblage. The great abundance of *Reticulofenestra scrippsae* is notable. Samples 23, CC, 24, CC, 26, CC, and 28, CC (no recovery in 25, CC and 27, CC) are assigned to the lower Miocene

(NN 1 to NN 3) because of the presence of the following: *Chiasmolithus altus*, *Cyclicargolithus floridanus*, *R. pseudumbilica*, and *R. scrippsae*.

The *Triquetrorhabdulus carinatus* Zone (NN 1) is evident in Samples 29, CC and 30, CC. Particularly indicative of this are *Discolithina vigintiforata*, *C. floridanus*, *Reticulofenestra bisecta*, *Orthorhabdulus serratus*, *Triquetrorhabdulus carinatus*, and *Zygrhablithus bijugatus*.

Samples 31, CC, 32, CC, and 36-2, 39 cm (34, CC is barren) contain uppermost Oligocene assemblages from the *Sphenolithus cipoensis* Zone (NP 25). Present are *Helicopontosphaera recta*, *C. floridanus*, *D. vigintiforata*, *O. serratus*, *R. bisecta*, *S. moriformis*, and *Z. bijugatus*.

About 100 meters of basalt occur next. Recovery in Core 43 was limited to the core-catcher sample, sandy calcareous mud. Nannofossils present include *Chiasmolithus oamaruensis*, *Helicopontosphaera* cf. *H. recta*, *Isthmolithus recurvus*, *Reticulofenestra hillaie*, *Sphenolithus predistentus*, *S. moriformis*, and *Z. bijugatus*. This assemblage suggests the lower upper Oligocene (NP 22) 123. The remaining cores are basalt.

PHYSICAL PROPERTIES OF SEDIMENTS

Eighty-five sonic velocity measurements, 73 water content measurements, and 65 wet bulk density measurements were made on samples through the sediment column, and are plotted against sub-bottom depth and core number in Figures 8, 9, and 10.

Water content and wet bulk density show a characteristic inverse relationship, with nominal values of 0.5 and 1.5, respectively. The most notable systematic variations in the physical properties of the sediment column are the minimum of 0.35 in water content, centered at about 100 meters, and the corresponding maximum of about 1.7 in wet bulk density. This fluctuation corresponds to a decrease in drilling rate beginning at Core 12, but is not reflected in sonic velocity values or analog GRAPE records.

Sonic velocity measurements show two highs — at 160 and 260 meters — that correspond to reflecting horizons (at 200 and 390 ms of two-way travel time) in the seismic reflection profiles. These correlate in terms of average sediment velocity; they also correlate in terms of depth-in-hole. Two other velocity peaks, at 27 meters and 279 meters, are single-valued highs and appear to be measurement errors.

PALEOMAGNETISM OF THE SEDIMENTS

The sediments recovered from Hole 407 are generally unsuitable for paleomagnetism measurements: most of them have been disturbed considerably in drilling. Ten specimens were taken, however, between depths of 117 meters and 224 meters, in an attempt to select undisturbed material. Unfortunately, it was not possible to measure these specimens until after they had dried out, by which time they had become very friable, so that containment in the plastic holder was a problem.

Measured intensities were of the order of a few μG (10^{-5} emu/cm³), typical of sediments, but the directions fluctuated upon AF demagnetization, particularly when the relative declination was considered, and the angular standard deviation within the six positions constituting a

single measurement reached values not explicable in terms of the instrumental noise level. In nine out of ten cases, the directions had changed appreciably and the intensity increased, four days after the initial measurements and AF demagnetization to a peak field of 500 Oe (50 mT).

It would seem that no significant conclusion can be drawn from these specimens. Deformation may have occurred in sampling and spinning and tumbling in the AF demagnetizer, so that internal coherence and orientation may no longer be very good.

CHEMISTRY OF SEDIMENTS

Chemistry of Interstitial Solutions

The composition of interstitial solutions of biogenic sediments has been shown to reflect reactions within the

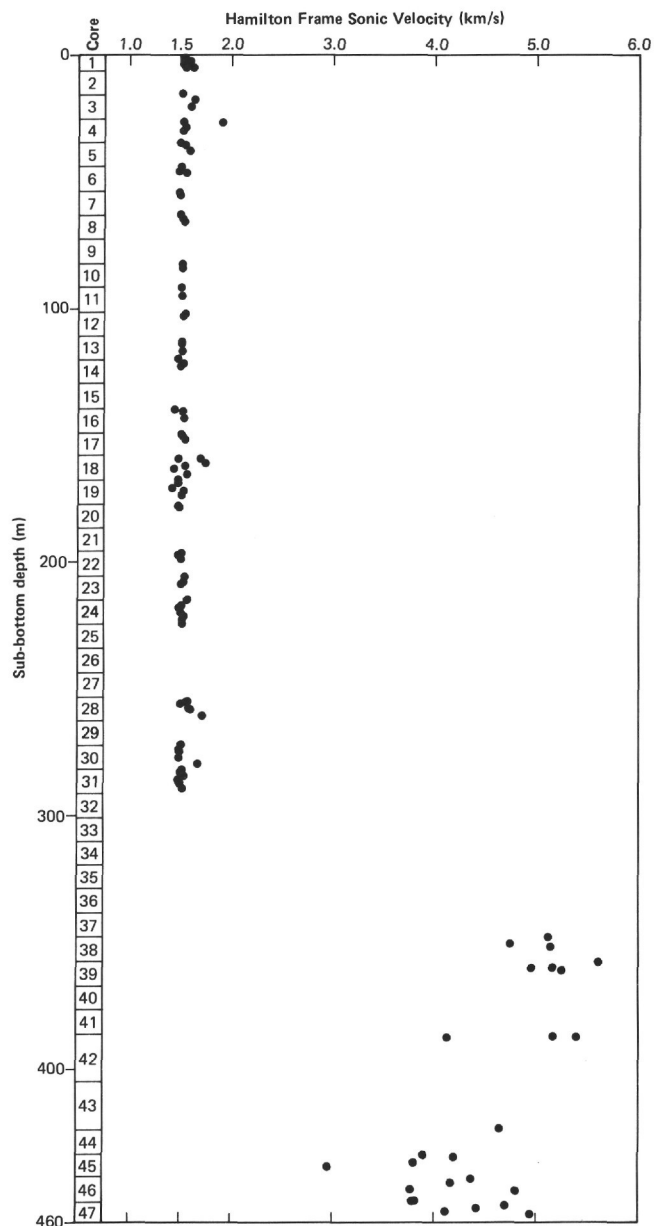


Figure 8. Sonic velocity versus depth, Site 407.

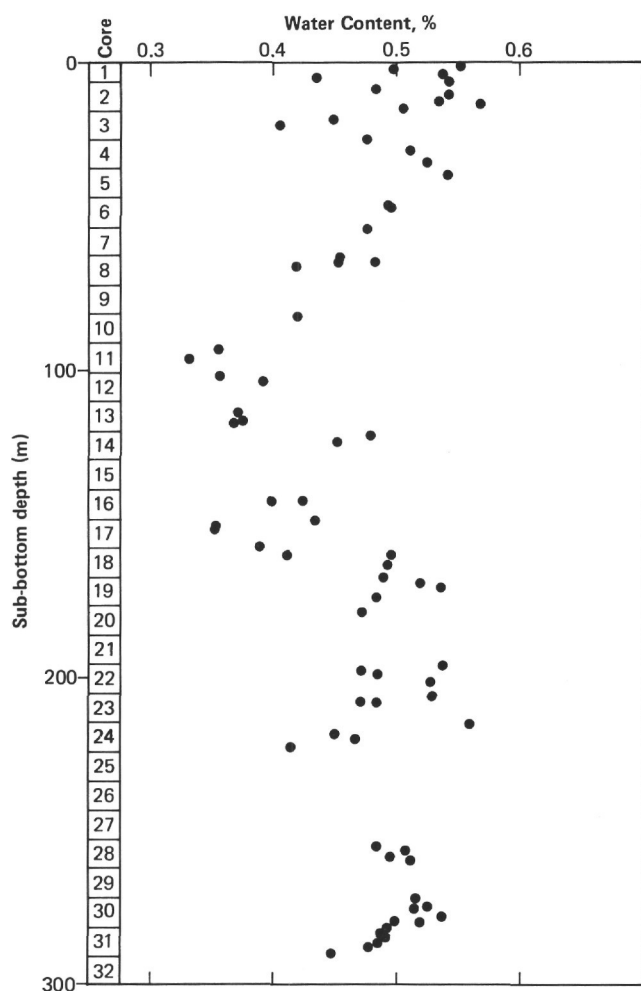


Figure 9. Water content versus depth, Site 407.

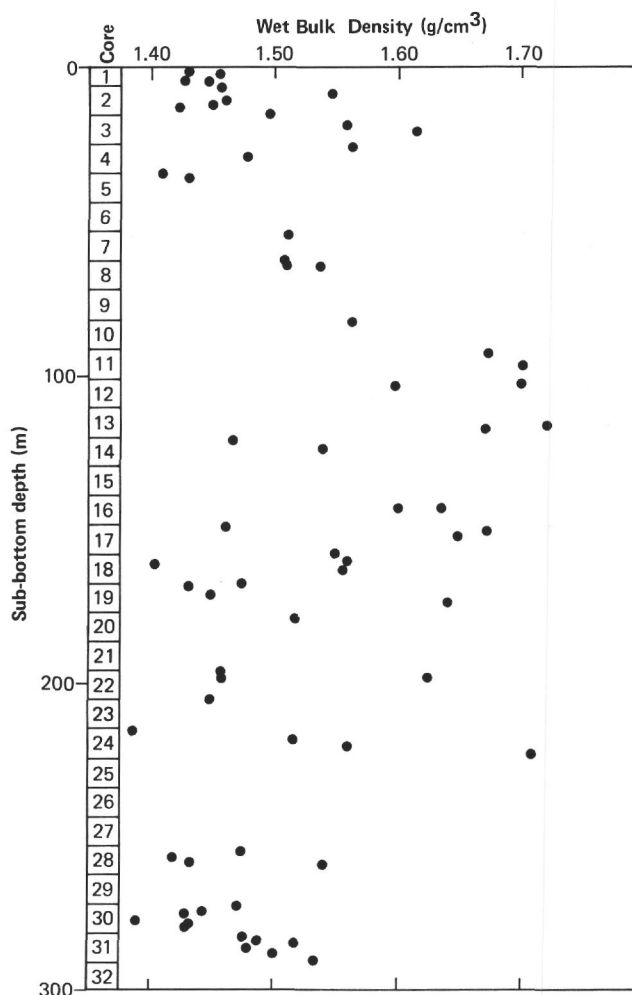


Figure 10. Wet bulk density versus depth, Site 407.

sediment and sediment-solute interactions (Sayles and Manheim, 1975). It is therefore possible to study the early stages of diagenesis in such sediments by analyzing the interstitial solutions. Pelagic clays deposited slowly (less than 1 cm/1000 years) in the abyssal basins of the ocean are the only sediments to show little evidence of reaction in the pore waters. Evidence of diagenetic reactions in the pore solutions is lacking most probably because of the completion of reaction and dissipation of the resulting pore fluids by diffusion near the seawater/sediment interface, in consequence of slow deposition rates (Sayles and Manheim, 1975).

Results of interstitial water analyses for alkalinity, pH, chlorinity, Ca, and Mg are shown in Figure 11. From the variables measured, it appears that the interstitial solutions are indistinguishable from seawater throughout the sedimentary succession. However, post-depositional reactions can be seen to have taken place within these sediments: e.g., the alteration of volcanic ash fragments and layers. The sedimentation rate at this site varied from less than 0.5 cm/1000 years to more than 4 cm/1000 years (Figure 12), which is significantly greater than the rates for pelagic clays mentioned above. The absence of changes in the interstitial water composition of these relatively rapidly

deposited ocean-floor sediments is somewhat surprising. Most sediments recovered at this site were highly disturbed and soupy, because of the drilling. That the interstitial solutions are chemically similar to sea water may be because the sediments were significantly contaminated by seawater used as drilling fluid during their recovery, with the result that in subsequent sampling of the interstitial solutions we have really sampled sea water.

Regardless of the methods used in recovery, the samples have been standard in the Project for a number of years, and it seems more likely that some other unknown cause keeps the composition of interstitial solutions here close to that of sea water.

PALEOENVIRONMENTAL INTERPRETATION

Sediments cored at Site 407 suggest major changes in bottom current activity between the Oligocene and the Quaternary.

Low sediment accumulation rates and slight current laminations, highlighted by dark mineral placers (e.g., Cores 28 and 30), are evident in the upper Oligocene through the lower Miocene; this suggests slight or sluggish bottom current action. Unconformities within the middle to upper Miocene are attributed to erosion by bottom currents,

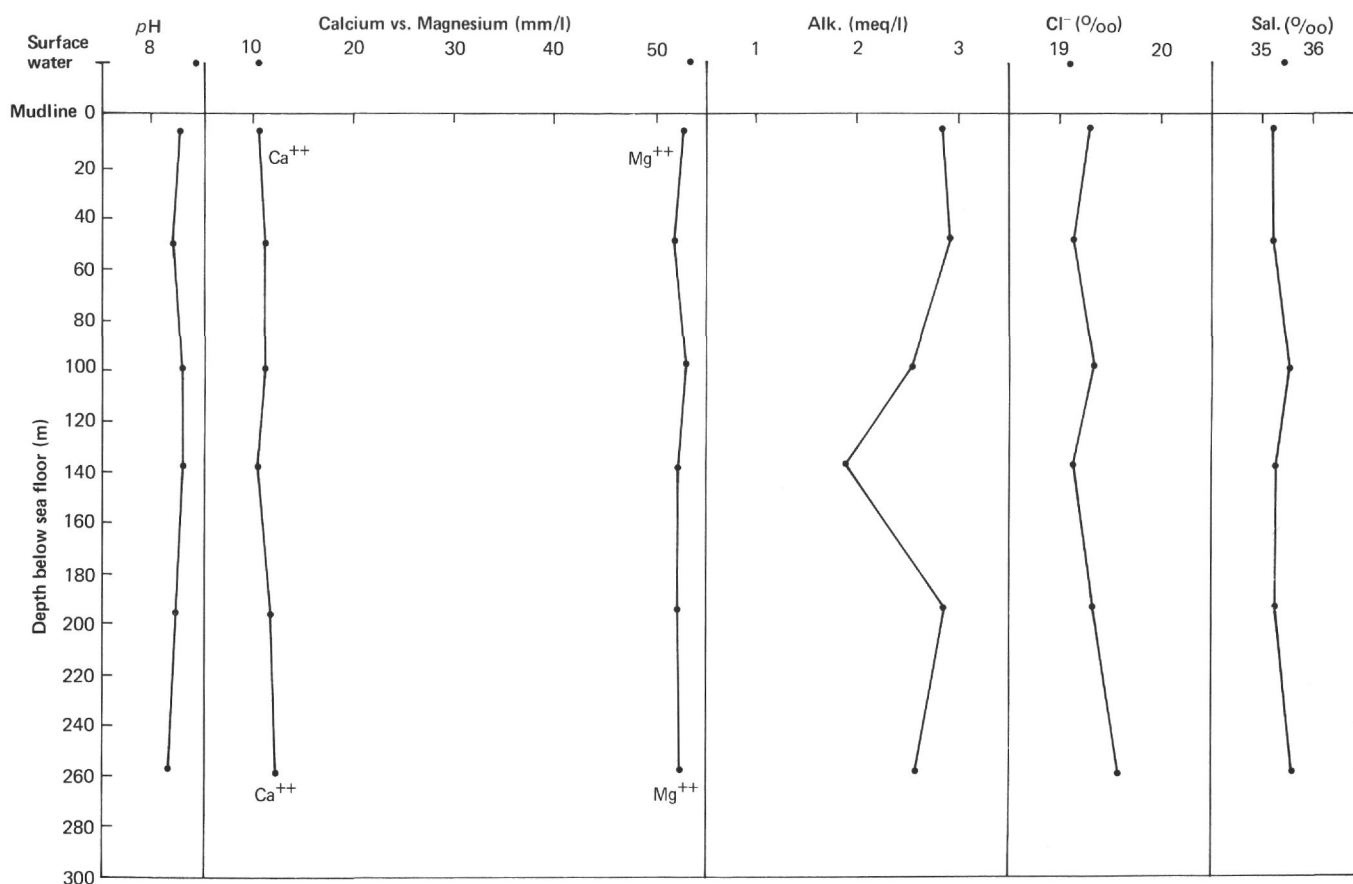


Figure 11. *Interstitial water chemistry at Site 407.*

whereas the high sediment accumulation rate calculated for the Pliocene indicates a change from an erosional to a depositional bottom current regime.

Unit 1 (Cores 1 to 6; 0 to 46.3 m) is principally calcareous sandy mud with interlayered nannofossil ooze and terrigenous mud. Ice-rafted detrital grains (sand to gravel size) and volcanic ash (both fresh and altered) are present in variable abundance; combined with the variable carbonate content, this suggests that glacial/interglacial contrasts in surface temperature, Icelandic glaciation, and sea ice cover were the principal mechanisms controlling sediment deposition throughout the Pleistocene. Graded bedding, indicating turbidity currents, occurs only in Core 5 (36.2 to 39.5 m); coring disturbance and burrowing may, however, have prevented recognition higher in the section of graded turbidites comparable to those at Site 408. Airgun records near the drill site (e.g., Figure 5) show flat-lying, highly reflective surface sediments with multiple reflectors that suggest ponded turbidites.

The sharp compositional and textural boundary between Units 1 and 2 (sandy calcareous mud above nannofossil ooze) suggests an erosional hiatus, with Pleistocene glacial sediments (turbidites?) overlying non-glacial Pliocene deposits. This interpretation is compatible with our understanding of bottom current activity on the west flank of Reykjanes Ridge. Increased production of bottom water at the Iceland-Faeroes Ridge (eastern basin of the North Atlantic) would be expected to have occurred during the

climatic deterioration in the Pliocene; glacial conditions started about 3 m.y. ago, according to Laughton, Berggren, et al. (1972). We suggest that the depositional regime changed dramatically after the initiation of late Pliocene glaciation, resulting in erosion or non-deposition of silt- and clay-size sediments, because of increased velocity of the thermohaline bottom current and/or erosion by turbidity currents. Turbidites and ice-rafted coarser sediments (Unit 1) from Iceland were deposited rapidly and probably episodically during the Pleistocene, and probably represent only a portion of the material originally deposited during the last 3 m.y. Our model of current-controlled deposition at Sites 407 and 408 is further developed in Shor and Poore (this volume).

Unit 2 (Cores 6 to 18; 46.3 to 160.7 m) is a nannofossil ooze containing only minor accessory components. Coring disturbance was intense, particularly above Core 13. Compaction increases markedly below this level (from "ooze" to "chalk"), and disturbance is consequently reduced to a moderate level. Four thin (5 to 15 cm) ash horizons cause a change in consolidation within Core 10, from fairly firm above to soupy below; this, if widespread, could be a zone of slippage in other parts of the region, where slopes are somewhat steeper. The silt-size detrital grains (> 2% throughout) are mainly quartz, opaques, and traces of hornblende (probably windblown).

Foraminifer and nannofossil assemblages both change significantly at the base of Unit 2 (between 17, CC and 18,

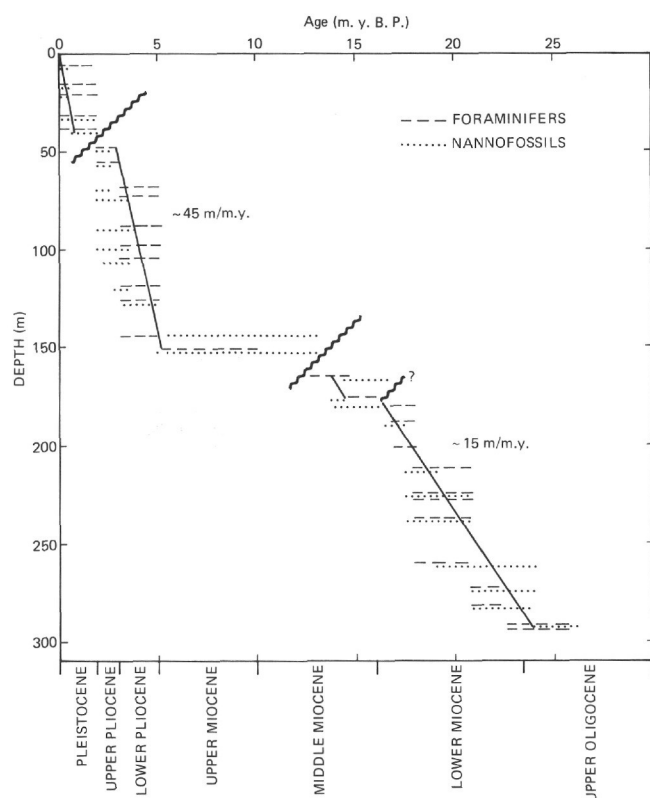


Figure 12. Sediment accumulation rates for Hole 407. Ages of foraminifers and nannofossil zone boundaries are from Berggren (1972b).

CC; see Biostratigraphy), suggesting a hiatus between middle and upper Miocene deposits. This level brackets a change from nannofossil chalk above to siliceous nannofossil chalk below (Core 18; 160.7 m), and may represent a change in flow regime as well. Smear slides from slightly above the 160.7-meter contact contain a relatively high percentage of glauconite (1 to 3%) and broken foraminifer fragments, which we tentatively interpret as evidence of reworking and/or erosion caused by bottom currents.

Green to black lithified clasts (sand size) are scattered through the ooze below 149.5 meters (Core 17). The darker grains are principally volcanic ash; the green clasts appear to be lithified fine-grained glauconitic ooze, and in some instances the glauconite shows evidence of forming by alteration from ash grains. They may be burrow fills, or they could be redeposited fragments of glauconitized laminations resulting from winnowing and fractionation of sand and silt components by bottom currents. They are compositionally similar to thin laminations deeper in the section, both at this site and at Site 408, which suggests that they may be related to current activity rather than to bioturbation. If so, they appear to represent redeposition of older material, since no laminations occur unbroken in Unit 2.

Unit 3 (160.7 to 272.0 m) contains an increased number of lithified clay clasts and volcanic ash grains; thin laminations in Core 28 are highlighted by these components (apparently current-sorted). The increased biogenic silica in

this unit, compared with that in Unit 2, could be the result of either lower deposition rates of carbonate relative to siliceous biogenic sediments, or removal of fine-grained carbonate by bottom currents; our preliminary examination does not enable us to decide which mechanism was responsible.

Unit 4 (Cores 30 to 32; 272.0 to 300.5 m) is nannofossil chalk in Core 30; basaltic sand and gravel increase downcore to form a conglomerate by Core 32. The basalt clasts are mostly angular and up to 4 cm in diameter, and so imply a local source. A basement hill (buried) one to two kilometers east of Site 407 is the most likely source of this unit, and there appears to be a discontinuous set of reflectors immediately overlying acoustic basement on the underway airgun record, which originates at the base of this hill and extends past the drill site (Figure 5). A short (19-cm-thick) sequence of disturbed laminae in Section 30-6 is the only evidence of current winnowing in this unit. Its setting within a basal conglomerate suggests local currents or turbidity currents. The laminations (1 mm to 1.5 cm thick) are highlighted by dark mineral grains and sand/silt grains of basalt and volcanic glass.

SEDIMENT ACCUMULATION RATES

Sediment accumulation rates have been calculated for the Pliocene and lower Miocene to Oligocene sections of Hole 407 (Figure 12). Age assignments based on nannofossils and foraminifers are in general agreement, although Pliocene nannofossil age assignments are slightly younger than foraminifer age assignments from the same samples.

The average accumulation rate of 15 m/m.y. for the lower Miocene to upper Oligocene sediments contrasts with the estimated Pliocene rate of 45 m/m.y.; the increase in the upper section is ascribed to deposition from bottom currents. The Miocene hiatus(es) is similarly ascribed to bottom current flow; erosion followed the initiation of overflow from the Norwegian Sea.

An accumulation rate of 20 m/m.y. is calculated for the Quaternary turbidite section. A portion of the Quaternary may be missing.

BASEMENT LITHOSTRATIGRAPHY

Lithostratigraphy and Major Volcanologic and Petrographic Characteristics

After penetrating 281.5 meters of sedimentary section, we drilled nearly 177 meters of basalt and basaltic breccia at Site 407. About 25 per cent of the igneous section was recovered as core; recovery for the entire hole was 40 per cent. Basalt first appears as clasts in a matrix of fossiliferous clay, in Cores 30, 31, and 32. The remainder of the recovered material is basalt, except for some interlayered clay in Cores 35, 36, and 43.

Since no facilities for determining rock chemistry were available aboard ship, igneous stratigraphy was initially defined according to the presence of interlayered sediments, changes in magnetic polarity and drilling rate, and macroscopic and microscopic petrographic characteristics. Subsequent geochemistry has enabled us to define four major lithostratigraphic units.

Macroscopic examination of the basalt cores was useful in reconstructing some igneous stratigraphy. Eight fragments with fine-grained margins (Table 3) may represent parts of quickly cooled margins of lava flows. Thirty fragments with glass margins (Table 3), especially abundant in Cores 45, 46, and 47, are probably pieces from the quenched skins of pillow basalt (Figure 13). In Core 37, Section 1, an abrupt change in grain size suggests another contact between flows. This change in grain size is also closely bracketed by samples that indicate a reversal of the magnetic field.

Interlayered sediments also help define boundaries between flows or groups of flows (see stratigraphic summary sheets, Figures 14 and 15). Four such boundaries are present within the igneous section.

Correlation between the rate of penetration during drilling and the core material recovered helps to further define the nature of the igneous section. Generally, constant weight is maintained on the drill bit, and the bit is turned at constant speed during drilling. Thus, differences in penetration rate primarily reflect relative resistances of rock types to drilling. In a general way, the rate of drilling decreases with depth in the hole (Figures 6 and 16), because of increased compaction of sediments with depth and eventual penetration of the far more resistant igneous section. An even closer correlation between drilling rate and rock type is possible from examination of the drilling recorder strip chart (geolograph), which shows depth of penetration, in half-meter intervals, versus time. By assigning "hard" rocks to times of slow penetration and "soft" rocks to time

of fast penetration, a hypothetical subdivision of flow units has been constructed (Figure 15). Many ambiguities exist in such a reconstruction, but for the most part all recovered core material can be assigned to an appropriate time of easy or hard drilling. Much of the easily drilled material was never recovered as core, and in most cases, we can only guess at its identity. Easily drilled material may represent fossiliferous sediment or largely tuffaceous or rubbly parts of flows, but in any event it implies a break between lava flows, or flow units.

Magnetic polarity and inclination define a threefold magnetic stratigraphy. As mentioned above, a large change in grain size in Core 37, Section 1, is closely bracketed by samples of opposite magnetic polarity; the overlying rocks are normally magnetized and the underlying rocks reversely magnetized. The uppermost part of the igneous section (≥ 345 m) and the lowest part (≥ 428 m) also have distinctively different magnetic inclinations (see Table 4), and may correspond to periods of different rates of eruption, implied by contrasting abundances of sediment interlayered with flows of the two zones (Figure 15).

The petrographic character of the rocks provides additional control for defining flow units. All the lavas are aphyric or sparsely phryic basalt. Variation in groundmass texture within flows appears to be as great as variation between flows. Abundance of phenocrysts never exceeds 5 per cent, but phenocryst assemblages appear distinctive for some flows. Additional characteristics, such as occurrence

TABLE 3
Basalt Samples that Show Evidence of Chilled Margins

Glassy Margins			Fine-grained Margins		
Core	Section	Interval (cm)	Core	Section	Interval (cm)
37	1	110	35	2	30-40
38	2	52	38	2	15
40	1	30	42	1	45
41	1	0	44	1	0
42	1	0	44	1	60
44	1	40	46	3	120
44	1	60	47	2	110
45	1	25	47	2	120
45	2	75			
45	2	80			
45	2	85			
45	2	110			
45	2	115			
45	2	120			
45	2	130			
45	3	25			
45	4	30			
46	2	100			
46	2	115			
46	2	120			
46	3	40			
46	3	90			
46	3	150			
46	4	0			
46	4	60			
47	2	115			
47	3	135			
47	3	140			
47	4	80			
47	4	85			



Figure 13. Chilled margin of submarine flow. Note veinlets of calcite in the glass (dark band).

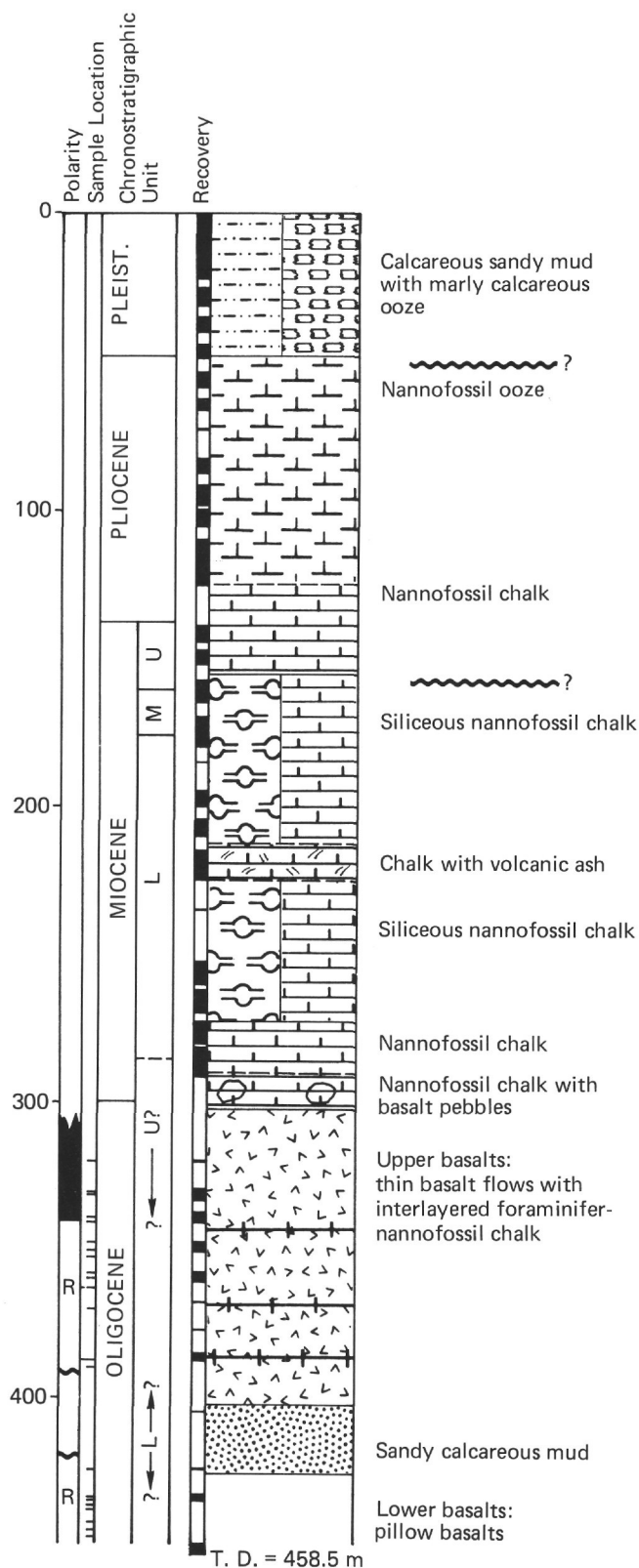


Figure 14. Summary stratigraphic column, Hole 407.

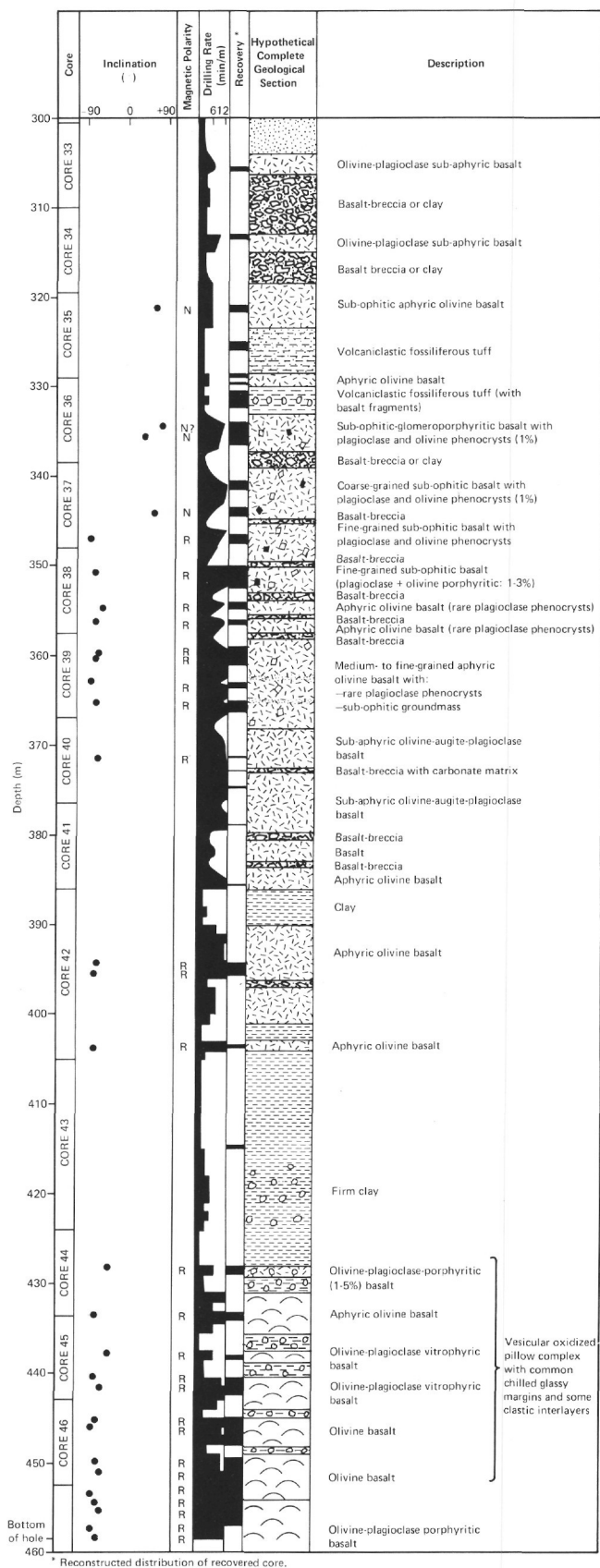


Figure 15. Stratigraphic column of basement rocks, Hole 407.

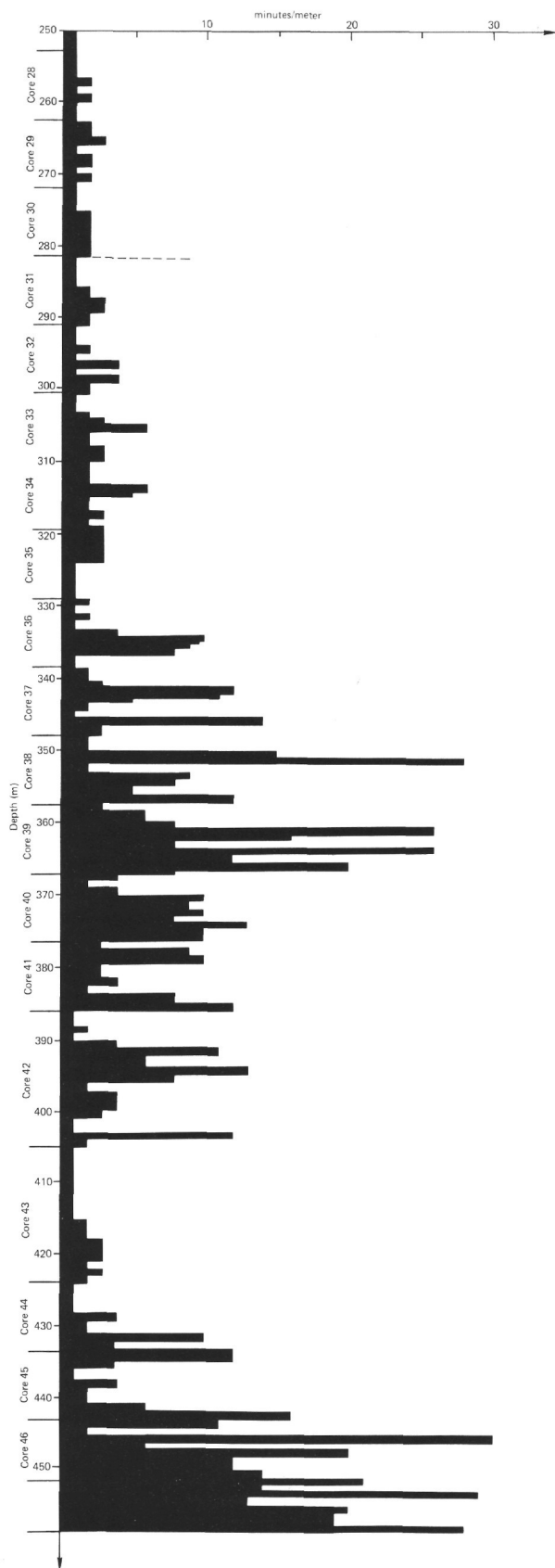


Figure 16. Average drilling rates versus depth, Hole 407.

of microcumulates and plagioclase phenocryst compositions, are also useful in differentiating flows.

Table 5 summarizes the division of the lavas, on petrographic criteria, into units. Apart from the breccia blocks in Cores 31 and 32, the petrographic character of which clearly differs from the underlying lavas, 12 units are defined. In all but one case (at 454 m in the pillow complex), a petrographic boundary corresponds to a flow boundary, as defined by drilling rates and other criteria previously discussed. The exception is a boundary in the pillow complex close to the bottom of the hole; this contact may not have shown up in the drilling rate log because the drill bit was failing rapidly at that time.

Figure 15 summarizes the igneous stratigraphy of Hole 407, based on all criteria available on board. Twenty-five flows or flow units are defined; these vary in thickness from 1 to 10 meters, and have an average thickness between 3 and 5 meters, depending on one's interpretation of the easily drilled but unrecovered part of the section. Observed contacts between igneous units are horizontal or nearly so. Some plagioclase grains and trains of vesicles are similarly oriented, and are consistent with a flow interpretation of the igneous units.

The best geochemical indicators for defining lithostratigraphic units are plotted in Figure 17. Four units are apparent. The differences between them are particularly well seen in K_2O , TiO_2 , Fe_2O_3 , and Ce/Y .

In Unit 1, these variables take high values, and in Unit 2, low values. Unit 3 has Ce/Y similar to Unit 1, but lower K_2O and Fe_2O_3 . It is a more variable unit than Unit 2. Unit 4 comes below the layer of sediments, and is broadly similar to Unit 2, although Ce/Y is significantly lower. Unit 4 is particularly variable. There is a clear inverse relationship between Fe and Mg , and Ni follows Mg .

IGNEOUS PETROGRAPHY

Petrography of the Volcanic Rocks

Volcanic Fragments in the Sediments

Fragments of pale brown volcanic glass, generally palagonitized or chloritized (Figure 18), occur in many of the sediments recovered in Hole 407. Grains of feldspar, quartz, pyroxene, magnetite, amphibole, biotite, and altered olivine, all believed to be of volcanic origin, are also present. Identification of biotite and amphibole, and distinction of quartz from feldspar, is difficult in smear slides. Most of the glass fragments are pale brown, vesicular (Figure 19), and sometimes contain elongated cavities. These fragments are probably basaltic. Ash layers, particularly in the interval 86 to 90 meters (Pliocene), also contain colorless glassy fragments with relatively low refractive index, suggestive of a silicic composition.

Volcaniclastic Breccia

A breccia of basalt lapilli (50%) and ash (30%) in a matrix of nannofossil ooze was recovered in the depth interval 280 to 305 meters. Fragments reach 10 cm diameter, and are usually angular but sometimes rounded. Angular fragments of complex shape (Figure 20) suggest

TABLE 4
Paleomagnetism Data – Hole 407

Sample (Interval in cm)	Depth Sub-Bottom (m)	NRM Intensity (10^{-3} emu cm^{-3})	Initial Inclination ($^{\circ}$)	Stable Inclination ($^{\circ}$)	MDF (Oe)	Comments
407-35-1, 37-39	319.9	3.1	+65.8	+63.7	40	Basalt, Magnetic Unit 1
407-35-1, 109-113	320.6	0.05	+43.6	+61.6	130	Tuff
407-35-2, 17-20	321.2	0.09	+71.1	+45.0	7100	Tuff
407-36-1, 93-96	329.9	0.09	+58.0	+57.8	100	Tuff
407-36-2, 9-11	330.3	0.08	+72.2	+68.2	150	Tuff
407-36-2, 74-76	331.3	4.7	+77.1	+73.2	40	Basalt
407-36-2, 91-93	331.4	3.5	+63.1	+73.1	90	Basalt
407-36-3, 9-11	332.1	5.6	+71.2	+69.9	Thermal	Basalt
407-36-3, 14-16	332.2	6.1	+63.5	+69.5	100	Basalt
407-36-3, 58-60	332.6	3.2	+72.8	+65.9	25	Basalt
407-37-1, 30-32	338.8	6.3	+77.4	+67.6	60	Basalt
407-37-1, 74-76	339.3	3.7	+78.2	+50.7	35	Basalt
407-37-1, 111-113	339.6	7.7	+73.2	+68.7	Thermal	Basalt
407-37-2, 74-76	340.8	2.7	-12.1	-85.8	150	Basalt, Magnetic Unit 2
407-38-1, 52-54	348.5	1.5	-43.9	-70.3	200	Basalt, Magnetic Unit 2
407-38-2, 59-61	350.1	2.2	-47.4	-56.6	Thermal	Basalt, Magnetic Unit 2
407-35-3, 56-58	351.6	4.3	-45.2	-73.8	130	Basalt, Magnetic Unit 2
407-38-3, 81-83	351.8	4.1	+56.6	-73.4	150	Basalt, Magnetic Unit 2
407-39-1, 49-51	358.0	2.5	-53.9	-65.2	Thermal	Basalt, Magnetic Unit 2
407-39-2, 58-60	359.6	1.0	+14.5	-70.3	80	Basalt, Magnetic Unit 2
407-39-3, 42-44	360.7	2.6	-43.3	-78.7	180	Basalt, Magnetic Unit 2
407-39-3, 48-50	361.0	2.1	-23.9	-77.2	Thermal	Basalt, Magnetic Unit 2
407-39-3, 140-142	361.9	2.6	+35.5	-66.1	35	Basalt, Magnetic Unit 2
407-40-1, 59-61	367.6	2.8	-49.7	-63.4	300	Basalt, Magnetic Unit 2
407-41-1, 100-102	377.5	4.3	-42.3			Basalt, Magnetic Unit 2
407-42-1, 77-79	386.8	4.8	+30.4	-63.8	Thermal	Basalt, Magnetic Unit 2
407-42-1, 87-89	386.9	2.7	-34.7	-67.0	180	Basalt, Magnetic Unit 2
407-42-2, 143-145	388.9	5.3	+51.1	-66.5	20	Basalt, Magnetic Unit 2
407-44-1, 17-19	424.2	8.2	-24.5	-34.7	150	Basalt, Magnetic Unit 3
407-44-1, 68-70	424.7	18.5	-38.4	-43.3	160	Basalt, Magnetic Unit 3
407-45-1, 69-71	424.2	10.5	-25.6	-68.6	110	Basalt, Magnetic Unit 3
407-45-2, 40-42	435.4	1.9	-53.3	-36.4	250	Basalt, Magnetic Unit 3
407-45-3, 122-124	437.7	11.4	-34.5	-67.0	100	Basalt, Magnetic Unit 3
407-45-4, 53-55	438.5	14.4	-48.1	-49.6	350	Basalt, Magnetic Unit 3
407-45-4, 58-60	438.6	15.6	-57.9	-57.2	200	Basalt, Magnetic Unit 3
407-46-1, 15-17	443.2	3.9	-56.8			Basalt, Magnetic Unit 3
407-46-1, 63-65	443.6	1.8	-53.2	-56.7	7400	Basalt, Magnetic Unit 3
407-46-2, 59-61	445.1	6.4	-54.1	-67.7	7300	Basalt, Magnetic Unit 3
407-46-3, 66-68	446.7	4.6	-65.1	-64.7	220	Basalt, Magnetic Unit 3
407-46-4, 68-72	448.2	2.5	-56.4	-54.2	280	Basalt, Magnetic Unit 3
407-47-1, 48-50	453.0	6.5	-67.2	-68.1	80	Basalt, Magnetic Unit 3
407-47-2, 14-16	454.2	1.9	-34.3	-58.0	250	Basalt, Magnetic Unit 3
407-47-2, 88-70	454.9	1.3	-47.7	-53.7	200	Basalt, Magnetic Unit 3
407-47-3, 20-22	455.7	3.0	-39.8	-58.7	90	Basalt, Magnetic Unit 3
407-47-4, 40-43	457.4	2.3	-54.6	-64.4	210	Basalt, Magnetic Unit 3

direct fallout from a nearby subaqueous gas-rich eruption occurring in soft mud. All fragments contain scattered phenocrysts of augite and plagioclase in an aphanitic groundmass (Figure 21). The composition of the plagioclase (An_{48-30}) suggests an evolved magma with a high Fe/Fe + Mg ratio, similar to the lavas of Unit 1 beneath.

Upper Lava Sequence

The first sequence of lava flows encountered (304 to 404 m) is interstratified with sediments in the upper part (304 to 399 m, see Figure 15).

304 to 317 meters: two flow units, probably about 2 meters thick each, were sampled in core catchers 33 and 34. They contain olivine (1 to 4%) and plagioclase (2 to 7%) phenocrysts, associated with rare later clinopyroxene, in a

black, predominantly glassy groundmass (Figure 22). Plagioclase phenocrysts show normal zoning (An_{68-55}).

317 to 332 meters: parts of two flow units were recovered. The rocks are sparsely phryic olivine basalt with olivine and plagioclase (An_{70-60}) phenocrysts. The groundmass is sub-ophitic to glassy. Both the groundmass and the olivine are altered to smectite. Sulfide veinlets are present. The first two groups of flow units correspond to geochemical Unit 1.

332 to 350 meters: parts of three flow units of plagioclase (1 to 5%) and olivine (1 to 3%) porphyritic basalts with sub-ophitic to ophitic groundmass were recovered in this interval. Plagioclase compositions are An_{76-60} . Olivine and glass are altered to smectite, and smectite also occurs in subvertical cracks and fractures

TABLE 5
Petrographic Criteria of Basement Units, Site 407

Core-Section	No. of Flows	Hard Rock Thickness (m)	Soft Rock Thickness (m)	Total Thickness (m)	Phases at the Liquidus (Chilled Margin Mineralogy or Phenocrysts)	Groundmass Structure	Other: Alteration Comments
31, 32	Blocks breccia				Plagioclase (An ₄₆₋₃₀)-clinopyroxene	Aphanitic or glassy	Altered olivine also present
33, 34	2	4.5	8.5	13.0	Olivine-plagioclase (An ₆₈₋₅₅)	Intersertal	Olivine altered to smectite
35 to 36-1	2	6.5	8.5	15.0	Olivine	Sub-ophitic to glassy	(An ₇₀₋₆₀ in plag.) to smectite
36-2 to 38-1	3	14.5	4.0	18.5	Plagioclase (An ₇₆₋₆₀)-olivine	Sub-ophitic to ophitic	Carbonate veins to smectite
38-2	1	3.0	1.0	4.0	Plagioclase (An ₇₀₋₅₀)-olivine	Sub-ophitic	Plagioclase microcumulates into smectite
38-3 to 39	3 (5)	13.0	1.5	14.5	Rare plagioclase (An ₆₄₋₅₀)	Sub-ophitic	Pigeonite? (2nd-generation cpx)[Fe-Ti rich rock] into smectite
40 to 41	4	16.0	4.0	20.0	Olivine-plagioclase-augite (An ₆₄₋₄₆)	Subvariolaritic-hyalophitic	Smectite chlorite + calcite filling
42	3	11.0	5.0	16.0	Aphyric	Intersertal	Pyrite filling cavities and cracks
		Sediment		19.0	(lower Oligocene)		
44-1	1	1.5	1.5	3.0	Olivine-plagioclase (An ₇₅₋₇₂)	Sub-ophitic	ol-pl microcumulate - smectite and pyrite
45-1 to 45-2, 6 cm	1	4.5	2.0	6.5	Olivine	Aphyric intersertal	Olivine altered, glass, too
45-2, 13 cm to 46-4	3	7.5	4.0	11.5	Olivine-plagioclase (An ₇₆₋₆₂)	Vitrophyric to glassy	Partly palagonitized
47-1 to 47-2, 2 cm	1	5.0	0.5	5.5	Olivine	Sub-ophitic coarse-grained	Olivine altered, plagioclase (An ₅₅₋₅₀)
47-2, 3 cm to bottom	1	4.5	0.0	4.5	Olivine-plagioclase	Sub-ophitic-intersertal (An ₅₅₋₅₀)	Fe-Ti-rich alteration: chlorite, calcite, zeolite

filled by later calcite. The boundary between geochemical Units 2 and 3 occurs within this group of flow units, but is not from phenocryst assemblages. This boundary is principally defined by trace elements, and is not readily apparent in the major elements.

350 to 354 meters: this interval has only one flow unit. The rock is similar to the overlying unit, except that plagioclase microcumulates up to 2 cm in diameter (Figure 23) are present.

354 to 368 meters: three or possibly five flow units of sparsely phyric to aphyric basalt with rare plagioclase phenocrysts are present in this interval. Olivine microphenocrysts are altered. Plagioclase compositions are An₆₄₋₅₀, and two generations of clinopyroxenes lie in a sub-ophitic groundmass. The second generation is pleochroic from pale brown to violet, suggesting iron-titanium enrichment.

368 to 388 meters: four flows of phyric to sparsely phyric basalts occur in this interval. All contain plagioclase An₆₄₋₄₆ (1 to 5%), clinopyroxene (1 to 3%), and olivine (2 to 5%) microphenocrysts (0.1 to 0.6 mm), sometimes in glomeroporphyritic masses. Texture is variolitic to glassy toward the flow margins. Smectite and chlorite replace glass and olivine; vesicles and fissures are filled by chlorite.

388 to 404 meters: three flows of nearly aphyric olivine basalt are present in this interval. Rare grains of olivine, plagioclase (An₆₂), and clinopyroxene coexist in a predominantly glassy groundmass. Olivine and glass are altered to smectite; some of the larger plagioclase phenocrysts show zonation and inclusions of crystallized basaltic magma (Figure 24), and may not have been in equilibrium with the liquid.

Lower Lava Sequence

Between 404 and about 428 meters, drilling rates increased. A minor amount of sediment was recovered from this interval, but the entire interval was probably soft sediment. Below here, good recovery was obtained from a series of what are probably pillow lavas. These correspond to geochemical Unit 4, which is a variable unit of basic character.

428 to 431 meters: one flow of olivine (5%) and plagioclase (5%) porphyritic basalt was penetrated. Phenocrysts reach 1 mm diameter, and occur as microcumulative assemblages (1 cm diameter). Olivine is also abundant in the sub-ophitic groundmass.

431 to 437 meters: olivine phyric (7 to 14%) pillow basalt with an intersertal groundmass occurs in this interval.

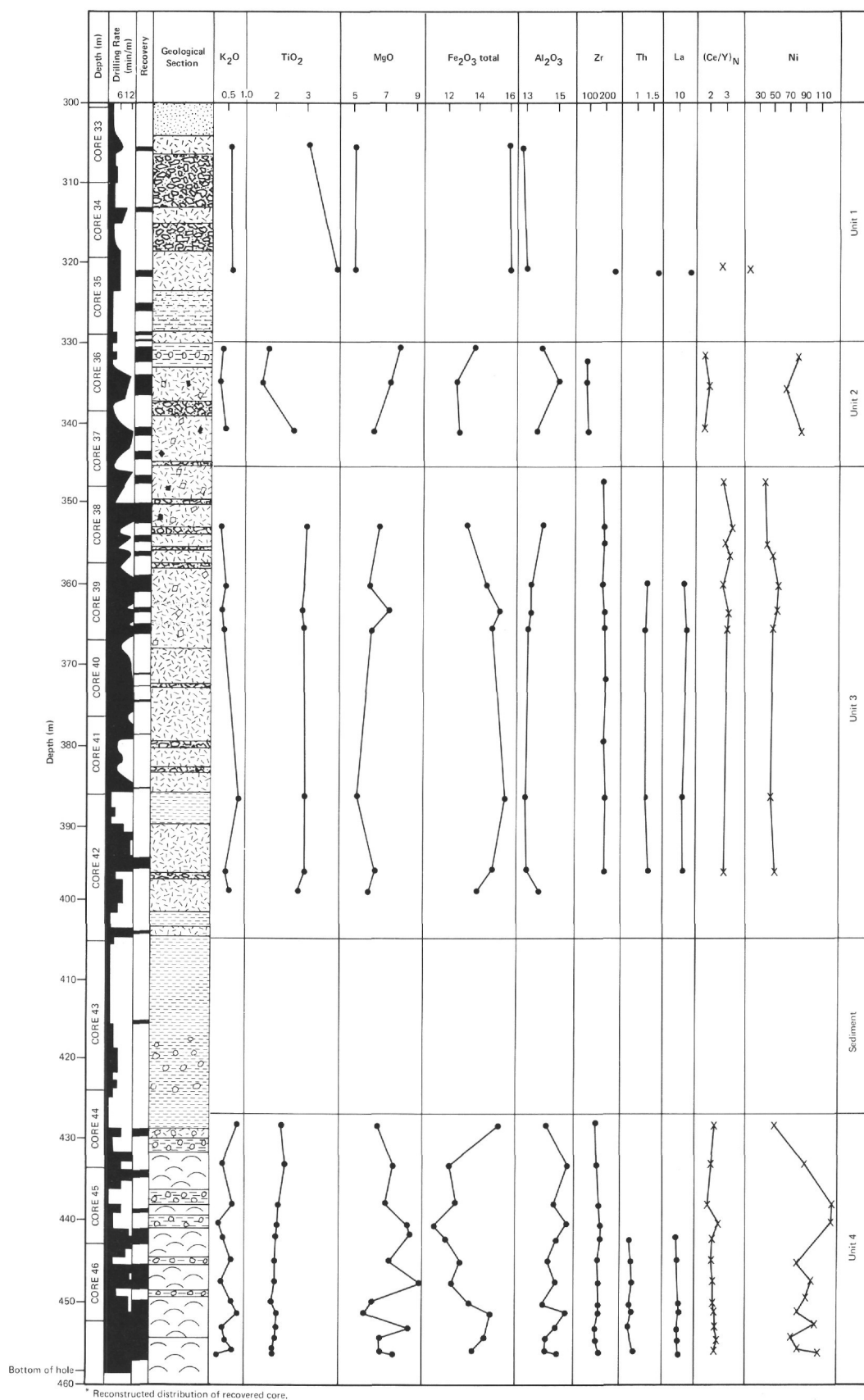


Figure 17. Chemistry of basement rocks, Hole 407.

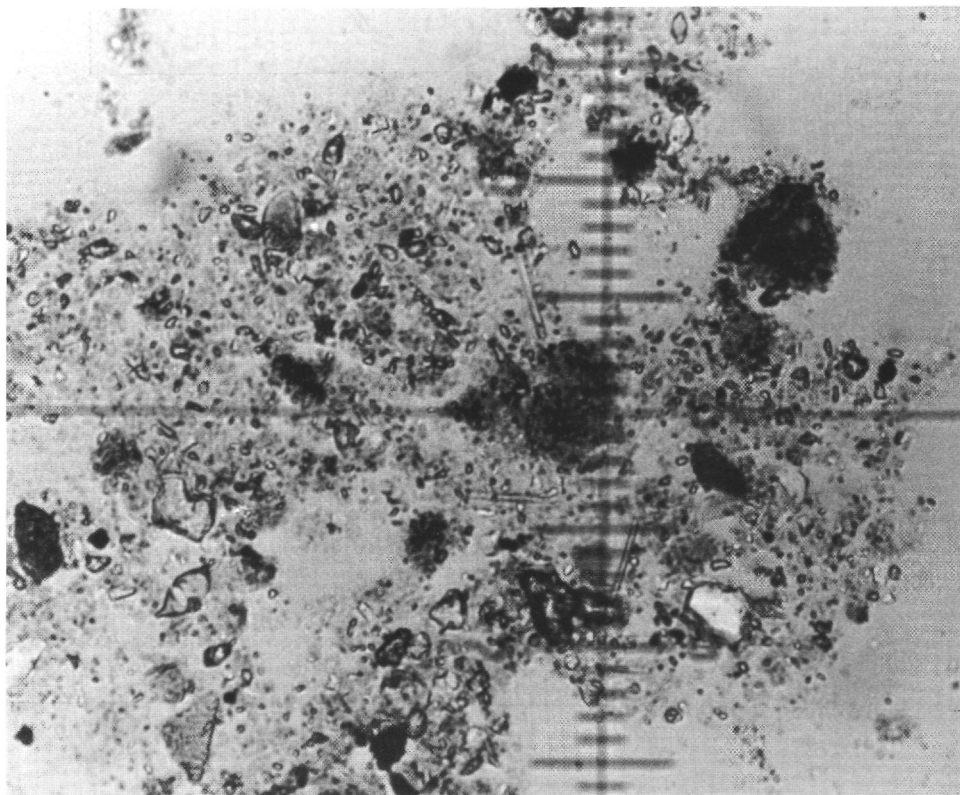


Figure 18. *Basaltic glass fragments in nannofossil ooze. Fresh basaltic glass is darker and has ill-defined contours (X10).*

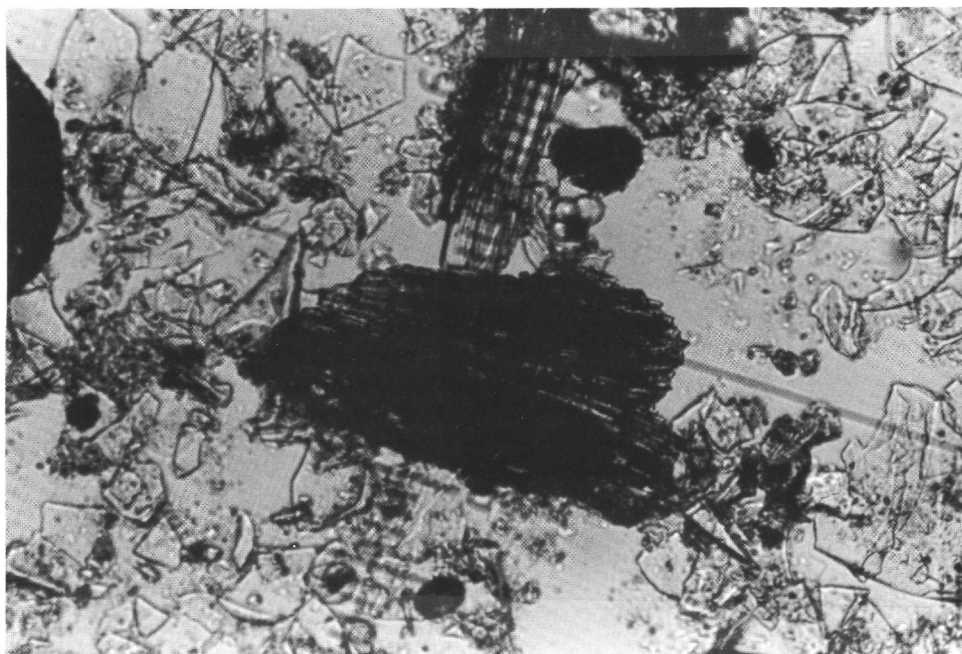


Figure 19. *Colorless shards of rhyolitic glass associated with pale brown shards of basaltic glass having elongated cavities (fibrous glass lapilli) (X10), 86-90-meter layer.*



Figure 20. Volcanic breccia with round and angular fragments (Sample 32-1, 40-55 cm).

The rock is highly altered; serpentine has replaced the olivine, and chlorite and calcite fill vesicles.

437 to 448 meters: three units of olivine and plagioclase phyric pillow basalts are present in this interval. Plagioclase grains are An₇₆₋₆₂, and zoned normally. An intersertal groundmass texture contains palagonitized glass. Relatively fresh glassy fragments are preserved in pillow margins. Concentric spalling of glassy margins has resulted in alternating bands of glass and calcite fillings (Figure 25).

448 to 454 meters: one thick flow of phyric basalt yielded almost continuous recovery in this interval. The rock is coarse grained with sub-ophitic texture and olivine phenocrysts. The groundmass contains plagioclase An₅₅₋₅₀ and two generations of pyroxenes. Olivine is oxidized and replaced by chlorite and calcite.

454 to 458 meters: Hole 407 ends in a pillowed sequence of aphyric basalt with a sub-ophitic to intersertal texture. Olivine and plagioclase grains occur in glassy margins. Two generations of pyroxenes are present in the groundmass, and are associated with plagioclase (An₅₅₋₅₀) in a sub-ophitic texture. Chlorite has replaced glass and olivine, and zeolite and younger calcite line fissures (vertical joints, pipe vesicles, and horizontal veins) (Figure 26).

Discussion

Although the nature of the lava encountered in Hole 407 appears fairly constant at first sight, a detailed petrographic study allows various magnetic units to be distinguished. Olivine is a constant phenocryst (or microphenocryst) phase, and is frequently associated with plagioclase. The most primitive-looking basalts are plagioclase and olivine, slightly phyric (332 to 354 m, 428 to 431 m, 437 to 448 m, 454 to 458 m). Rocks that contain relatively sodic plagioclase appear to be somewhat evolved (317 to 332 m), and can be called iron-rich andesine basalts.

In the lower lava sequence, clinopyroxene occurs only in the groundmass (437 to 454 m), whereas in the upper sequence, some clinopyroxene microphenocrysts are present (280 to 305 m). This suggests that the upper lava sequence is more alkalic. Note, however, that the clinopyroxene phenocrysts always occur in the most evolved lavas, and may therefore be related to fractionation processes rather than to characteristics of primary magma.

One of the bases for choosing the location of Hole 407 was that the greatest depth on the Iceland-Greenland Ridge might correspond with a time of reduced activity of the proposed Iceland plume (Vogt, 1972).

The geochemistry of the lavas from this hole shows, however, that they are more enriched in compatible elements than those from the other holes or those erupted now at this latitude on the Reykjanes Ridge. This observation is not consistent with the original proposal, and appears to contradict one of the bases on which the Iceland plume was proposed (Schilling, 1973).

ALTERATION PETROGRAPHY

Through all the basalts of Hole 407, the same assemblage of alteration minerals is present. This includes calcite, smectite, celadonite, pyrite, an unidentified zeolite,

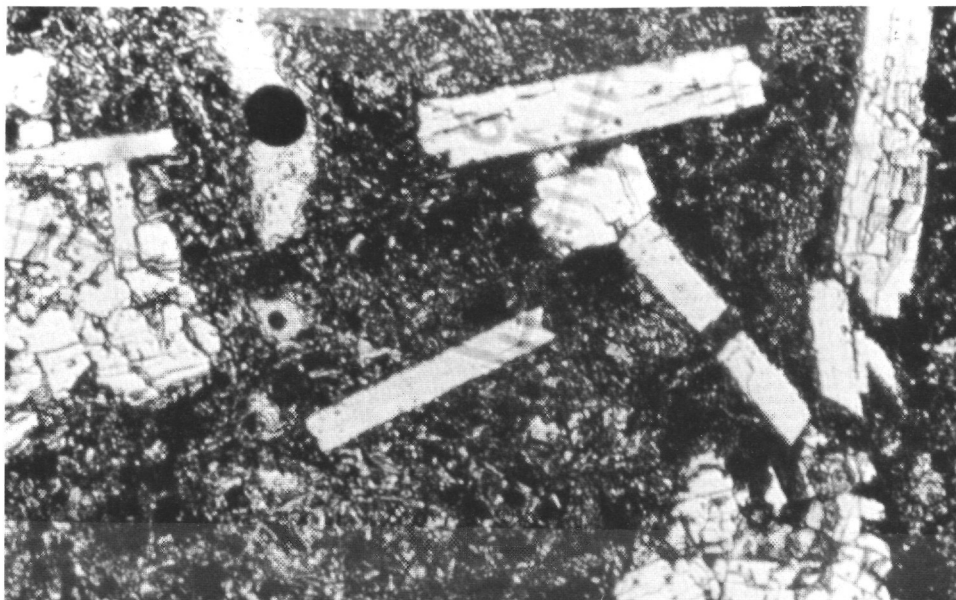


Figure 21. *Plagioclase and clinopyroxene phenocrysts in basaltic fragment of the volcaniclastic breccia (280 to 285 m) (X10).*



Figure 22. *Olivine and plagioclase porphyritic basalt with cryptocrystalline, rather glassy, groundmass (309 to 317 m) (X10).*

unidentified alteration products of titanomagnetite (leucoxene), and an orange iron oxide. There is no clear appearance of new minerals or disappearance of old ones down the hole. The intensity of alteration does generally increase downward, however, so that, in particular, the proportion of smectite forming in the basalt and the degree of alteration of titanomagnetite grains become greater at depths below 430 meters than higher up.

Not all the minerals can coexist, and one of the most striking features of the core is the alternation of orange to brown oxidized zones with dark gray reduced zones in the lower cores. In the oxidized zones, the orange iron oxide is present and the pyrite absent. The reverse is true for the reduced zones. The other minerals show no special bias toward one kind of zone or the other. The oxidized zones are apparently associated with the pillow lava fragments,



Figure 23. *Plagioclase phenocrysts in basalt with tendency to form microcumulate assemblage. One altered olivine phenocryst is evident (322 to 350 m) ($\times 10$).*

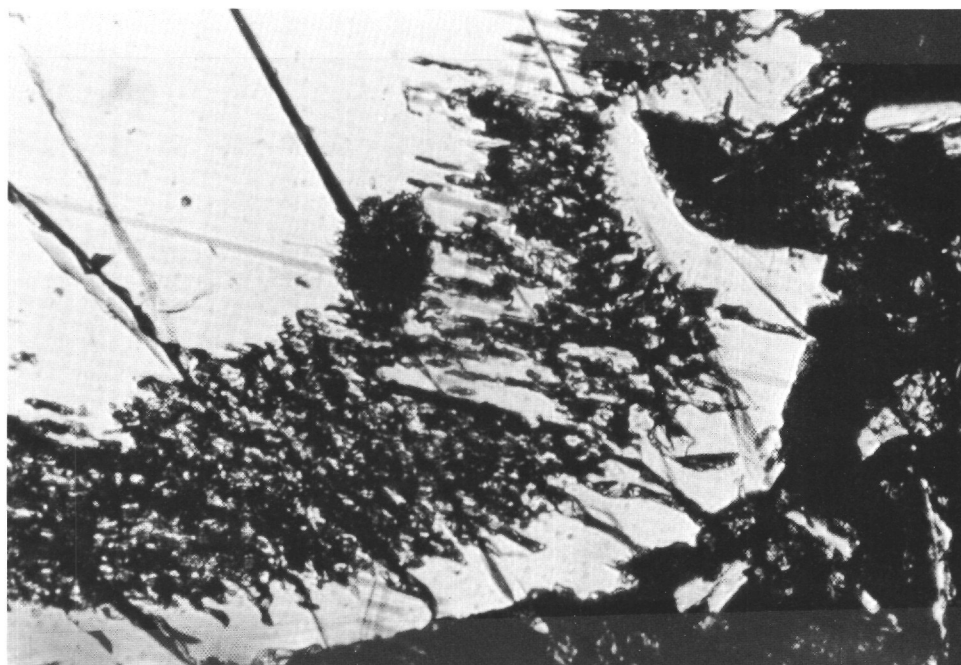


Figure 24. *Plagioclase phenocrysts showing signs of instability during crystallization. Numerous inclusions of basaltic glass are evident in outermost zone.*

and oxidized lengths of core have frequent chilled or glassy margins. The reduced zones, on the other hand, especially in the lower part of the core, are coarse-grained ophitic basalt in continuous lengths, and perhaps represent thicker flows or intrusions.

The different alteration minerals are strongly associated with particular alteration sites in the rocks. Thus, smectite is found replacing olivine and glass, and filling veins and vesicles; calcite occurs mostly as vein filling, though it sometimes replaces the cores of olivine crystals; zeolites are

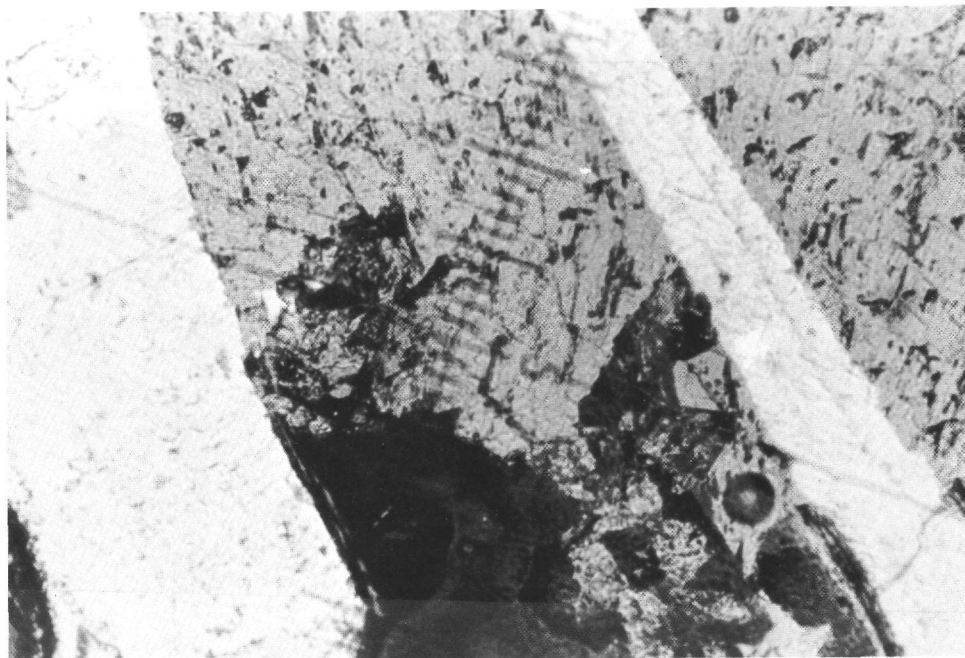


Figure 25. Spalling phenomena at pillow margin. Glassy, partly recrystallized skins are interlayered with calcite filling (white) (437 to 448 m) ($\times 10$).

present only as vein filling, usually in association with glassy zones of pillows or flow margins (Figure 27); pyrite fills veins and is also present as clusters of crystals in vesicles; and celadonite and iron oxide appear to be present only as vein fillings and coating to joints.

The minerals that resist alteration are as interesting as the newly formed minerals. Some fragments of fresh (or apparently fresh) basalt glass remain all the way to the bottom of the hole, as has been observed, too, in the deeper holes into the ocean crust drilled on Legs 37 and 45. This is despite the very extensive development of smectite and calcite in many of the rocks at this level. It is presumably attributable to the massive and unjointed nature of the fragments of glass, so that alteration must proceed in them by diffusion of ions through the atomic structure, rather than by transport of material along cracks and crystal boundaries, as must happen in originally crystalline rocks.

Equally remarkable is the preservation of plagioclase. Olivine survives only if totally immersed in glass: the almost complete lack of attack on plagioclase is surprising. There are some places where threads of smectite do occur in plagioclase, but it is always difficult to demonstrate a replacement relationship. Nowhere does there appear the extensive zeolitization of the plagioclase that might be expected from the associated minerals.

Pyrite occurs as two generations: as primary magmatic pyrite, in the form of minute circular blebs scattered through the rock, and as much larger, more euhedral, secondary crystals. Textural relationships indicate that this secondary pyrite may have been the last mineral of the secondary materials to crystallize (Figure 28).

Although it would be useful to attempt some estimate of temperatures involved in this alteration, not enough is yet known about the stability fields of the minerals that have

been identified here to make such an attempt reasonable. Certainly temperatures did not rise above 400°C, the approximate lower temperature of the greenschist facies, and they were probably at least 100°C below this, since the plagioclase has not been attacked. It is possible that the alteration was caused by cold seawater alone, percolating slowly into the volcanic pile. This is suggested by the general relationship observed between age of crust and degree of alteration on Leg 49.

BASEMENT PALEOMAGNETISM

Forty-one specimens of basalt and four of fossiliferous limy tuff were taken from depths of 319.5 to 458.5 meters (Cores 35 through 47) in Hole 407. Paleomagnetism measurements were made on 34 of these aboard *Glomar Challenger*, and on 11 in the shore laboratory, using similar apparatus. NRM intensities of the basalts were between 10^{-3} and 1.8×10^{-2} emu cm $^{-3}$, and of the tuffs around 8×10^{-5} emu cm $^{-3}$ (Figure 29 and Table 4).

Thirty-four specimens were subjected to progressive alternating-field (AF) demagnetization; peak fields reached up to 700 Oe (70 mT). Five were thermally demagnetized at temperatures increasing to 500°C in 50°C increments. Near neighbors in the core of two of these specimens were demagnetized by the AF method to compare the two sets of demagnetization characteristics. The stable inclination is taken as the result of that demagnetization step which produces little further directional change and leaves more than about 20 per cent of the initial intensity. Each stable inclination may leave an associated uncertainty of $\pm 2^\circ$.

Polished thin sections corresponding to 27 of the basalts were examined in reflected light up to a magnification of $\times 400$, on the ship.

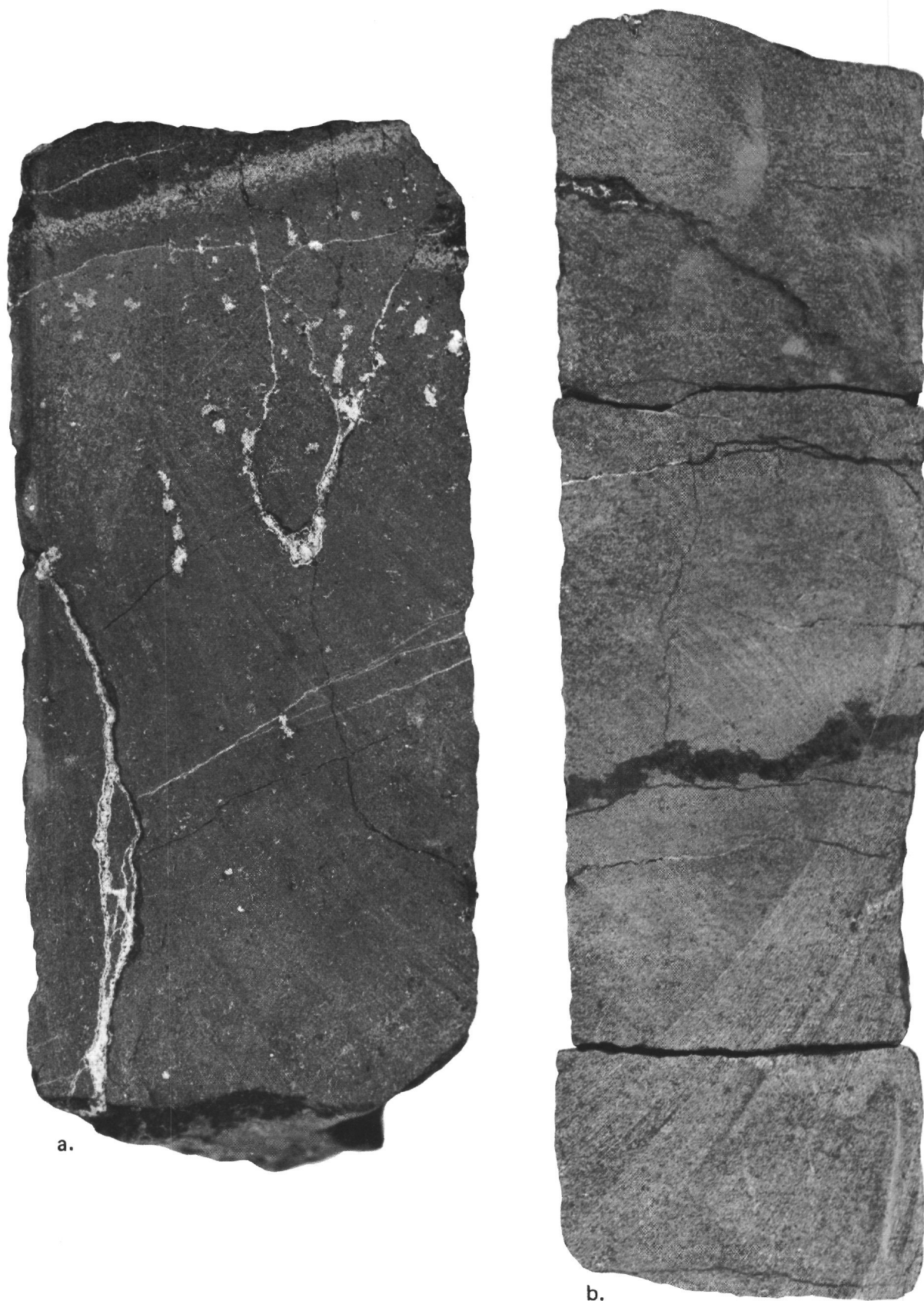


Figure 26. Vertical joints and pipe vesicles (a) and horizontal veinlets (b) filled with chlorite and calcite. Sample A is a pillow margin (46-2, 120-125 cm). Sample B is a flow interior (45-2, 95-105 cm).

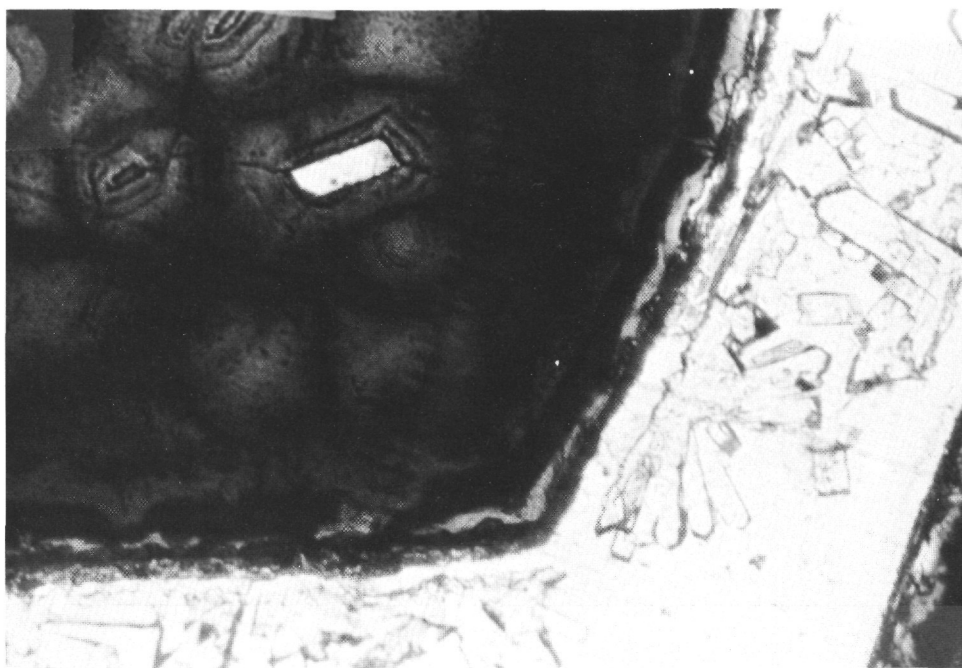


Figure 27. *Vein filling of zeolite and calcite on glassy pillow margin. The basalt is slightly plagioclase porphyritic (454 to 458 m) ($\times 10$).*

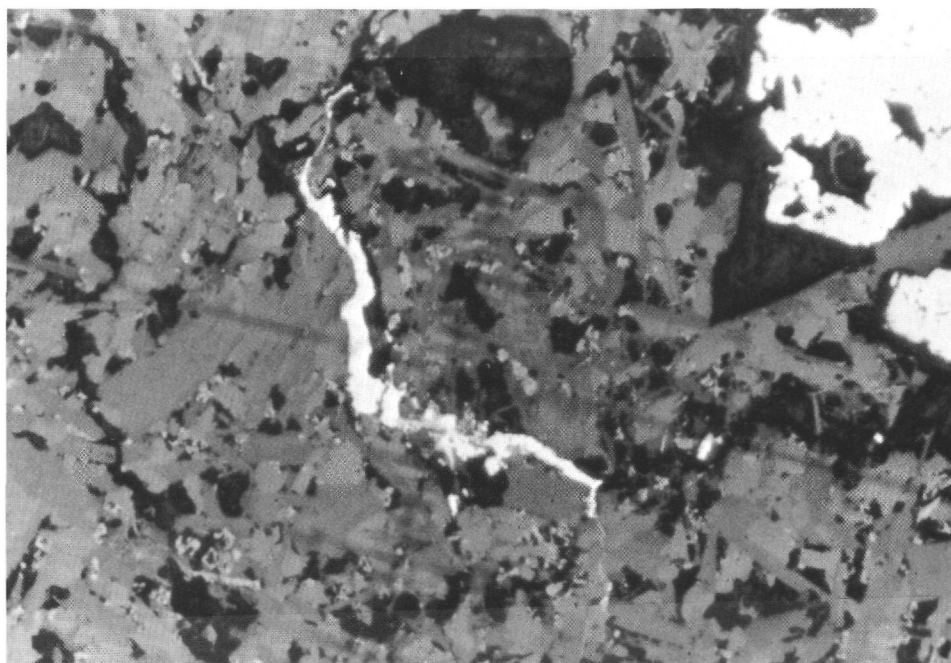


Figure 28. *Late pyrite filling cracks and cavities (reflected light, $\times 10$).*

Stable inclinations are summarized in Figures 29 and 30 and Table 4. The nine uppermost basalt specimens are normally magnetized, with mean stable inclinations $+ 67^\circ \pm 2.5^\circ$, and the stable inclinations of the tuffs in Cores 35 and 36 agree well with those of the interbedded basalts [the method of Briden and Ward [1966] was used to obtain the mean inclination in all cases where data are grouped]. The

stability of these uppermost specimens to AF demagnetization is low, with median destructive fields (MDFs) around 50 Oe (see later discussion). All the specimens from below 340 meters have stable reversed remanence. A reversal therefore occurs between specimens 37-1 and 37-2. These come from lithologically distinct pieces which could well belong to different flows; 37-1 is

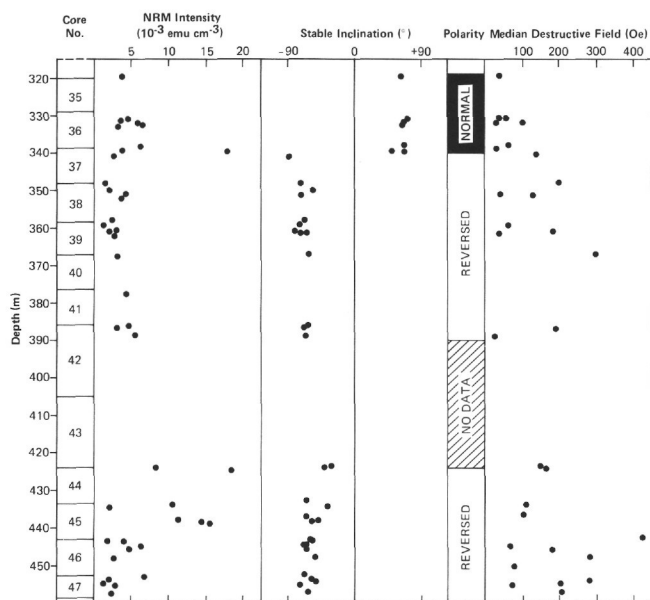


Figure 29. Downhole plot of paleomagnetism results, Hole 407.

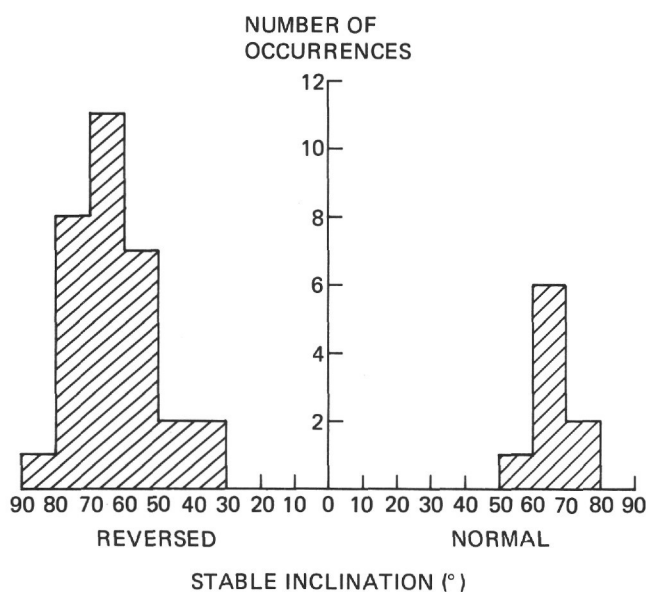


Figure 30. Distribution of stable inclinations, Hole 407.

coarse grained, 37-2 fine grained. The stable inclinations of the reversed specimens below the normal ones but above the sampling gap are grouped around $-72^\circ \pm 2^\circ$. Those of the reversed specimens below the sampling gap (424 to 458 m) are shallower, $-62^\circ \pm 4^\circ$. (The axial dipole field inclination for this site is 76.3° .) The three distinct groups of stable inclinations suggest three magnetic units or volcanic episodes.

Toward the bottom of the hole (below 444 m), some very brown, more oxidized basalts occur, interspersed with zones of dark basalt. Intensities and inclinations of the oxidized basalts do not differ appreciably, however, from those of the overlying and interspersed dark ones. The oxidized specimens sometimes show a slight difference in

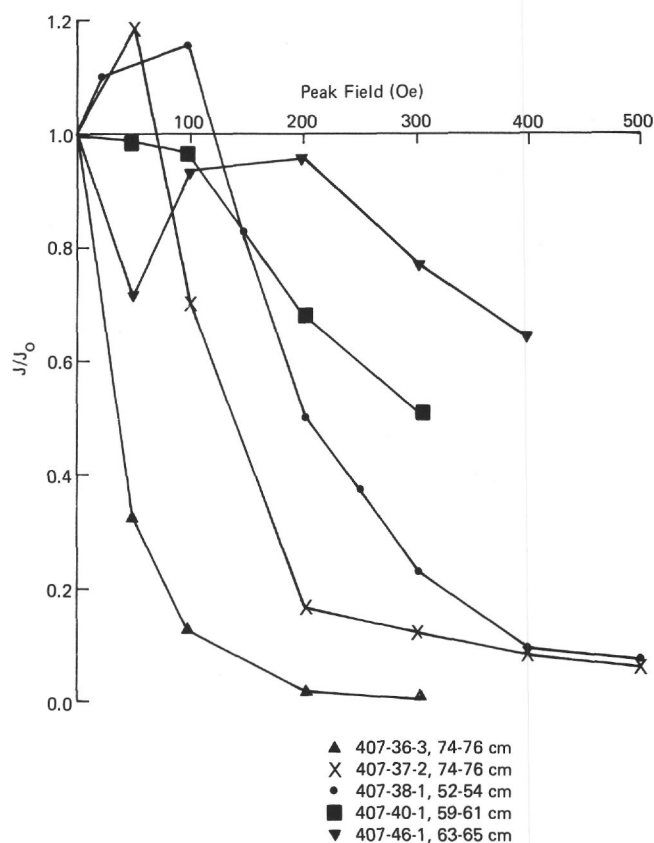


Figure 31. Examples of intensity changes upon AF demagnetization, Hole 407.

AF demagnetization behavior, with an initial drop in intensity up to 50 Oe, followed by a rise to 0.9 of the NRM value and then further decay, as in, for example, specimen 46-1 (Figure 31). Such behavior may indicate a two-component magnetization. In thin section the oxidized basalts show very corroded titanomagnetite.

Table 6 gives the results of preliminary observations on the polished thin sections. Since there is no apparent correlation between the proportion of primary magnetic minerals remaining and the NRM intensity, the magnetization may arise mainly from the contribution of grains much smaller than 0.01 mm, which could not be observed at the maximum magnification of $\times 400$.

AF Demagnetization

Figures 31 and 32 show examples of response to AF demagnetization. As mentioned earlier, the normally magnetized specimens (making up magnetic Unit 1) are characterized by very low MDFs, and after subjection to a peak field of 300 Oe their remanence intensity is only a few per cent of its original value. Five of the reversed specimens (38-3; 39-2; 39-3, 140-142 cm; 42-1, 77-79 cm; 42-2) had apparently normal NRMs which changed sign very early (50 Oe); these are all above the sampling gap, and are interspersed with other specimens having reversed NRM but otherwise similar demagnetization characteristics. This group (magnetic Unit 2) has widely ranging MDFs (average value 150 Oe), and stability is typically reached by 300 Oe, after early steepening of the inclination with little change in the relative declination. Similar behavior on AF

TABLE 6
Opaque Petrography, Hole 407

Specimen (Interval in cm)	Approx. % of Primary Phase of Magnetic Minerals Remaining	Approx. Grain size (mm)	Comments	
35-1, 38-40	50	0.1	Normal polarity	Magnetic Unit 1
36-2, 75-77	65	0.1		
36-3, 60-61	65	0.1		
37-1, 89-91	100	0.03		

37-2, 74-76	50	0.1	Reversed interval above sampling gap	Magnetic Unit 2
38-1, 53-55	100	0.03		
38-3, 88-90	100	0.1-0.01		
39-1, 55-57	100	0.03-0.01		
39-2, 44-48	65	0.1		
39-3, 47-51	100	0.1-0.01		
40-1, 59-62	100	0.01		
42-1, 87-89	100	0.02		
42-2, 141-143	100	0.03	-----	
44-1, 17-19	100	0.03	Reversed interval below sampling gap	Magnetic Unit 3
45-1, 69-71	50	0.1		
45-2, 40-42	25	0.1		
45-3, 122-124	50	0.1		
45-4, 53-55	25	0.1		
46-1, 63-65	50	0.1		
46-2, 59-61	50	0.1		
46-3, 66-68	No oxide visible			
46-4, 68-72	70	0.01		
47-1, 44-46	50	0.03		
47-2, 10-12	25	0.1		
47-2, 86-88	50	0.1		
47-3, 24-26	50	0.1		
47-4, 44-46	100	0.01		

demagnetization has been noticed in earlier DSDP work. A steep positive component induced by drilling and/or a low-stability viscous remanence caused by the present earth's field may have been removed. The behavior of the intensities would support this: 20 out of 30 reversed specimens show an increase in intensity above the initial value after low-field demagnetization. The normally magnetized specimens also suggest the removal of a steep normal component by their tendency to move to shallower inclinations upon demagnetization.

The specimens from the lowest basalts sampled (magnetic Unit 3) show much smaller changes of direction upon AF demagnetization than do those from magnetic Unit 2. The MDFs of magnetic Unit 3 are between 80 and 310 Oe, and average 175 Oe.

Thermal Demagnetization

Reversed specimens 38-2, 39-1, 39-3 (48-50 cm), and 42-1 (77-79 cm) were thermally demagnetized in increments of 50°C (Figure 33). Three types of behavior are apparent. Specimens 38-2 and 39-1 have thermal stability similar to the TRM of titanomagnetite, with a blocking temperature of approximately 450°C. Specimen 42-1 has the same blocking temperature, but apparently contains a

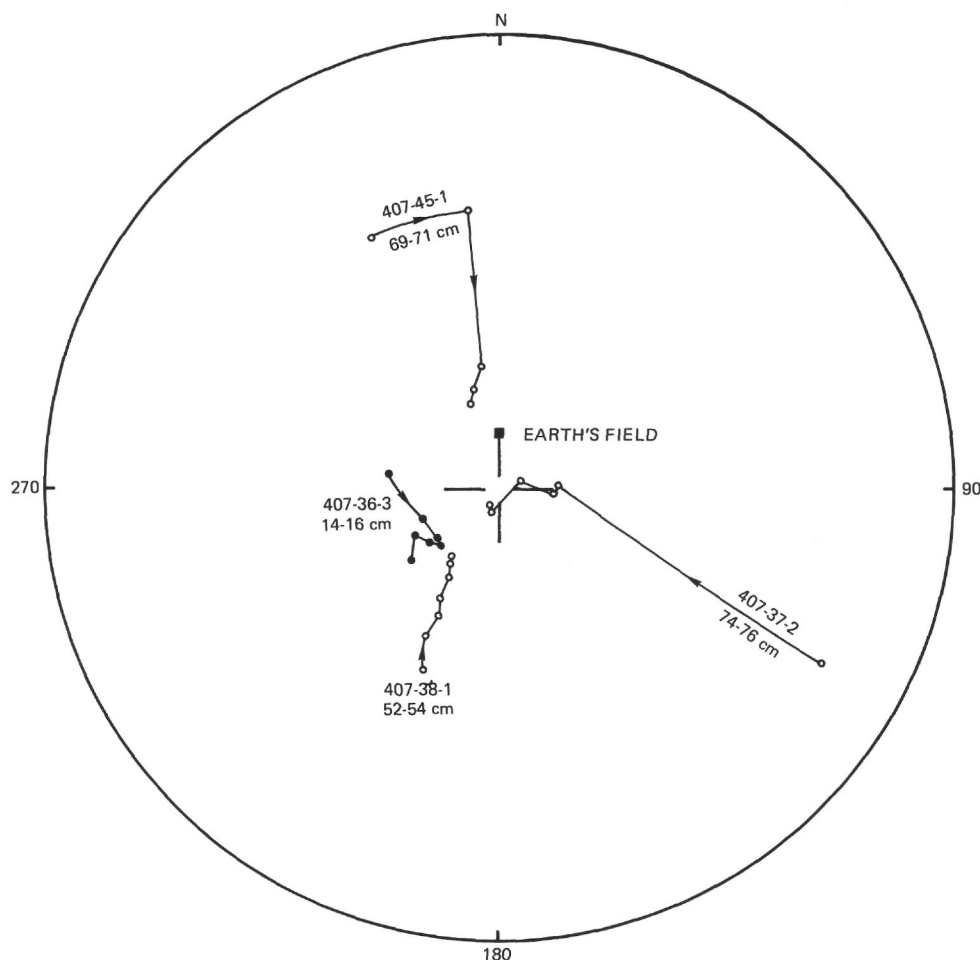


Figure 32. Stereographic (equal-angle) projection, showing examples of changes of paleomagnetic direction upon AF demagnetization, Hole 407. Solid circles denote lower hemisphere, open circles are upper hemisphere, squares represent the axial dipole inclination.

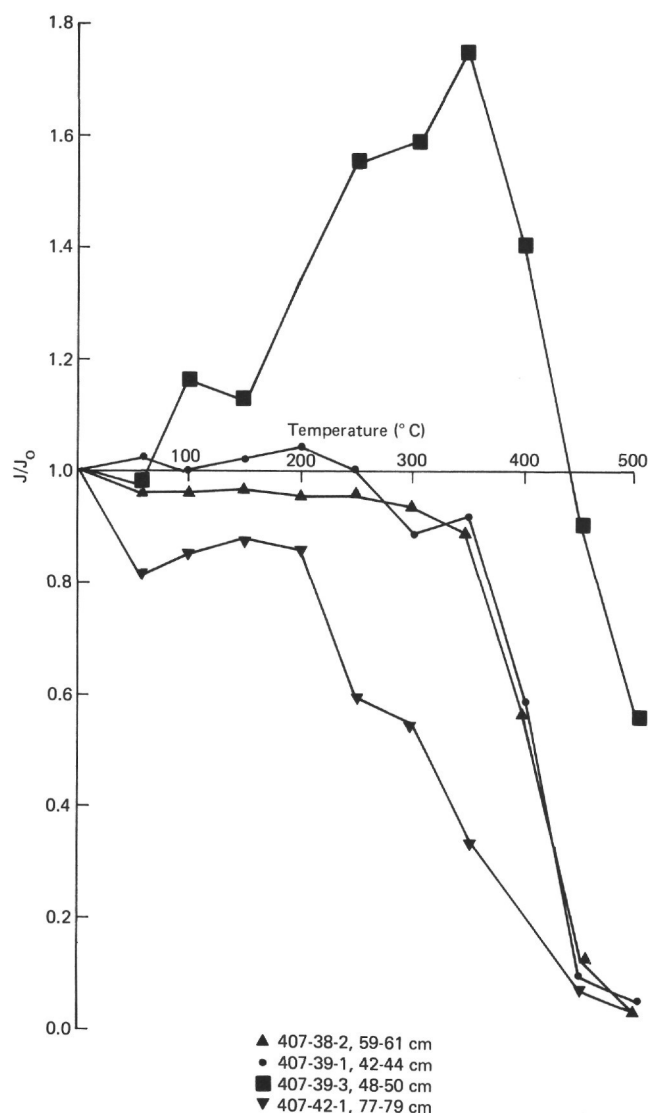


Figure 33. Examples of intensity changes upon thermal demagnetization, Hole 407.

less stable component of reversed NRM, which was demagnetized below 200°C. The Curie temperatures of the ferromagnetic minerals would be expected to be just above their blocking temperatures. Specimen 39-3 has a very anomalous demagnetization curve; its intensity gradually increased upon heating, and reached a peak after 350°C. Shore-based thermomagnetic measurement and X-ray analysis may provide more information on the causes of these different thermal modes.

The associated directional changes (Figure 34) are very small even at high temperatures, except for specimen 42-1, which changes appreciably below 100°C, implying an unstable component. AF demagnetization produced a very similar change for a specimen a few centimeters away. From 200°C to 350°C each specimen remains very constant in direction, with all four inclinations close to 60°. This is slightly shallower than the inclinations of AF demagnetized specimens (comparing 38-2 with 38-1, 39-1 with 39-2, and 39-3 with another 39-3 [Figure 35]) and shallower than the

axial dipole inclination of 76.3°. However, on heating to 400°C and above, the inclinations steepen consistently to between 70° and 75°, in agreement with the AF results. This may indicate two components of magnetization, one perhaps formed by later oxidation.

None of these thermal demagnetization results indicates self-reversal. This is particularly unlikely for specimens 38-2 and 39-1. The graphs of Figure 34 suggest more than one magnetic phase. The slight increase of intensity after heating to 150°C for specimen 42-1, and 350°C for 39-1, may be a result of inversion of either titanomagnetite or pyrrhotite to magnetite with higher magnetization. This thermal experiment shows, however, that the existence of these minerals does not substantially change the direction and polarity of the remanent magnetization. The direction of the stable remanence can therefore be taken as a reliable indicator of the geomagnetic field at the time these rocks were formed.

Summary

The most significant findings (Table 7) from these paleomagnetism studies are (1) inclinations which match or are shallower than the axial geocentric dipole inclination and (2) almost entirely reversed polarity under normal anomaly 13 (35 to 36 m.y.). Because of the present magnetic field direction, anomaly peaks in this area are skewed toward the southeast of the center of the magnetized bodies that generate the anomaly. We took great care to position the site on the northwest flank of the anomaly, so that the hole would be drilled in the center of the body. The 130 meters sampled from Layer 2 are largely reversed with approximately the correct inclination (there is no evidence for tilting or other tectonic disturbance). A similar situation on a larger scale was encountered on Leg 45 (Hole 395A). The uppermost third of the basalt recovered from 576 meters of basement below a normal anomaly was normally magnetized, and the remaining two-thirds was reversed. According to LaBrecque et al. (1977), the anomaly 13 normal polarity interval is divided by a reversed interval (35.26-35.45 = N, 35.45-35.52 = R, 35.52-35.86 = N); evidently we have drilled into this body. The occurrence of normal crust overlying reversed crust is explained by onlap of the younger normally magnetized rocks (Kidd, 1977; see model in Luyendyk et al., this volume).

The NRM intensities of the basalts from Hole 407 are comparable to, or slightly higher than, those from other DSDP basement holes. The arithmetic mean of the intensities of all the 41 specimens is 5.2×10^{-3} emu cm⁻³.

PHYSICAL PROPERTIES OF BASEMENT ROCKS

About two dozen sonic velocity and GRAPE measurements were made on samples of basement rocks; results are plotted in Figures 36 and 37, respectively. Note that the basement sonic velocity measurements are also plotted with sediment velocities in Figure 8.

The GRAPE densities and sonic velocities show a curious negative gradient with depth away from the basalt/sediment interface; both sonic velocity and apparent density peak near that interface. This is possibly a consequence of alteration of the basalts, with concurrent cementation and void filling,

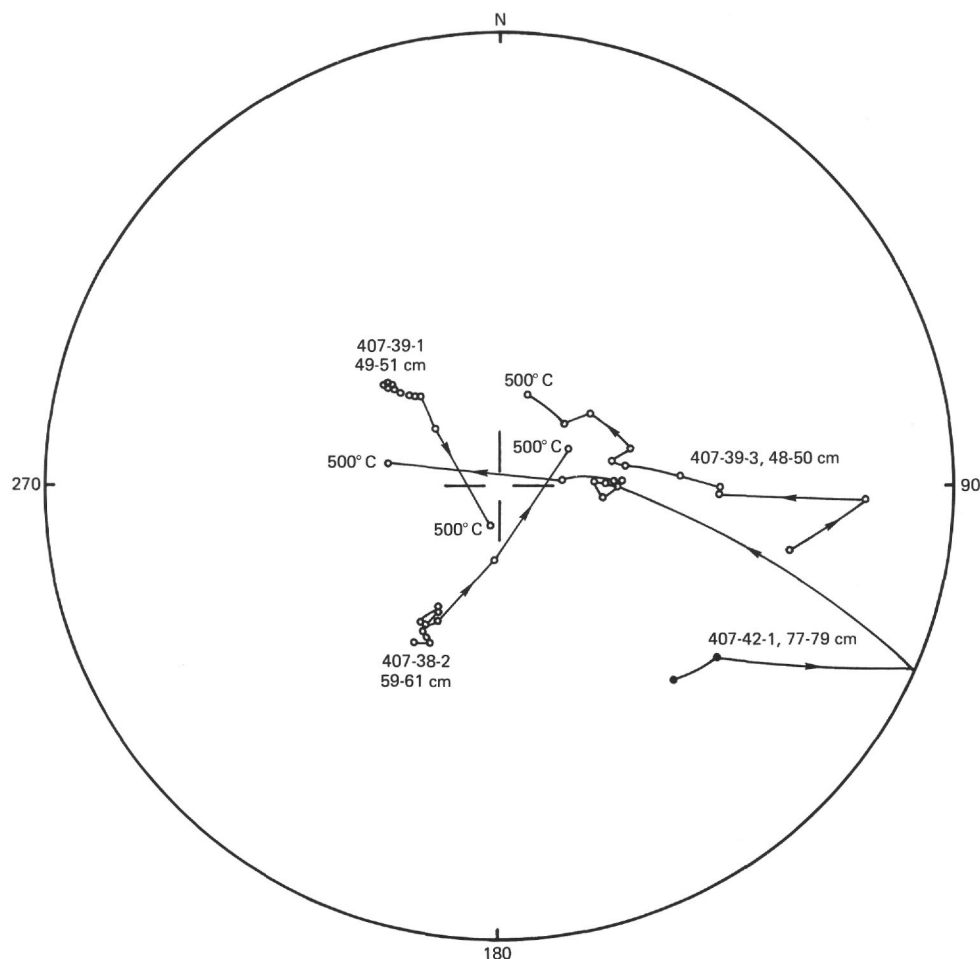


Figure 34. Stereographic (equal-angle) projection, showing directional changes upon thermal demagnetization, Hole 407. Solid circles denote lower hemisphere, open circles upper hemisphere.

or of two distinct flow units, above and below Core 43, representing different episodes of eruption of lavas with different densities and sonic velocities.

The GRAPE apparent density, despite its inherent scatter, generally parallels the sonic velocity values; this also suggests that the higher velocities may reflect lower porosities near the top of the basement layer.

CORRELATION OF SEISMIC REFLECTION MEASUREMENTS WITH DRILLING RESULTS

Underway reflection profiles obtained while approaching and leaving the site, and *Meteor-42B* site survey profiles, show a simple layering of semi-transparent sediment, about 200 to 300 ms (DT) thick, overlying acoustic basement. Over the beacon, the transparent section is 390 ms (DT) thick. On site, we deployed a SSQ 41 sonobuoy and fired a 5-in.³ airgun as the buoy drifted away from the ship (Figure 38). This record showed two reflectors, one at 200 ms and another at 390 ms (DT) sub-bottom.

Four methods can be used to determine velocities to convert these times to sub-bottom depth with the information on hand. These are: assuming a sound velocity in the sediments; assuming a bottom water sound velocity

and sediment sound velocity gradient; using interval velocities calculated from the sonobuoy profile; and using laboratory-determined sound velocities. For the first method, commonly assumed velocities are 1.5 km/s and 2.0 km/s. These give sub-bottom depths of 150 meters, 292 meters and 200 meters, 390 meters. Talwani et al. (1971), in determining sediment thicknesses from sonobuoy results over the ridge, used the relation

$$H = V_0 (e^{\alpha t} - 1) / \alpha$$

(Houtz et al., 1968), where H is the sediment thickness, V_0 the sediment surface sound velocity (1500 assumed), α the gradient (1.0 s^{-1} assumed), and t the one-way time. The resulting values are 158 meters and 323 meters sub-bottom.

The interpretation of wide-angle reflection data obtained with sonobuoys follows the methods outlined by Le Pichon et al. (1968) and Houtz et al. (1968). First, the individual reflection times are picked as a function of x , distance. Then a plot is made of T^2 (reflection time squared) versus x^2 . For each individual reflector the plots will be straight lines with a slope of $1/V_{iAV}^2$, where V_{iAV} is the average velocity down to the interface separating layers i and $i + 1$. To determine

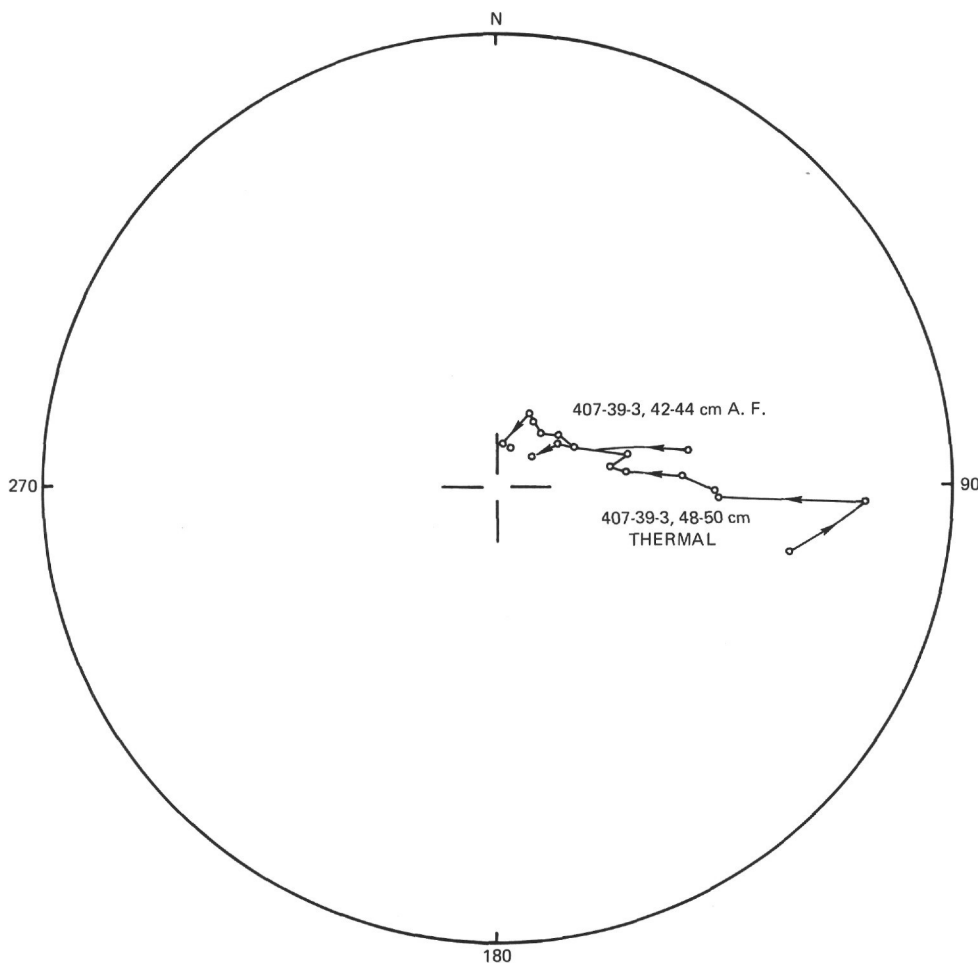


Figure 35. Comparison of directional changes upon AF and thermal demagnetization, using two specimens from Core 39, Section 3, Piece 4.

TABLE 7
Summary of Paleomagnetism Data, Hole 407

Unit	Thickness (m)	NRM Intensity (emu cm^{-3})	Stable Inclination ($^{\circ}$)	MDF (Oe)
1	20	6.0×10^{-3}	$+67 \pm 2.5$	50
Uppermost, normally magnetized	(320-340)			
2	48	3.0×10^{-3}	-72 ± 2	150
Reversed, above sampling gap and sediment section	(341-389)			
3	24	6.7×10^{-3}	-62 ± 4	175
Reversed, below sampling gap and sediment section	(424-458)			

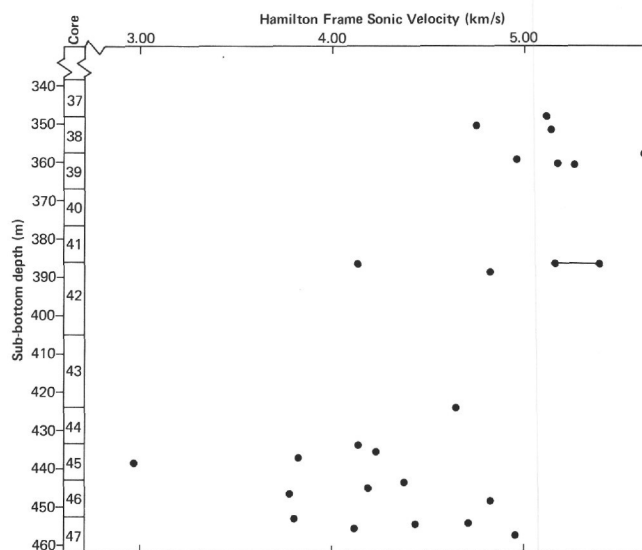


Figure 36. Sonic velocity versus depth.

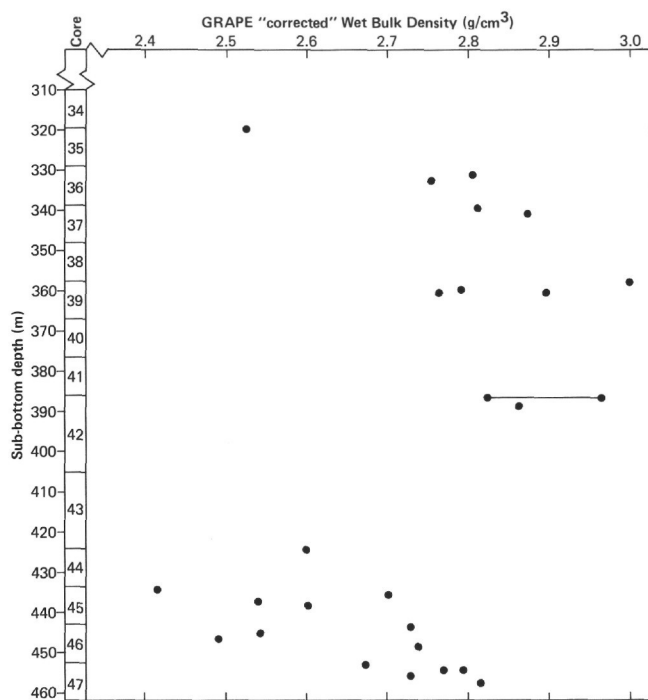


Figure 37. GRAPE "corrected" wet bulk density vs. depth.

the interval velocities, which are those average velocities between the $i-1$ and i interfaces, the following method is used. The average velocity down to the second interface (the intermediate reflector in this case) can be considered a weighted average

$$\frac{V_1 Z_1 + V_2 \Delta Z_2}{Z_2} = V_{2AV}$$

By rearranging terms and substitution,

$$V_2^2 = \frac{V_2^2 \Delta V T_2 - T_1^2 \Delta V T_1}{T_2 - T_1}$$

Similarly for deeper intervals:

$$V_3^2 = \frac{V_3^2 \Delta V T_3 - V_2^2 \Delta V T_2}{T_3 - T_2}$$

and so on. Figure 39 and Table 8 show the results of this analysis. The water sound velocity, V_1 , was determined from Matthews' tables checked against drill-string length.

Laboratory velocity measurements on the Hamilton Frame give an average V_p of 1.52 km/s (1.48 to 1.71) for the sediments above the first basalt. The depth of the intermediate reflector would then be 152 meters and the deeper acoustic basement 296 meters.

Two pieces of drilling information can be used to estimate the depth to reflecting horizons: lithologic contrasts and changes in drilling rate. Not all lithologic changes will produce reflections, but drilling rate changes may

presumably be related to acoustic impedance contrasts (allowing for changes in bit weight, pump pressure, etc.). Changes in drilling rate are correlated with recovered lithology to arrive at a detailed stratigraphy. Another factor to consider in recognizing reflectors is the thickness of the zone of acoustic impedance contrast. Generally, the zone should be $\frac{1}{4}$ of the acoustic wavelength, or in this case 2 meters thick. The situation in this hole is more complicated. Many thin lava flows are interlayered with sediments. The exact effect of this on the incoming acoustic signal would require detailed analysis. The most prominent reflection would probably return from somewhere deeper than the shallowest thin flow.

Possible reflecting horizons, selected from combined lithologic-drilling information, are shown in Figure 40 and Table 9. Prominent reflections are likely at 140 and/or 185 meters (Unit 3), and at the upper contacts of the upper and lower basalts. The reflection depths indicated by the various seismic analyses indicate fairly consistently that the first reflector is within the sediment sequence. Most likely it is a stiff clay unit first encountered in Cores 21 and 22 near 185 meters. On the other hand, the deeper reflection, acoustic basement, comes from either the upper or lower basalt units. From study of the drilling rates, it would be extremely unlikely that a significant reflection did not originate within the upper basalts. Results from the assumed gradient calculation appear most suitable. As for the sonobuoy calculation, it must be recalled that the reflection points for the ray paths are not exactly at the drill site, but were displayed up to a maximum of 700 to 800 meters.

HEAT FLOW

Three downhole sediment temperatures were measured at sub-bottom depths of 196, 243.5, and 281.5 meters. A self-contained temperature recorder was provided by R. von Herzen and A. Erickson (von Herzen et al., 1971), and the shipboard operation was conducted by K. Kobayashi. Method of measurement and analysis is the same as for preceding cruises.

An example of temperature records is shown in Figure 41; a sediment temperature of 16.2°C was obtained from this record. Temperatures of 11.2° and 21.5°C were obtained at sub-bottom depths of 243.5 and 281.5 meters, respectively. Immediately before and after the bottom penetration, the minimum temperature of about 3.7°C was recorded. As seawater is circulated in the drill string during lowering of the probe, it can be safely assumed that the probe records the average water temperature. In this portion of the North Atlantic, the minimum of recorded temperature is roughly equal to temperature at the bottom surface (zero sub-bottom depth).

Three *in-situ* sediment temperatures, recorded at sub-bottom depths of 0, 196, and 281.5 meters, are quite linear with sub-bottom depths. Temperature gradient obtained from this linear relationship is 6.36°C/100 meters. A temperature given at a sub-bottom depth of 243.5 meters is extraordinarily low, compared with the others. This value was not included in the following calculations, since slump sediment, caused by the preceding drilling or deficient penetration of the probe, may be suspected at this depth.

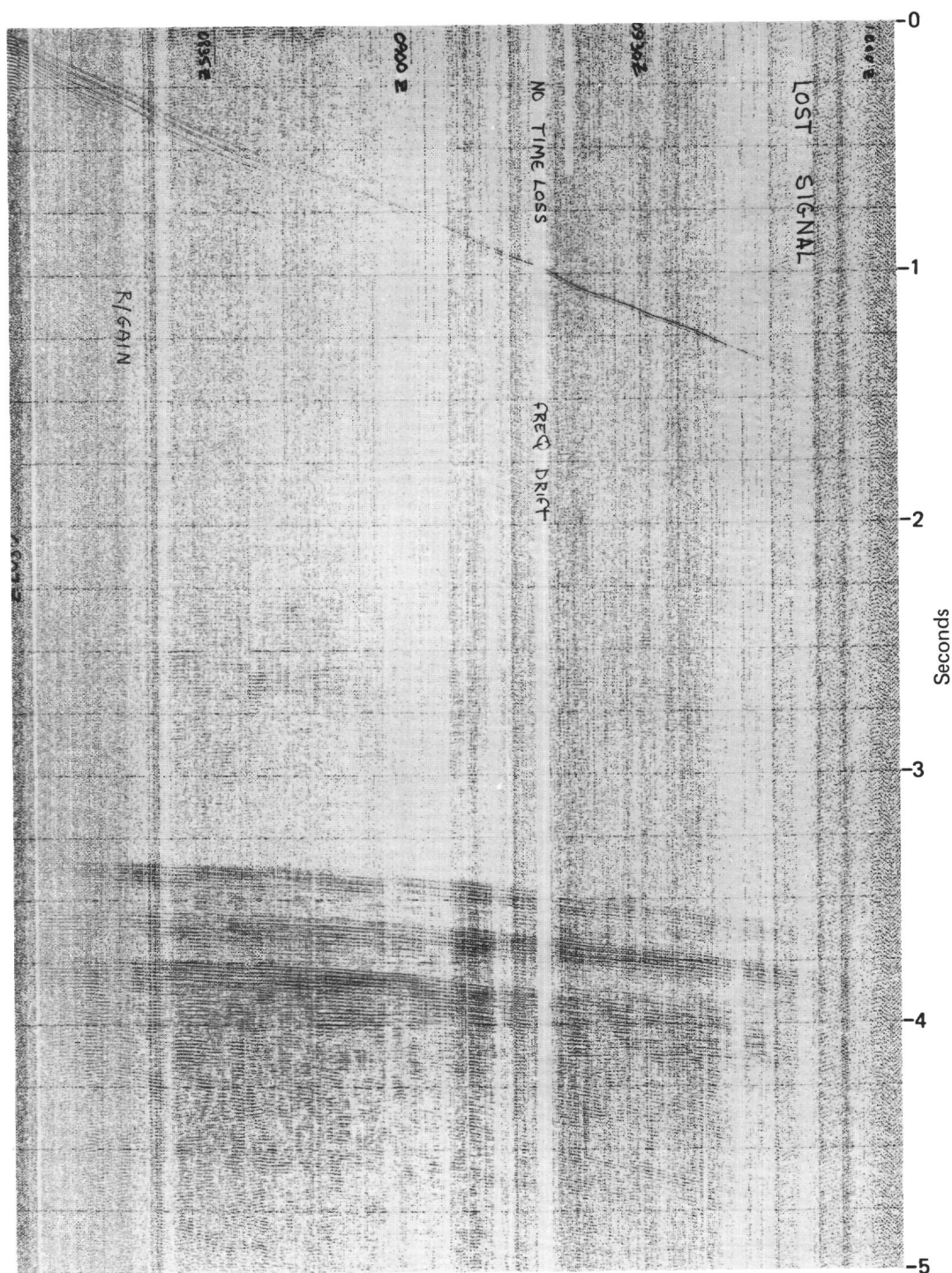


Figure 38. Sonobuoy profile run while on Site 407.

Thermal conductivity was measured on unsplit sections of cores, using a shipboard needle-probe apparatus. Seven analog measurements were made with cores taken from sub-bottom depths of 197.7, 199.5, 202.2, 253.9, 256.7, 291.0, and 291.4 meters. Values of thermal conductivity are mutually consistent among six measurements, and only one is abnormal (Table 10). The averaged value of thermal conductivity is 2.18 ± 0.10 mcal/cm s°C, excluding the abnormal one. Heat flow at Site 407 above the sediment of

281.5 meters sub-bottom depth is thus 1.39×10^{-6} cal/cm²s = 1.39 H.F.U.

SUMMARY AND CONCLUSIONS

On the basis of lithologic characteristics (Figures 7 and 14), four sedimentary units have been distinguished (depths are recovery depths not correlated with drilling logs). Three additional thin zones of interlayered sediment occur within the basalt.

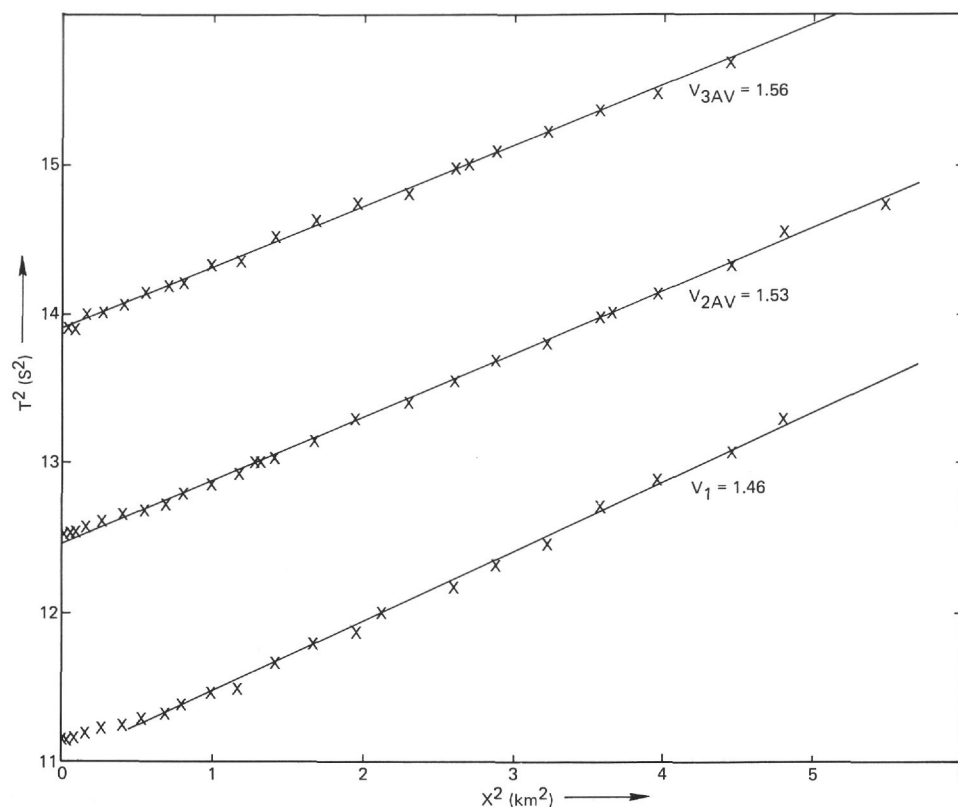
Figure 39. Plot ($x^2 - T^2$) of reflections recorded on sonobuoy 407-1.

TABLE 8
Average and Interval Velocities From Sonobuoy 407-1

Average V	Interval V	Depth (km)	Thickness
1.48 km/s	1.48	2.472	2.472
1.51 km/s	1.94	2.666	0.194
1.56 km/s	2.32	2.886	0.220 = 414 meters sub-bottom

TABLE 9
Sub-Bottom Depths to Reflecting Horizons (m)

	R ₁ (200 ms)	R ₂ (390 ms)
1. Assumed velocities 1.5 - 2.0	150-200	292-390
2. Assumed gradient 1.0 s ⁻¹	158	323
3. Sonobuoy 1.94, 2.32	194	414
4. Laboratory 1.52	152	296

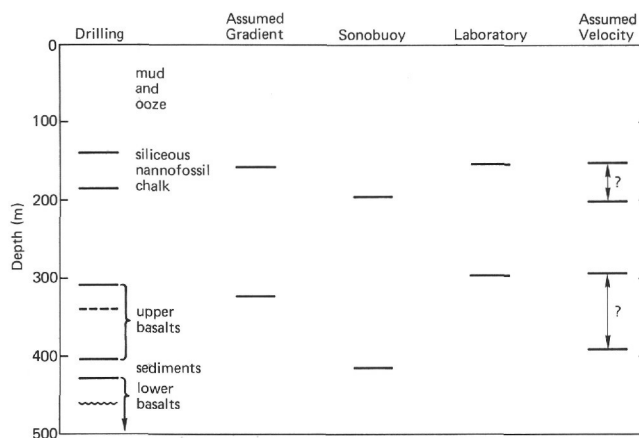


Figure 40. Reflection horizons from combined drilling-lithologic information, Hole 407.

Unit 1 (0 to 46.3 m): Pleistocene calcareous sandy mud with intervals of calcareous and marly calcareous ooze of variable volcanic ash content (up to 20%).

Unit 2 (46.3 to 160.7 m): Pliocene to upper Miocene nannofossil ooze (46.3 to 124.0 m) and nannofossil chalk (124.0 to 160.7 m).

Unit 3 (160.7 to 272.0 m): middle to lower Miocene siliceous nannofossil chalk with an interbedded chalk-volcanic ash zone between 215 and 224.5 meters.

Unit 4 (272.0 to 300.5 m): lower Miocene nannofossil chalk (272.0 to 280.0 m) and lower Miocene to upper Oligocene nannofossil chalk basalt pebble gravel.

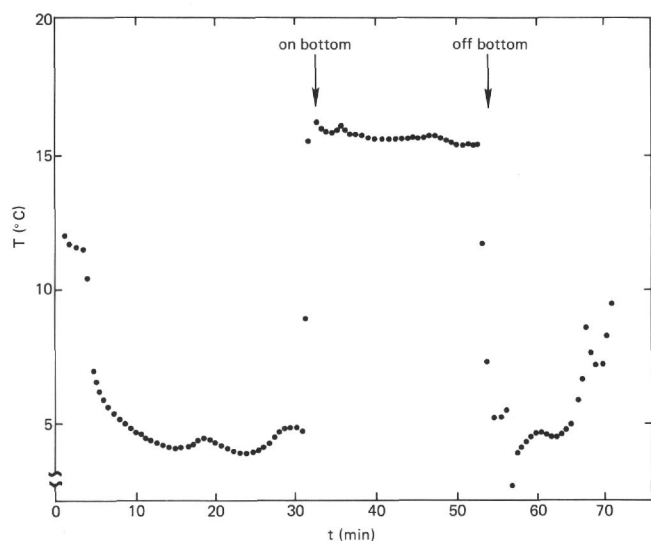


Figure 41. Temperature record at Hole 407, 196 meters below mudline.

TABLE 10
Thermal Conductivity of Sediments

Core	Section	Interval (cm)	(in mcal/cm s °C)	
			Uncorrected Conductivity	Corrected Conductivity
22	2	13	2.27	2.25
22	2	31	2.20	2.18
22	2	58	2.12	2.10
28	1	90	1.75	1.73
28	3	70	2.20	2.18
31	6	51	2.33	2.31
31	6	90	2.14	2.12
			2.21	2.18±0.10
average (Section 28-1 included)			(2.14)	(2.12)

Interlayered sediments: upper Oligocene foraminiferal nannofossil chalk (320.3 to 321.3 m), upper Oligocene nannofossil chalk (329.4 to 331.2 m) and "mid-" Oligocene sandy calcareous mud (405 to 405.4 m).

Sediments cored at Site 407 suggest major changes in bottom current activity between the Oligocene and Quaternary.

Low sediment accumulation rates and slight current laminations, highlighted by dark mineral placers (e.g., Cores 28 and 30), occur in the upper Oligocene through lower Miocene, which suggests slight or sluggish bottom current action. Unconformities in the middle to upper Miocene are attributed to erosion by bottom currents, whereas the high sediment accumulation rate calculated for the Pliocene indicates a change from an erosional to a depositional bottom current regime.

Immediately above the first basalt lava flows is a sediment composed of basalt clasts in a nannofossil chalk matrix. The shape of the clasts, often intricately cusped,

suggests a close local source, most probably nearby active volcanism. This is the most evolved lava erupted at this site.

The main interest in the igneous rocks at this site was to determine whether there was any evidence that the crust in this area showed a geochemical anomaly, relative to oceanic crust, similar to that found in dredged rocks at the crest of the Reykjanes Ridge along a mantle flow line from Site 407. Geochemical studies show that, on the average, this anomaly is even more pronounced at Site 407 than at the Reykjanes Ridge along the flow line on which Site 407 lies (see Wood et al., this volume). This poses the problem that the Icelandic mantle plume, if one exists, was apparently more developed about 38 m.y. ago than it is now.

At Site 407 there is evidence of off-axis volcanism. A layer of sediment 20 meters thick lies between two lava flows. Consideration of fossils in this and in sediment directly above the upper basalt sequence suggests that the upper and lower lava sequences occurred as much as 10 m.y., or as little as 1 m.y., apart.

Paleomagnetism suggests two breaks in volcanism. A magnetic polarity change 40 meters below the top of the upper lava sequence is one, and a change in inclination between the lower and the upper lavas, in about the same position as the sediment layer, is the other. The magnetic evidence does not indicate the duration of the volcanic episode or of the breaks. The magnetic anomaly pattern in the region indicates a basement age of 35 to 36 m.y., corresponding to lower Oligocene or upper Eocene.

Volcanological evidence bearing on the problem is of two kinds. The first is the angular basalt clast-nannofossil chalk sediment overlying the upper lava sequence. As indicated above, the intricate shape of the clasts very strongly suggests an origin by eruption of lava into a soft sediment as it formed, and thus that the enclosing sediment is of the same age as or older than the last eruption at this site. The second is the contrast between the upper lava sequence, composed of rather massive flows, and the lower lava sequence, composed mostly of pillows. This suggests some change in eruptive mechanism, and hence perhaps a break in volcanism at the time the sediment interlayer was deposited.

The foraminifers and nannofossils indicate a late Oligocene date for Core 32 (the basalt clast-nannofossil chalk sediment), and thus date the last eruption, if the volcanological evidence is believed. Both methods indicate that the sediment recovered from the sediment layer between the two lava sequences is lower to upper Oligocene. Sediments recovered from within the upper lava sequence are upper Oligocene (Cores 35 and 36). Therefore, the lower lavas were laid down in the early Oligocene and the upper lavas in the late Oligocene. This indicates a gap of several million-years in the continuity of volcanism and ranks as one of the most important finds at this site.

The question should be asked whether the lower lava sequence shows any evidence of petrographic anomaly, compared with normal mid-ocean ridge lavas. One criterion that has been suggested turns on the presence or absence of clinopyroxene phenocrysts in the lavas. The present-day lavas of Iceland and the upper parts of the Reykjanes Ridge

contain them, but in ocean-floor basalts they are rather rare. Some of the basalts in the lower lava sequence contain clinopyroxene phenocrysts, but these crystals are not common enough for us to be certain that in the Oligocene there was an eruptive anomaly, compared with normal ocean-floor basalt. Another possible indicator of anomalous lavas is vesicularity. Vesicularity of lavas at Site 407, however, is not unusual. Thus, it is not certain that the primary crust at Site 407 is anomalous relative to normal ocean floor.

The paleomagnetism measurements of the basalts show that the top 40 meters or so of basalt are normally magnetized, and below an apparently sharp transition, the rest are stably and reversely magnetized. Thermal demagnetization studies indicate that this reversed magnetization was not produced by self-reversal, and these lavas appear to have been erupted at a time when the earth's field was reversed (35.45 to 35.52 m.y.; LaBrecque et al., 1977). Within the reversed unit is a marked change in inclination, coinciding with the thick sediment band (404 to 428 m) between the upper and lower lava sequences.

Evidence was presented above that some or all of the upper lava sequence (depending on the final results of the paleontological dating) represents off-axis volcanism, occurring perhaps 10 m.y. later than the ridge volcanism. On this interpretation, the normally magnetized, and perhaps some of the reversely magnetized, lavas would have been produced off-axis during some later polarity episode, while the primary crust was entirely reversely magnetized. In view of the care with which the site was positioned on anomaly 13 so as to intersect the normally magnetized crust producing the anomaly, this interpretation causes problems. It could be that the hole by chance penetrated rock representing a short reversely magnetized period within a longer normally magnetized episode. Alternatively, because of the skewness expected of the anomalies at these latitudes, and the expected trapezoidal shape of the anomaly-producing body, caused by dip of lavas toward a spreading center, it is possible that the lavas sampled are the succeeding reversely magnetized lavas that have overlapped far enough over the anomaly-13-age normal lavas to be met in the drill hole. On this interpretation, the hole, if continued, would have soon

passed into normally magnetized lavas of that age. These possibilities are discussed by Luyendyk et al. (this volume).

REFERENCES

- Berggren, W.A., 1972a. Cenozoic biostratigraphy and paleobiogeography of the North Atlantic. In Laughton, A.S., Berggren, W.A., et al., *Initial Reports of the Deep Sea Drilling Project*, v. 12: Washington (U.S. Government Printing Office), p. 965-1001.
- , 1972b. A Cenozoic time scale — some implications for regional geology and paleobiogeography, *Lethaia*, v. 5, p. 195-215.
- Briden, J.C. and Ward, M.A., 1966. Analyses of magnetic inclinations in borecores, *Pure Applied Geophysics*, v. 63, p. 133.
- Houtz, R.E., Ewing, J.I., and Le Pichon, X., 1968. Velocity and deep-sea sediments from sonobuoy data, *J. Geophysical Res.*, v. 73, p. 261.
- Kidd, R.G.W., 1977. The nature and shape of the sources of marine magnetic anomalies, *Earth Planetary Sci. Lett.*, v. 33, p. 310.
- La Brecque, J.L., Kent, D.V., and Cande, S.C., 1977. Revised magnetic polarity time scale for Late Cretaceous and Cenozoic time, *Geology*, v. 5, p. 330.
- Laughton, A.S., Berggren, W.A., et al., 1972. *Initial Reports of the Deep Sea Drilling Project*, v. 12: Washington (U.S. Government Printing Office).
- Le Pichon, X., Ewing, J.I., and Houtz, R.E., 1968. Deep-sea sediment velocity determination made while reflection profiling, *J. Geophysical Res.*, v. 73, p. 2597.
- Sayles, F.L. and Manheim, F.T., 1975. Interstitial solutions and diagenesis in deeply buried marine sediments: results from the Deep Sea Drilling Project, *Geochim. Cosmochim. Acta*, v. 39, p. 103.
- Schilling, J.G., 1973. Iceland mantle plume: geochemical study of the Reykjanes Ridge, *Nature*, v. 242, p. 565.
- Talwani, M., Windisch, C.D., and Langseth, M.G., Jr., 1971. Reykjanes Ridge Crest: a detailed geophysical study, *J. Geophysical Res.*, v. 76, p. 473.
- Vogt, P.R., 1972. Evidence for global synchronism in mantle plume convection and possible significance for geology, *Nature*, v. 240, p. 338.
- von Herzen, R.P., Fiske, R.J., and Sutton, G., 1971. Geothermal measurements on Leg 8. In Tracey, J.I., Sutton, G.H., et al., *Initial Reports of the Deep Sea Drilling Project*, v. 8: Washington (U.S. Government Printing Office), p. 837-849.

SITE 407		HOLE		CORE 1		CORED INTERVAL: 0.0-6.0 m	
TIME-ROCK UNIT	BIOSTRAT ZONE	FOSSIL CHARACTER		SECTION	METERS	GRAPHIC LITHOLOGY	LITHOLOGIC DESCRIPTION
		FORAMS	NANNOS				
QUATERNARY	N22/N23 NN20						
					</		

Explanatory notes in Chapter 1

SITE 407		HOLE		CORE 2		CORED INTERVAL: 6.0-15.5 m		
TIME-ROCK UNIT	BIOSTRAT ZONE	FOSSIL CHARACTER		SECTION	METERS	GRAPHIC LITHOLOGY	DRILLING DISTURBANCE SEDIMENTARY LITHOLOGIC SAMPLE	LITHOLOGIC DESCRIPTION
		FORAMS	NANNOS					
QUATERNARY	N22 NN20							
				</				

[illegible]

Explanatory notes in Chapter 1

[illegible]

SITE 407		HOLE		CORE 5		CORED INTERVAL: 34.5-44.0 m	
TIME-ROCK UNIT	BIOSTRAT ZONE	FOSSIL CHARACTER			SECTION METERS	GRAPHIC LITHOLOGY	LITHOLOGIC DESCRIPTION
		FORAMS	NANNOS	RADS			
QUATERNARY	N22 NN19				1	0.5 1.0	olive gray (5Y 4/2) olive (5Y 5/3)
					2		Smear Slides 1-42 1-128 2-15 2-113 qtz. 2 2 7 2 fspr. 3 2 Tr 10 H. min. 2 2 1 5 clay 30 34 60 40 volc. glass 20 10 2 15 palagonite 10 20 zeolite 1 Tr carb. unsp. 10 5 3 forams 15 10 2 10 nannos 25 20 3 20 silic. micro. 1 Tr Carbonate Bomb 1-85 20% 2-35 23% 3-10 21%
					3		olive gray (5Y 4/2)
		Ag	Cg		CC	VOID	

SITE 407		HOLE		CORE 6		CORED INTERVAL: 44.0-53.5 m	
TIME-ROCK UNIT	BIOSTRAT ZONE	FOSSIL CHARACTER			SECTION METERS	GRAPHIC LITHOLOGY	LITHOLOGIC DESCRIPTION
		FORAMS	NANNOS	RADS			
PLIOCENE	N21-2 NN18				1	0.5 1.0	olive gray (5Y 4/2) olive gray (5Y 4/2) and gray (5Y 5/1) light yellowish brown (10YR 6/4)
					2		very pale brown (10YR 7/3) brown (10YR 5/3) light olive gray (5Y 6/2) light yellowish brown (10YR 6/4) white (10YR 8/1) with mottles of above
		Ag	Ag		3		Carbonate Bomb 1-50 15% 2-57 60% 3-65 77%
					CC	VOID	light gray (10YR 7/1) CC=20 cm

SITE 407		HOLE		CORE 7		CORED INTERVAL: 53.5-63.0 m	
TIME-ROCK UNIT	BIOSTRAT ZONE	FOSSIL CHARACTER			SECTION METERS	GRAPHIC LITHOLOGY	LITHOLOGIC DESCRIPTION
		FORAMS	NANNOS	RADS			
Early PLIOCENE	N21 NN18				1	0.5 1.0	white (5Y 8/1) and light gray (5Y 7/1) mixed
		Ag	Ag		2		Smear Slides 1-80 2-62 qtz. Tr fspr. Tr clay 5 volc. glass/palagonite 10 carb. unsp. 1 3 forams 5 3 nannos 90 65 silic. micro. 4 15 Carbonate Bomb 1-70 74% 2-76 75%
					CC	VOID	

SITE 407		HOLE		CORE 8		CORED INTERVAL: 63.0-72.5 m	
TIME-ROCK UNIT	BIOSTRAT ZONE	FOSSIL CHARACTER			SECTION METERS	GRAPHIC LITHOLOGY	LITHOLOGIC DESCRIPTION
		FORAMS	NANNOS	RADS			
Early PLIOCENE	N19 NN18				1	0.5 1.0	light gray (5Y 6/1 & 5Y 7/1) throughout
		Ag	Ag		2		Smear Slides 1-68 2-53 qtz. Tr H. min. Tr clay 1 volc. glass 1 carb. unsp. 5 0 forams 7 9 nannos 88 90 silic. micro. Tr Tr Carbonate Bomb 1-50 85% 2-50 88% 3-31 85%

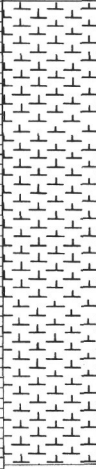
Explanatory notes in Chapter 1

SITE 407		HOLE		CORE 9		CORED INTERVAL: 72.5-82.0 m	
TIME-ROCK UNIT	BIOSTRAT ZONE	FOSSIL CHARACTER			SECTION METERS	GRAPHIC LITHOLOGY	LITHOLOGIC DESCRIPTION
		FORAMS	NANNOS	RADS			
Early PLIOCENE	N19 NN15/NN18	Ag	Ag		1		NANNOFOSSIL OOZE Very poor recovery of intensely disturbed nanno ooze similar to Core 8. <u>Smear Slides</u> 1-44 1-64 qtz. Tr carb. unsp. 1 forams 9 10 nannos 90 90 silic. micro. Tr Tr
							light gray (5Y 6/1 and 5Y 4/1) light gray (5Y 7/1) CC=30 cm (10 cm VOID)

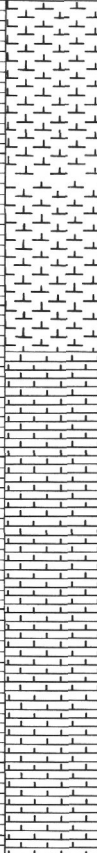
SITE 407		HOLE		CORE 10		CORED INTERVAL: 82.0-91.5 m	
TIME-ROCK UNIT	BIOSTRAT ZONE	FOSSIL CHARACTER			SECTION METERS	GRAPHIC LITHOLOGY	LITHOLOGIC DESCRIPTION
		FORAMS	NANNOS	RADS			
Early PLIOCENE	N19 NN15/NN18	Ag	Am		1		NANNOFOSSIL OOZE Highly disturbed core due to sharp change in water content below ash layer in Section 3 - soupy and creamy below. Lithified sediment clasts in Sections 1 and 2 have slight enrichment in heavy minerals, ash-otherwise nanno-fossil ooze. <u>Smear Slides</u> Major lith. 1-66 2-58 Sed. clasts 2-121 Ash 3-52 qtz. Tr Tr 3 2 fspr. Tr H. min. Tr clay Tr volc. glass 7 10 6 90 forams 93 90 90 5 nannos Tr silic. micro. Tr
							Carbonate Bomb 1-70 95% 3-87 90% black (5Y 2.5/1) black (5Y 2.5/1) black (5Y 2.5/1) black (5Y 2.5/1) CC=15 cm

Explanatory notes in Chapter 1

SITE 407		HOLE		CORE 11		CORED INTERVAL: 91.5-101.0 m	
TIME-ROCK UNIT	BIOSTRAT ZONE	FOSSIL CHARACTER			SECTION METERS	GRAPHIC LITHOLOGY	LITHOLOGIC DESCRIPTION
		FORAMS	NANNOS	RADS			
Early PLIOCENE	N19 NN15/NN18	Ag	Ag		1		NANNOFOSSIL OOZE Homogeneous light gray to white nannofossil ooze with firm, slightly darker layer from 70-130 cm in Section 2 apparently due to presence of small amount of ash and opaques. Small erratics (?) in 0-30 cm of Section 1. <u>Smear Slides (Major lithology)</u> 1-36 1-95 2-81 4-81 qtz. Tr fspr. 1 H. min. 1 Tr volc. glass/ palagonite forams 7 5 7 5 nannos 90 94 93 95 carb. unsp. Tr Tr Tr Tr silic. micro. Tr Tr Tr Tr
							gray (5Y 5/1) light brownish gray (2.5Y 6/2) light gray (5Y 7/1) CC=35 cm (15 cm VOID)

SITE 407		HOLE		CORE 12		CORED INTERVAL: 101.0-110.5 m																																																																					
TIME-ROCK UNIT	BIOSTRAT ZONE	FOSSIL CHARACTER			SECTION METERS	GRAPHIC LITHOLOGY	DRILLING DISTURBANCE STRUCTURE LITHOLOGIC SAMPLE	LITHOLOGIC DESCRIPTION																																																																			
		FORAMS	NANNOS	RADS																																																																							
Early PLIOCENE	N19 NN15/NN17				0.5		50	gray (N6 and N5) in alternating laminae	<u>NANNOFOSSIL OOZE</u> Dominantly gray to light gray, intensely deformed, soft. Trace amounts of volcanic glass and amphibole. Small amounts of foraminifer (<10%). Deformation obliterated any original sedimentary structures that may have existed. <u>Smear Slides</u> <table><thead><tr><th></th><th>1-50</th><th>1-115</th><th>2-45</th><th>2-98</th></tr></thead><tbody><tr><td>nannos</td><td>90</td><td>99</td><td>85</td><td>100</td></tr><tr><td>forams</td><td>2</td><td>Tr</td><td>10</td><td>--</td></tr><tr><td>diatoms</td><td>2</td><td>Tr</td><td>--</td><td>--</td></tr><tr><td>rads</td><td>2</td><td>Tr</td><td>--</td><td>Tr</td></tr><tr><td>sp. spic.</td><td>1</td><td>Tr</td><td>2</td><td>Tr</td></tr><tr><td>carb. unsp.</td><td>3</td><td>Tr</td><td>3</td><td>--</td></tr><tr><td>volc. glass</td><td>1</td><td>--</td><td>--</td><td>--</td></tr><tr><td>amphibole</td><td>--</td><td>Tr</td><td>--</td><td>Tr</td></tr><tr><td>palagonite</td><td>--</td><td>Tr</td><td>--</td><td>Tr</td></tr><tr><td>zeolite</td><td>--</td><td>--</td><td>--</td><td>--</td></tr><tr><td>fspr.</td><td>--</td><td>--</td><td>--</td><td>--</td></tr></tbody></table> <u>Carbonate Bomb</u> <table><tbody><tr><td>1-72</td><td>91%</td></tr><tr><td>2-73</td><td>93%</td></tr><tr><td>3-72</td><td>91%</td></tr></tbody></table>		1-50	1-115	2-45	2-98	nannos	90	99	85	100	forams	2	Tr	10	--	diatoms	2	Tr	--	--	rads	2	Tr	--	Tr	sp. spic.	1	Tr	2	Tr	carb. unsp.	3	Tr	3	--	volc. glass	1	--	--	--	amphibole	--	Tr	--	Tr	palagonite	--	Tr	--	Tr	zeolite	--	--	--	--	fspr.	--	--	--	--	1-72	91%	2-73	93%	3-72	91%
			1-50	1-115	2-45		2-98																																																																				
		nannos	90	99	85		100																																																																				
		forams	2	Tr	10		--																																																																				
		diatoms	2	Tr	--		--																																																																				
		rads	2	Tr	--		Tr																																																																				
		sp. spic.	1	Tr	2		Tr																																																																				
		carb. unsp.	3	Tr	3		--																																																																				
		volc. glass	1	--	--		--																																																																				
		amphibole	--	Tr	--		Tr																																																																				
palagonite	--	Tr	--	Tr																																																																							
zeolite	--	--	--	--																																																																							
fspr.	--	--	--	--																																																																							
1-72	91%																																																																										
2-73	93%																																																																										
3-72	91%																																																																										
			1.0	115																																																																							
			2	45	light gray (N7) and white (N8) alternating laminae and spots. At 64-76 cm zone of Section 2 is some areas of grayish yellow green (5GY 7/2)																																																																						
			3	98	Gray (N5)-light gray (N7)-white (N8)-grayish yellow green (5GY 7/2) in alternating laminae																																																																						
			4	78	olive (5Y 5/3)																																																																						
				104	light gray (5Y 7/1)																																																																						
				6																																																																							

Explanatory notes in Chapter 1

SITE 407		HOLE		CORE 13		CORED INTERVAL: 110.5-120.0 m																																		
TIME-ROCK UNIT	BIOSTRAT ZONE	FOSSIL CHARACTER			SECTION METERS	GRAPHIC LITHOLOGY	LITHOLOGIC DESCRIPTION																																	
		FORAMS	NANNOS	RADS																																				
PLIOCENE	N19	NN15/NN16					<div>Drilling breccia mixture of gray (5Y 5/1), white (N8) with patch of pale yellowish green (10GY 7/2) at 1-92</div> <div>gray (5Y 5/1) and white (N8) mixed</div> <div>light gray (5Y 7/1)</div>																																	
								0.5	54	<div>NANNOFOSSIL 007E (0 to 3-60)</div> <div>AND NANNOFOSSIL CHALK (3-60 to end)</div> <div>Light gray, with traces to less than 2 percent of foraminifera, amphibole, volcanic glass, sponge spicules. Major change in core from soft to firm character of sediment. Intensely deformed from top to 3-45, homogeneous and apparently structureless for remainder.</div>																														
								1.0	72	<div>Smear Slides</div> <table><tr><td>1-54</td><td>2-72</td><td>3-60</td></tr><tr><td>nannos 100</td><td>95</td><td>92</td></tr><tr><td>forams Tr</td><td>1</td><td>2</td></tr><tr><td>sp. spic. Tr</td><td>Tr</td><td>1</td></tr><tr><td>volc. glass Tr</td><td>1</td><td>2</td></tr><tr><td>palagonite Tr</td><td>--</td><td>--</td></tr><tr><td>amphibole --</td><td>Tr</td><td>Tr</td></tr><tr><td>carb. unsp. --</td><td>--</td><td>2</td></tr><tr><td>zeolite --</td><td>--</td><td>--</td></tr><tr><td>fspr. --</td><td>--</td><td>--</td></tr></table>	1-54	2-72	3-60	nannos 100	95	92	forams Tr	1	2	sp. spic. Tr	Tr	1	volc. glass Tr	1	2	palagonite Tr	--	--	amphibole --	Tr	Tr	carb. unsp. --	--	2	zeolite --	--	--	fspr. --	--	--
								1-54	2-72	3-60																														
								nannos 100	95	92																														
								forams Tr	1	2																														
								sp. spic. Tr	Tr	1																														
								volc. glass Tr	1	2																														
								palagonite Tr	--	--																														
								amphibole --	Tr	Tr																														
carb. unsp. --	--	2																																						
zeolite --	--	--																																						
fspr. --	--	--																																						
2																																								
3	60	<table><tr><td>4-94</td><td>5-62</td><td>6-17</td></tr><tr><td>nannos 91</td><td>95</td><td>92</td></tr><tr><td>forams 2</td><td>2</td><td>1</td></tr><tr><td>sp. spic. 2</td><td>1</td><td>1</td></tr><tr><td>volc. glass 2</td><td>1</td><td>2</td></tr><tr><td>palagonite --</td><td>--</td><td>--</td></tr><tr><td>amphibole 1</td><td>1</td><td>1</td></tr><tr><td>carb. unsp. 2</td><td>--</td><td>1</td></tr><tr><td>zeolite 2</td><td>1</td><td>--</td></tr><tr><td>fspr. --</td><td>Tr</td><td>--</td></tr></table>	4-94	5-62	6-17	nannos 91	95	92	forams 2	2	1	sp. spic. 2	1	1	volc. glass 2	1	2	palagonite --	--	--	amphibole 1	1	1	carb. unsp. 2	--	1	zeolite 2	1	--	fspr. --	Tr	--								
4-94	5-62	6-17																																						
nannos 91	95	92																																						
forams 2	2	1																																						
sp. spic. 2	1	1																																						
volc. glass 2	1	2																																						
palagonite --	--	--																																						
amphibole 1	1	1																																						
carb. unsp. 2	--	1																																						
zeolite 2	1	--																																						
fspr. --	Tr	--																																						
4	94	<div>Carbonate Bomb</div> <table><tr><td>1-73</td><td>83%</td><td>4-81</td><td>84%</td></tr><tr><td>2-81</td><td>90%</td><td>5-53</td><td>85%</td></tr><tr><td>3-81</td><td>85%</td><td>6-53</td><td>85%</td></tr></table>	1-73	83%	4-81	84%	2-81	90%	5-53	85%	3-81	85%	6-53	85%																										
1-73	83%	4-81	84%																																					
2-81	90%	5-53	85%																																					
3-81	85%	6-53	85%																																					
5	62																																							
6	17																																							
CC																																								

SITE 407		HOLE		CORE 14		CORED INTERVAL: 120.0-129.5 m	
TIME-ROCK UNIT	BIOSTRAT ZONE	FOSSIL CHARACTER			SECTION METERS	GRAPHIC LITHOLOGY	LITHOLOGIC DESCRIPTION
		FORAMS	NANNOS	RADS			
Early Pliocene	N19 NN13/NN15				0.5		light gray (N7) to white (N8) intermixed throughout 1-0 to 4-30 NANNOFOSSIL CHALK (except for ooze 0-30 cm from top), light gray to white. Small amounts of foraminifera, volcanic glass, sponge spicules. Deformed throughout so that no sedimentary structures detectable. <u>Smear Slides</u> 1-83 2-88 3-60.5 4-30 CC nannos 99 96 93 98 97.5 forams Tr 3 1 1 1 volc. glass 1 1 1 1 1 sp. spic. Tr Tr 2 Tr Tr H. min. -- Tr 3 -- 0.5 palagonite -- -- Tr Tr <u>Carbonate Bomb</u> 1-72 75% 2-72 85% 3-72 78% 4-27 85% 0-70 few sand-size black grains
					1.0		
					2		
					3		
					30		white (N8)
					15		gray (5Y 6/1) to dark gray (5Y 4/1)

Explanatory notes in Chapter 1

SITE 407		HOLE		CORE 16		CORED INTERVAL: 139.0-148.5 m	
TIME-ROCK UNIT	BIOSTRAT ZONE	FOSSIL CHARACTER			SECTION METERS	GRAPHIC LITHOLOGY	LITHOLOGIC DESCRIPTION
		FORAMS	NANNOS	RADS			
Late Miocene	N19 NN9/NN11				0.5		white (N8) to light gray (N7)
					1.0		gray (5Y 6/1 to 5Y 5/1)
					2		white (N8)
					3		light gray (N7) with slight mottles of white (N8)
					CC		

SITE 407		HOLE		CORE 17		CORED INTERVAL: 148.5-158.0 m	
TIME-ROCK UNIT	BIOSTRAT ZONE	FOSSIL CHARACTER			SECTION METERS	GRAPHIC LITHOLOGY	LITHOLOGIC DESCRIPTION
		FORAMS	NANNOS	RADS			
Late Miocene	N16-N17 NN9/NN11				0.5		white (N8) to gray (5Y 6/1)
					1.0		light gray (N7) with white (N8) mottles
					2		gray (5Y 6/1) with light gray (5Y 7/1) mottles, many scattered silt-fn-sand black particles (possible burrow fill?)
					3		light brownish gray (2.5Y 6/2)
					CC		same as above

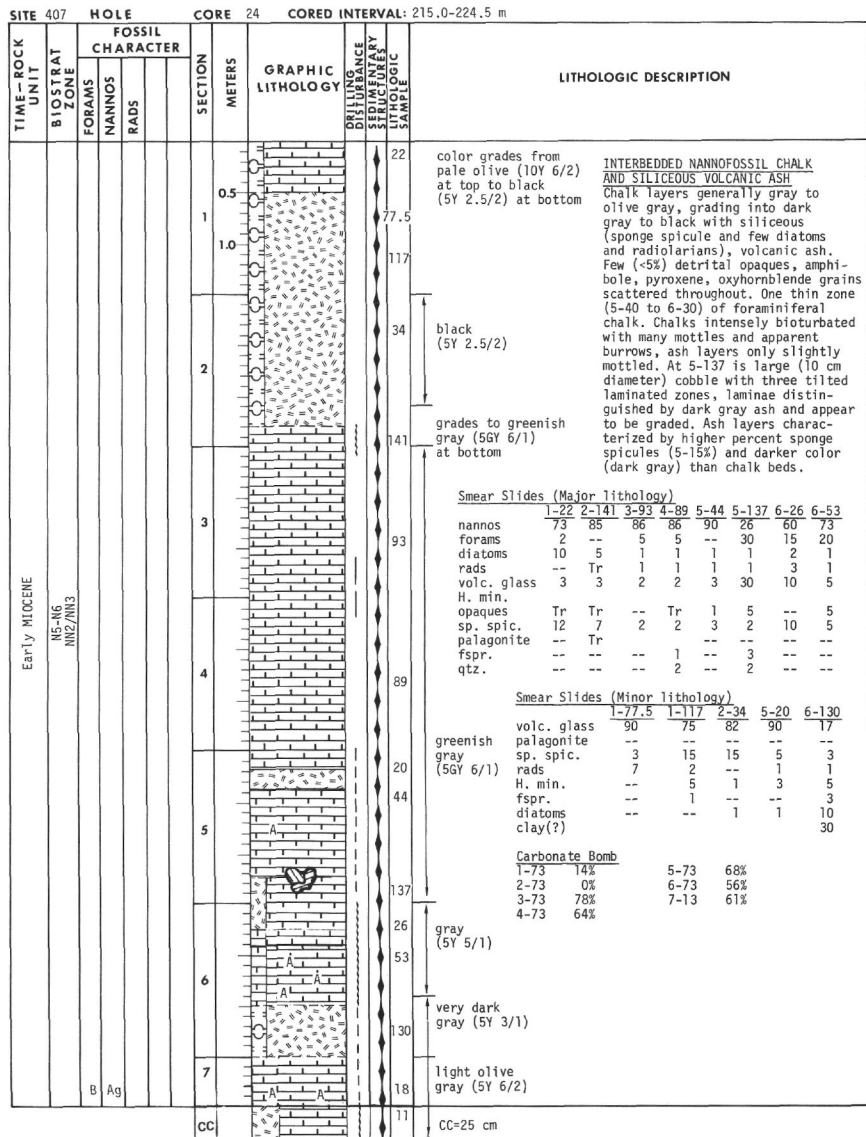
SITE 407		HOLE		CORE 20		CORED INTERVAL: 177.0-186.5 m	
TIME-ROCK UNIT	BIOSTRAT ZONE	FOSSIL CHARACTER			SECTION METERS	GRAPHIC LITHOLOGY	LITHOLOGIC DESCRIPTION
		FORAMS	NANNOS	RADS			
Middle Miocene	NN2-NN7				0.5		white (5Y 8/1) intermixed with gray (5Y 6/1)
					1.0		sand-size fragments, dusky green (5G 3/2) scattered throughout
		Cg	Ag				grayish yellow (5G 7/2) interlayered with grayish green (10G 5/2)
							pale olive (10Y 6/2)
							Smear Slides
							1-94 2-19 2-19 (frag.)
							nannos 94 89 81
							forams -- 2 5
							rads 3 3 2
							diatoms 2 -- --
							volc. glass 1 1 2
							opales Tr Tr Tr
							sp. spic. -- 5 10
							palagonite -- Tr Tr
							amphibole -- Tr Tr
							2-38 2-39
							nannos 89 90
							forams -- 3
							rads 5 1
							diatoms -- 1
							volc. glass -- 1
							opales Tr --
							sp. spic. 5 5
							palagonite -- --
							amphibole -- --
							Carbonate Bomb
							1-45 68%
							2-46 82%

SITE 407		HOLE		CORE 21		CORED INTERVAL: 186.5-196.0 m	
TIME-ROCK UNIT	BIOSTRAT ZONE	FOSSIL CHARACTER			SECTION METERS	GRAPHIC LITHOLOGY	LITHOLOGIC DESCRIPTION
		FORAMS	NANNOS	RADS			
Early Miocene?	NN4						dusky yellow green (5G 5/2)
		Rg	Ag				SILICEOUS NANNOFOSSIL CHALK Dusky yellow green, massive, no evidence of bioturbation, some trace of opaque minerals and volcanic glass, sponge spicules and radiolarians abundant (total 25% of core).
							Smear Slides
							1-35
							nannos 75
							rads 15
							sp. spic. 10
							volc. glass Tr
							opales Tr
							Carbonate Bomb
							1-45 42%

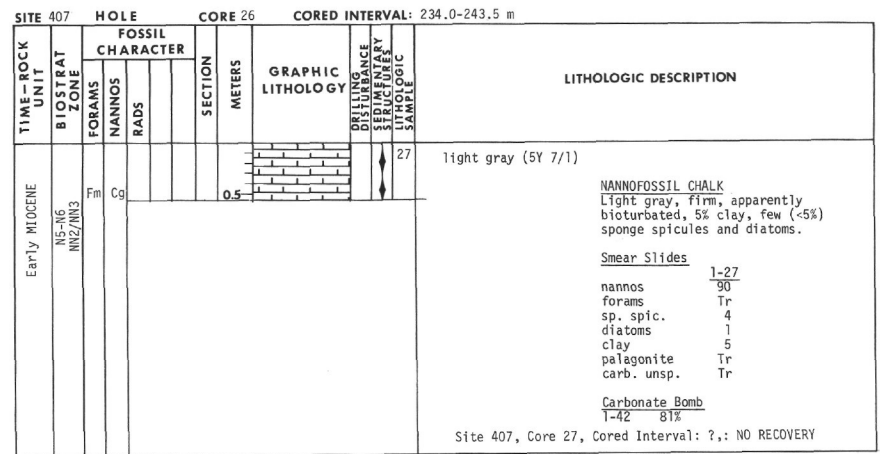
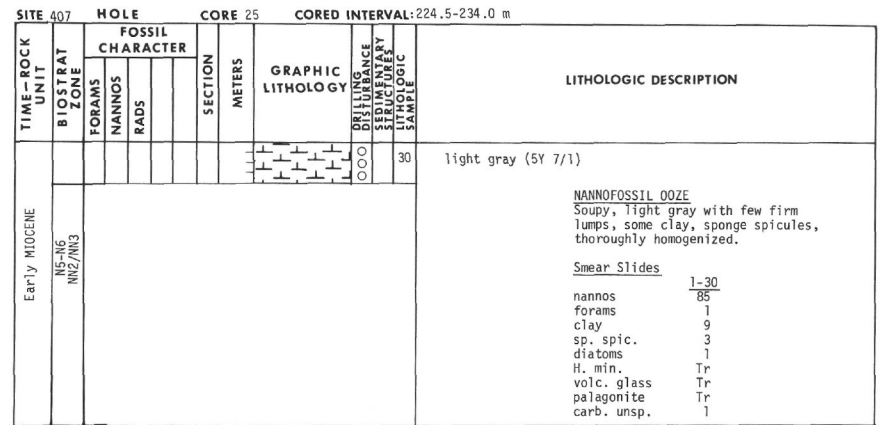
Explanatory notes in Chapter 1

SITE 407		HOLE		CORE 22		CORED INTERVAL: 196.0-205.5 m	
TIME-ROCK UNIT	BIOSTRAT ZONE	FOSSIL CHARACTER			SECTION METERS	GRAPHIC LITHOLOGY	LITHOLOGIC DESCRIPTION
		FORAMS	NANNOS	RADS			
Early Miocene	NN3/NN4				0.5		pale olive (10Y 6/2) with scattered sand-size frags.
					1.0		dusky green (5G 3/2) light olive gray (5G 6/1) gray (5Y 5/1) gray (5Y 6/1)
							Smear Slides
							1-43.5 1-81 1-88 1-119 2-81 3-56
							nannos 78 90 68 87 79 93
							forams 5 2 Tr 2 2 1
							diatoms -- Tr 2 3 5 2
							rads 5 2 -- Tr --
							sp. spic. 10 5 10 5 12 2
							volc. glass 2 1 20 3 2 1
							opaque -- 1 Tr -- -- Tr
							feldspar -- Tr -- -- --
							palagonite -- -- Tr -- -- 1
							amphibole -- -- -- -- -- Tr
							Carbonate Bomb
							1-73 55%
							2-73 53%
							3-73 51%

SITE 407		HOLE		CORE 23		CORED INTERVAL: 205.5-215.0 m	
TIME-ROCK UNIT	BIOSTRAT ZONE	FOSSIL CHARACTER			SECTION METERS	GRAPHIC LITHOLOGY	LITHOLOGIC DESCRIPTION
		FORAMS	NANNOS	RADS			
Early Miocene	NN5-NN6				0.5		gray (5Y 6/1)
					1.0		very dark gray (5Y 3/1) vol. ash
							light gray (5Y 7/1), intensely mottled
							Smear Slides (Major lithology)
							1-53 1-112 1-141
							nannos 88 83 77
							forams Tr -- 3
							diatoms 5 5 --
							rads 1 Tr 2
							sp. spic. 5 10 15
							volc. glass 1 2 2
							palagonite -- Tr 1
							opales -- Tr --
							amphibole -- -- --
							2-89 3-89.5
							nannos 80 82
							forams 1 2
							diatoms 1 3
							rads 1 1
							sp. spic. 15 10
							volc. glass 1 --
							palagonite -- 1
							opales Tr --
							amphibole Tr --
							few broken pieces
							Smear Slides (Minor lithology)
							1-128
							volc. glass 87
							diatoms 1
							rads 2
							sp. spic. 10
							Carbonate Bomb
							1-73 63%
							3-73 73%



Explanatory notes in Chapter 1



SITE 407 HOLE CORE 28 CORED INTERVAL: 253.0-262.5 m

TIME-ROCK UNIT	BIOSTRAT ZONE	FOSSIL CHARACTER	SECTION	METERS	GRAPHIC LITHOLOGY	DRILLING DISTURBANCE	STRUCTURE	LITHOLOGIC SAMPLE	LITHOLOGIC DESCRIPTION
Early Miocene	N5 NN1/NN2	Rm Cg	1	0.5	VOID			10	light olive gray (5Y 6/2)
			1	1.0					
			2					70	light brownish gray (2.5Y 6/2)
			3					66	
			4					66	
Early Miocene	N4 NN1	Rm Cg	5					7	
			CC						CC=20 cm

SILICEOUS NANNOFOSSIL CHALK
Light olive to brownish gray, firm calcareous sediments containing 5-10% volcanic glass and 5-15% siliceous microfossil debris-mainly sponge spicules. Coarse ash and occasional small basalt fragments are scattered throughout. Slight color banding highlighted by ash in Sections 4 and 5. Foram content varies from 5 to 20%; detrital grains 5-10%.

Smear Slides	1-10	2-70	3-66	4-66	5-7
qtz.	1	1	2	2	Tr
fspr.	1	10	5	3	10
Mica	3				
H. min.	3				
clay					
volc. glass	5	15	3	5	10
forams	7	20	5	10	5
nannos	75	50	75	65	60
diatoms	3	1	3	5	3
rads	2	1	3	5	2
sp. spic.	3	3	3	5	10

Carbonate Bomb	1-64	58%	4-64	45%
	2-64	58%	5-73	50%
	3-64	38%		

Explanatory notes in Chapter 1

SITE 407 HOLE CORE 29 CORED INTERVAL: 262.5-272.0 m

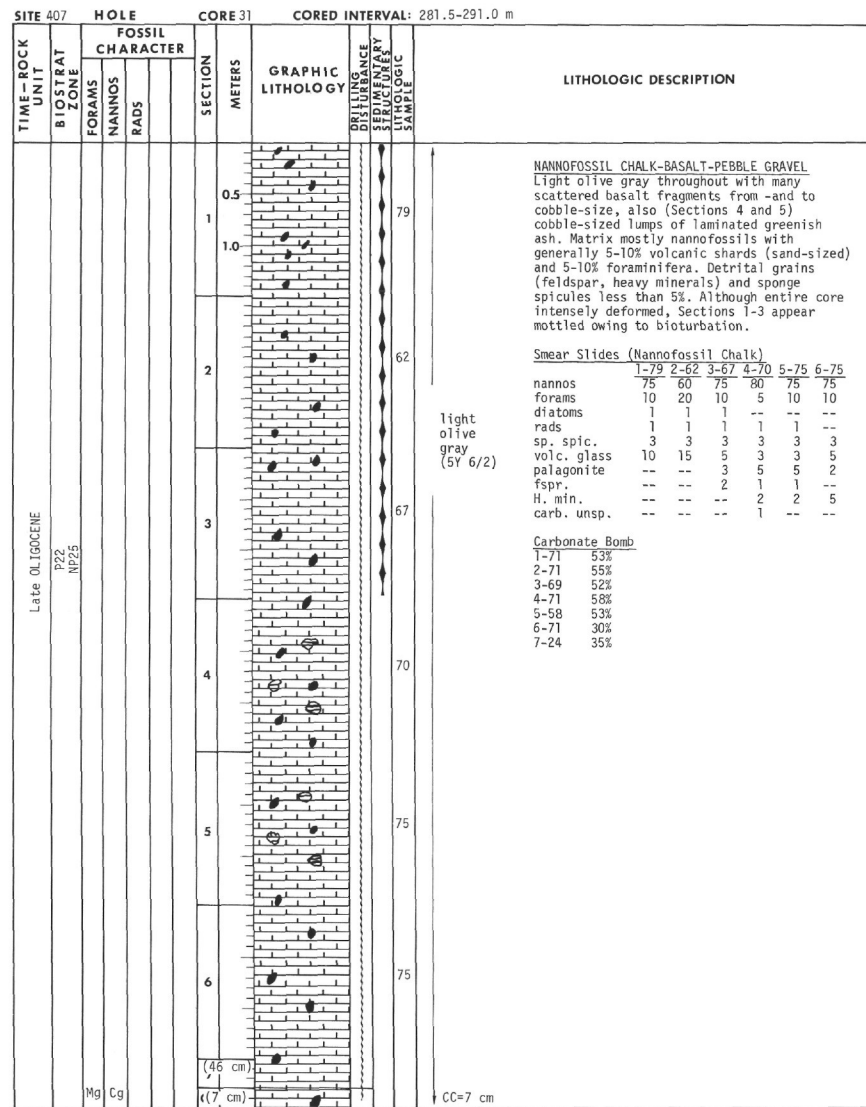
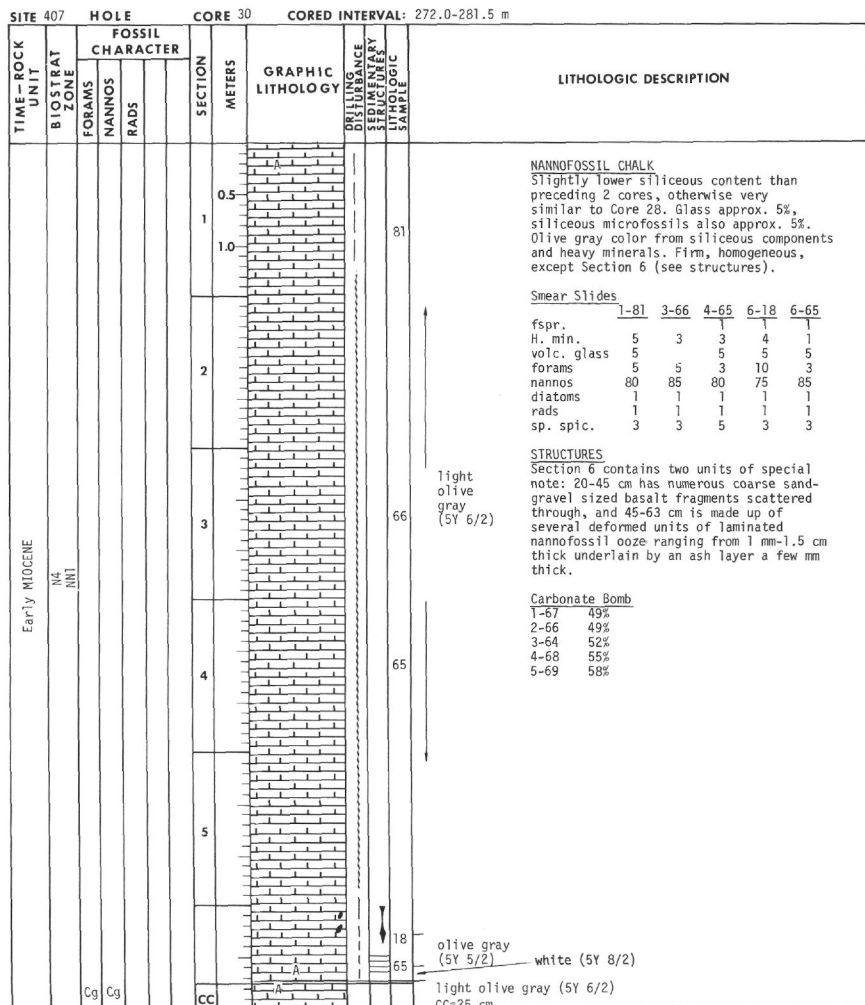
TIME-ROCK UNIT	BIOSTRAT ZONE	FOSSIL CHARACTER	SECTION	METERS	GRAPHIC LITHOLOGY	DRILLING DISTURBANCE	STRUCTURE	LITHOLOGIC SAMPLE	LITHOLOGIC DESCRIPTION
Early Miocene	N4 NN1	Rm Cg	1	0.5				85	light olive gray (5Y 6/2)
			1	1.0					
			2		VOID				
			3		VOID				
			4		VOID				
Early Miocene	N4 NN1	Rm Cg	5		VOID				
			6		VOID				
Early Miocene	N4 NN1	Rm Cg	CC						CC=20 cm

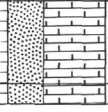
SILICEOUS NANNOFOSSIL OOZE
Highly disturbed soft (soupy) olive gray siliceous nannofossil ooze. Similar except in firmness to Core 28.

Smear Slides 1-85

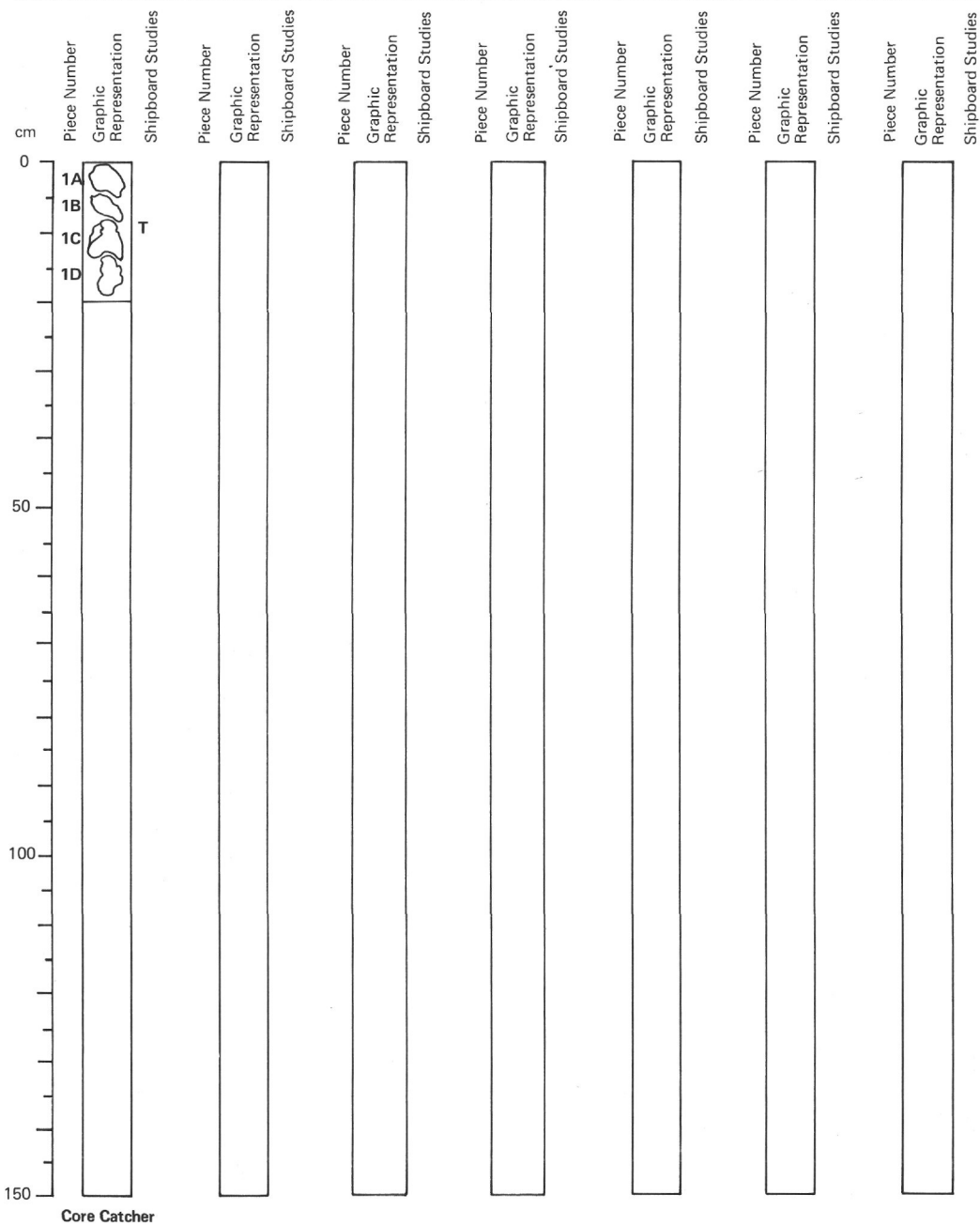
qtz.	2
fspr.	5
H. min.	5
volc. glass	5
forams	3
nannos	80
diatoms	1
rads	1
sp. spic.	5

Carbonate Bomb
1-57 42%
5-23 45%



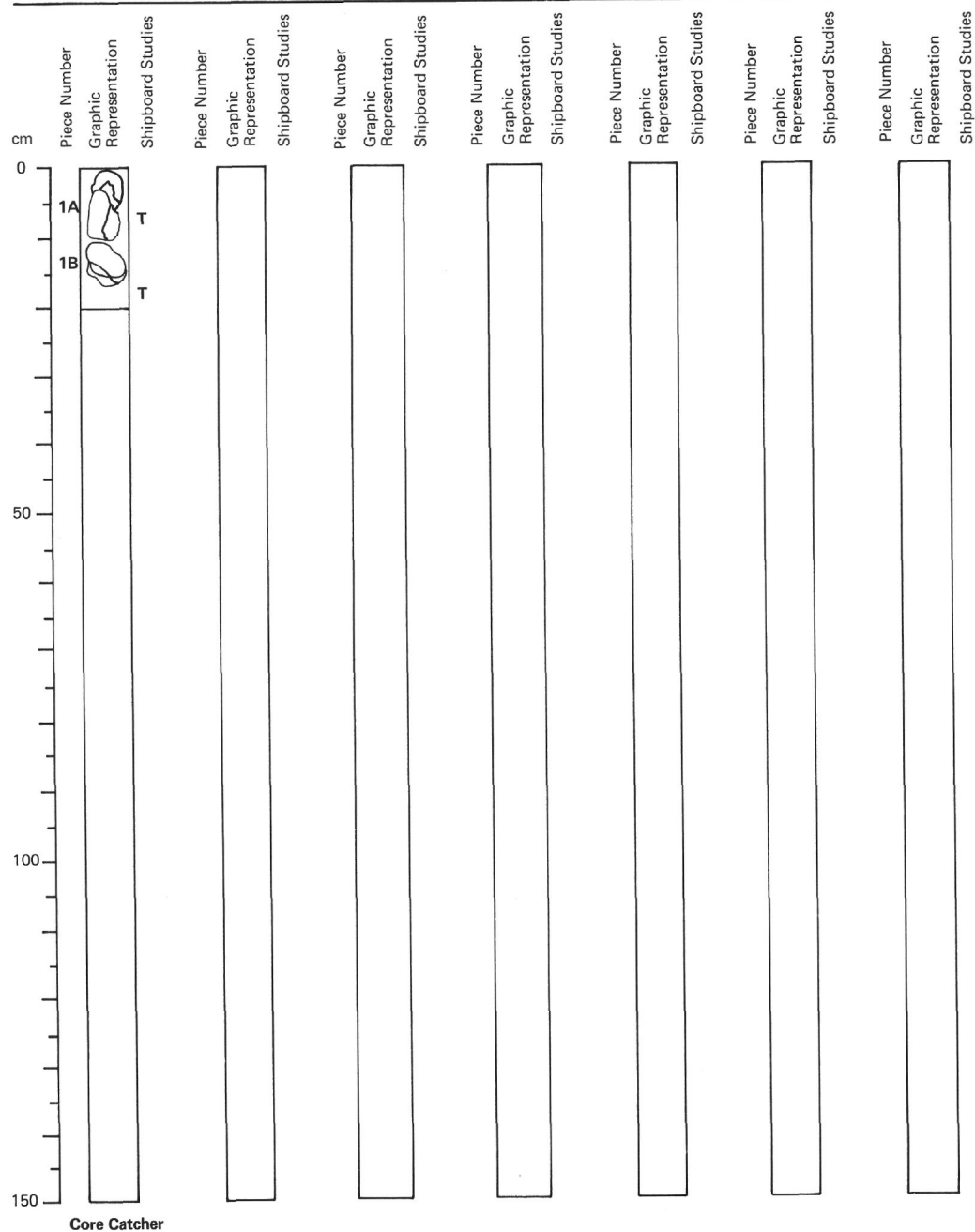
SITE 407		HOLE			CORE 32		CORED INTERVAL: 291.0-300.5 m	
TIME-ROCK UNIT	BIOSTRAT ZONE	FOSSIL CHARACTER			SECTION METERS	GRAPHIC LITHOLOGY	DIAGENETIC ALTERATION	LITHOLOGIC DESCRIPTION
		FORAMS	NANNOS	RADS				
Late Oligocene	P22-NP25	Cg	Cg		1		37	light olive gray (5Y 6/2) SANDY NANNOFOSSIL CHALK-BASALT-PEBBLE GRAVEL Nannofossil chalk matrix with 35% sand-size basalt fragments, 10% sponge spicules. Intensely deformed. Smear Slides (Nannofossil Chalk) nannos 1-37 basalt frags. 60 sp. spic. 30 Carbonate Bomb 1-25 27%
					CC 10		10	

Explanatory notes in Chapter 1



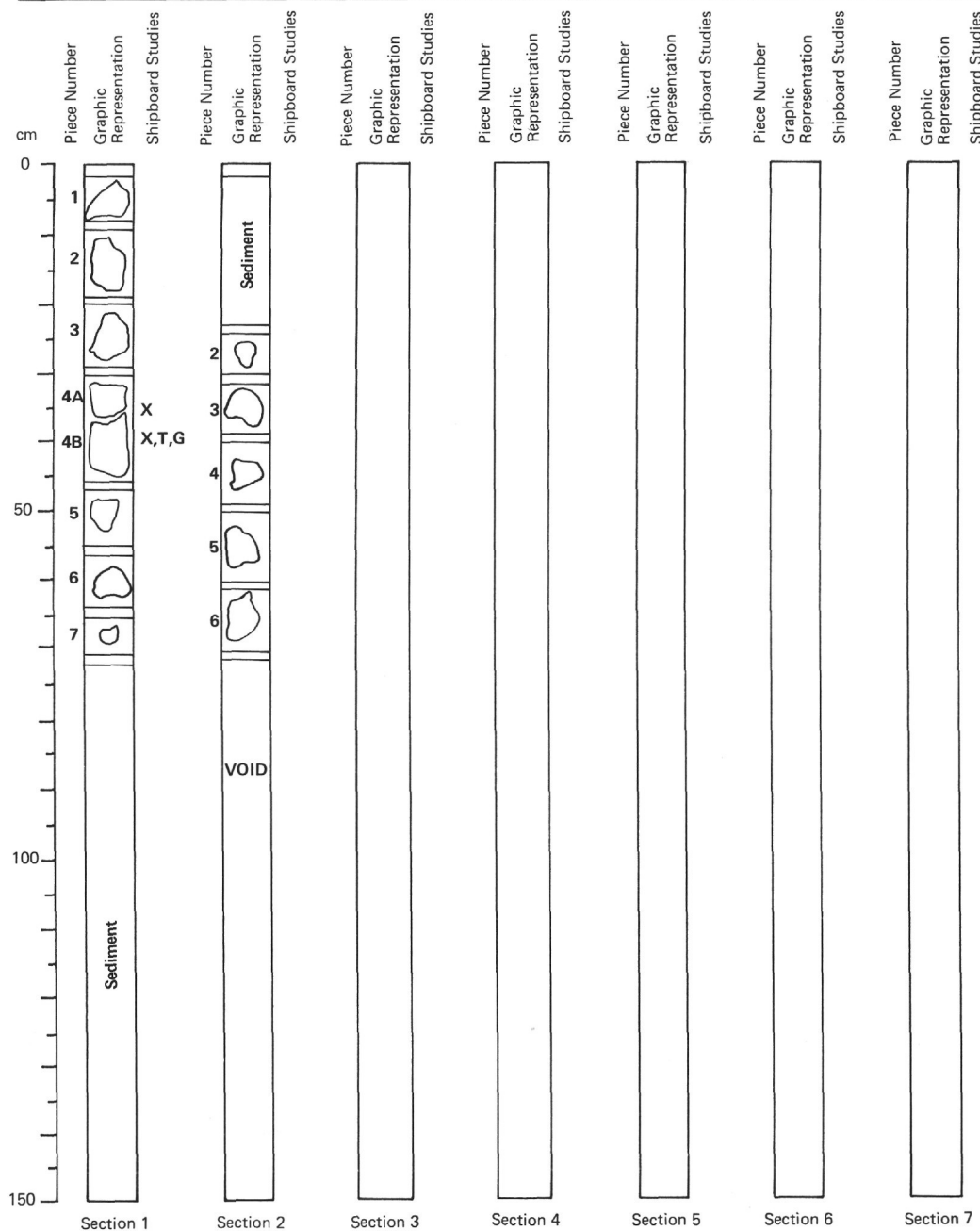
Aphyric hypocrystalline basalt with sparse vesicles (< 1 mm) and rare clots of plagioclase and olivine(?) to 2 mm. Red Fe-oxide weathered rinds up to 12 mm thick. Petrography: microporphyritic, normally zoned plagioclase microphenocrysts An₇₆₋₅₀, clinopyroxene microphenocrysts show some zoning and corrosion, olivine microphenocrysts altered to iddingsite and smectite. Groundmass contains plagioclase, clinopyroxene, opaques, olivine and fresh brown glass.

LEG 49 SITE 407 HOLE CORE 34 DEPTH 310.0-319.5 m



Interval 0-3 cm: basalt breccia with clasts of fine-grained holocrystalline basalt and basaltic glass in a clay(?) matrix.

Interval 3-21 cm: aphyric hypocrystalline basalt (2.5YR 6/0) with local vesicle clots (0.5-1.0 mm). Microscopic texture: sub-ophitic-interstitial. Olivine completely replaced by smectite, minor alteration of clinopyroxene. Pyrite in cavities. Estimated mineral per cent: plagioclase 32.0, clinopyroxene 21.1, olivine 1.1, opaques 7.4, pyrite 0.6, and glass 38.0.



Original core recovery was 1.5 meters. Styrofoam spacers make the length shown here greater than the amount recovered.

Interval 0-74 cm: aphyric holocrystalline basalt (2.5YR 4/0); up to 1% sulfide; vesicles 0.1-0.5 mm, rarely to 2 mm, vesicle rock (5-7%) zones.

Interval 74-150 cm: greenish-gray (5G 6/1) clay, shows bioturbation.

Interval 0-23 cm, Sect. 2: olive gray (5Y 4/1) clay, bioturbation.

Interval 23-70 cm: vesicular aphyric basalt (2.5YR 5/0) with rare plagioclase microphenocrysts, and 0.1 mm crystals of sulfide, vesicles to 3 mm partially filled with zeolites.

Petrography: sub-ophitic-hyalophitic, plagioclase An₇₀. Rare olivine altered to smectite, glass altered to smectite.

Mineral per cent: plagioclase 33, clinopyroxene 26, olivine 3, opaques 5, sulfide .5 and glass 33.

Interval 75-125 cm: greenish gray (5G 6/1) to olive gray (5Y 4/1) nannofossil-foraminiferal chalk, bioturbated.

Interval 150-175 cm: nannofossil chalk, olive gray (5Y 4/1).

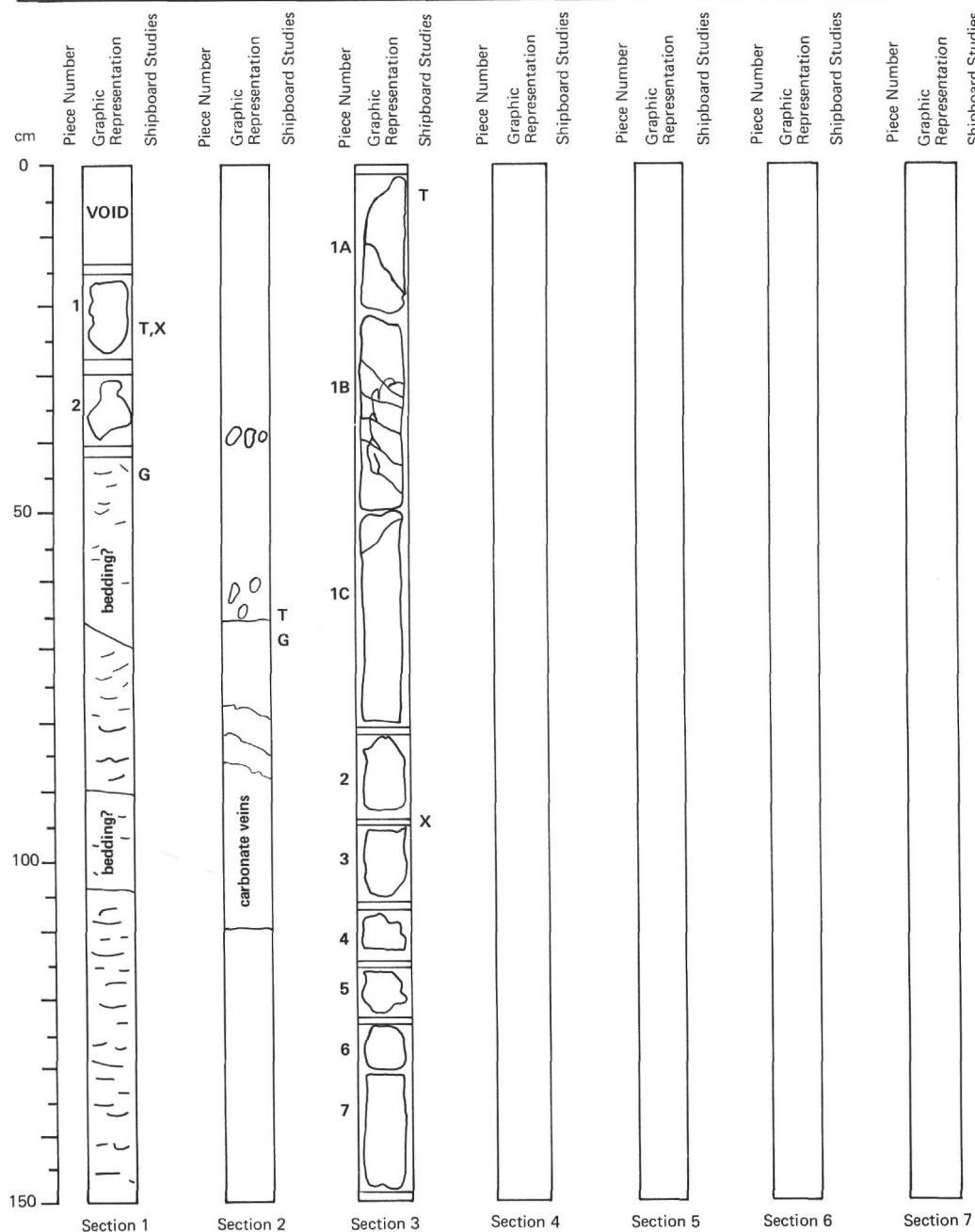
Shipboard Data

	Vp	NRM	Inc.
Sect. 1, 40 cm:	—	30.85	+64°

Smear Slides

	1-101	2-8
nannofossils	60	89
foraminifer	40	5
feldspar	TR	—
heavy minerals	TR	1
volcanic glass	TR	TR
clay	—	2
zeolite	—	3

Sediment age: Oligocene P20/P21 Zone



Original core recovery was 3.7 meters. Styrofoam spacers make the length shown here greater than the amount recovered.

Interval 20-40 cm, Sect. 1: fine-grained aphyric vesicular basalt, very rare plagioclase microphenocrysts to 4 mm. Approximately 1% vesicles average 0.5-1.0 mm, maximum 5 mm, 2.5YR 5/0.

Interval 40 cm, Sect. 1 to 65 cm, Sect. 2: nannofossil chalk, gray (5Y 5/1) with some basalt granules in upper part, 10% volcanic ash.

Interval 65 cm, Sect. 2 to 150 cm, Sect. 3: holocrystalline, porphyritic, amygdaloidal basalt (2.5YR 5/0). Plagioclase phenocrysts (< 1%) up to 5 mm. Amygdules to 3 mm, vary from 2-7%, carbonate veins 1 mm thick, zeolites(?) in amygdules.

Petrography: sub-ophitic-glomeroporphyritic, plagioclase microphenocrysts An₇₅, groundmass An₅₀₋₄₀. Olivine microphenocrysts altered to smectite. Clinopyroxene shows zoning. Five per cent glass altered to smectite. Rock strongly altered — smectite in groundmass and fractures. Carbonate in fractures.

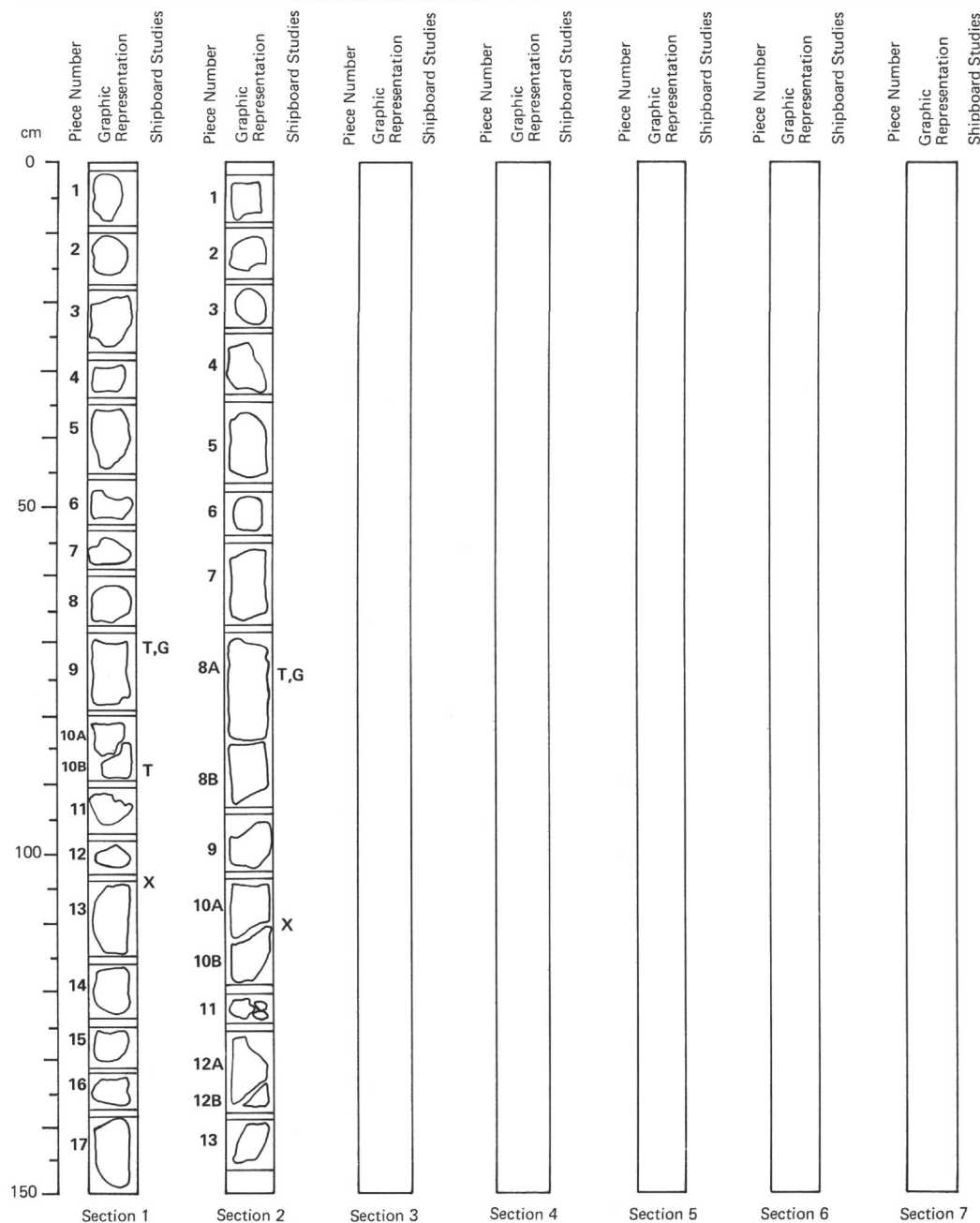
Shipboard Data

	Vp	NRM	Inc.
Sect. 2, 80 cm:	---	4687	+73° (?)
Sect. 2, 95 cm:	---	---	Normal
Sect. 3, 5 cm:	---	---	Normal
Sect. 3, 60 cm:	---	3246	+39°

Smear Slides

	2-24
nanofossils	82
foraminifer	2
volcanic ash	10
zeolite	3
heavy minerals	1
clay	2

Sediment age: Oligocene P20/P21, NP25 Zone



Original basalt recovery was 3.0 meters. Styrofoam spacers make the length shown here greater than the amount recovered.

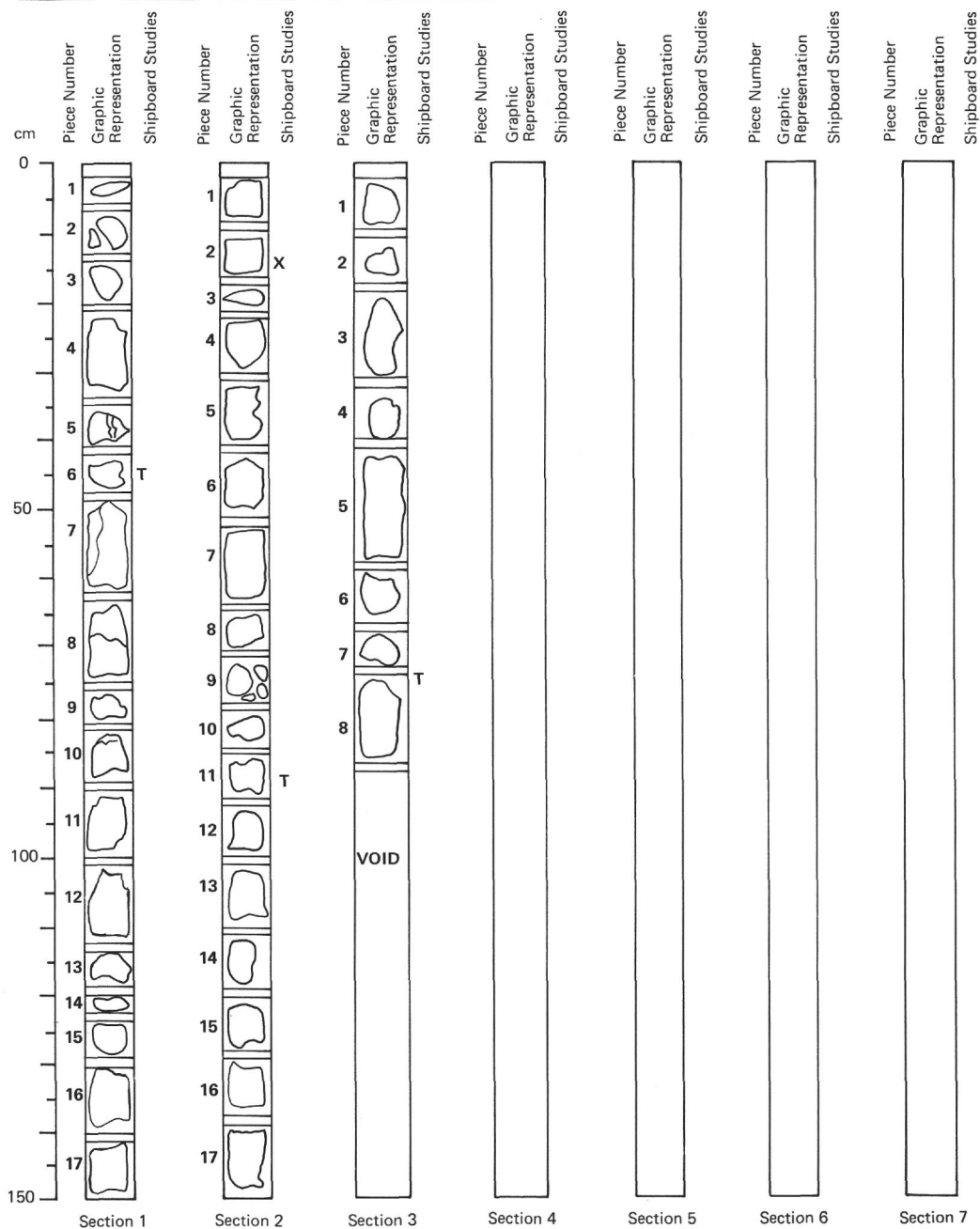
Interval 0-85 cm, Sect. 1: phyric basalt with rare amygdulites ~2 mm ϕ , most 1 mm ϕ occur < 1%. There are phenocrysts of plagioclase and altered olivine. Phenocrysts: plagioclase 0.7%, olivine 0.5%. Groundmass: plagioclase 39.1%, clinopyroxene 24.0%, olivine 2.0%, ilmenite 0.5%, magnetite 2.7%, pyrite 0.5%, glass 30.0% (2.5YR 5/0).

Interval 85-150 cm, Sect. 1: aphyric fine-grained basalt with rare phenocrysts of plagioclase. Groundmass: markedly finer-grained than #10A and above, phenocrysts: plagioclase < 1%, olivine (altered) < 1%. Groundmass: clinopyroxene 25%, plagioclase 35% (An_{76.66}), olivine < 10%, glass (altered) 30%, opaques 1-2% (2.5YR 4/0).

Interval 0-150 cm, Sect. 2: aphyric fine-grained vesicular basalt sulfides are present, very rare. There are phenocrysts of plagioclase and olivine (altered) very rare. Groundmass: plagioclase ~40%, olivine (altered) TR, opaques (magnetite and ilmenite) 3-5%, glass 5% (2.5YR 4/0).

Shipboard Data

	Vp	NRM	Inc.
Sect. 1, 35 cm:	---	---	Normal
Sect. 1, 60 cm:	---	3708	+51°
Sect. 1, 110 cm:	---	---	Normal
Sect. 2, 30 cm:	---	2656	-86°

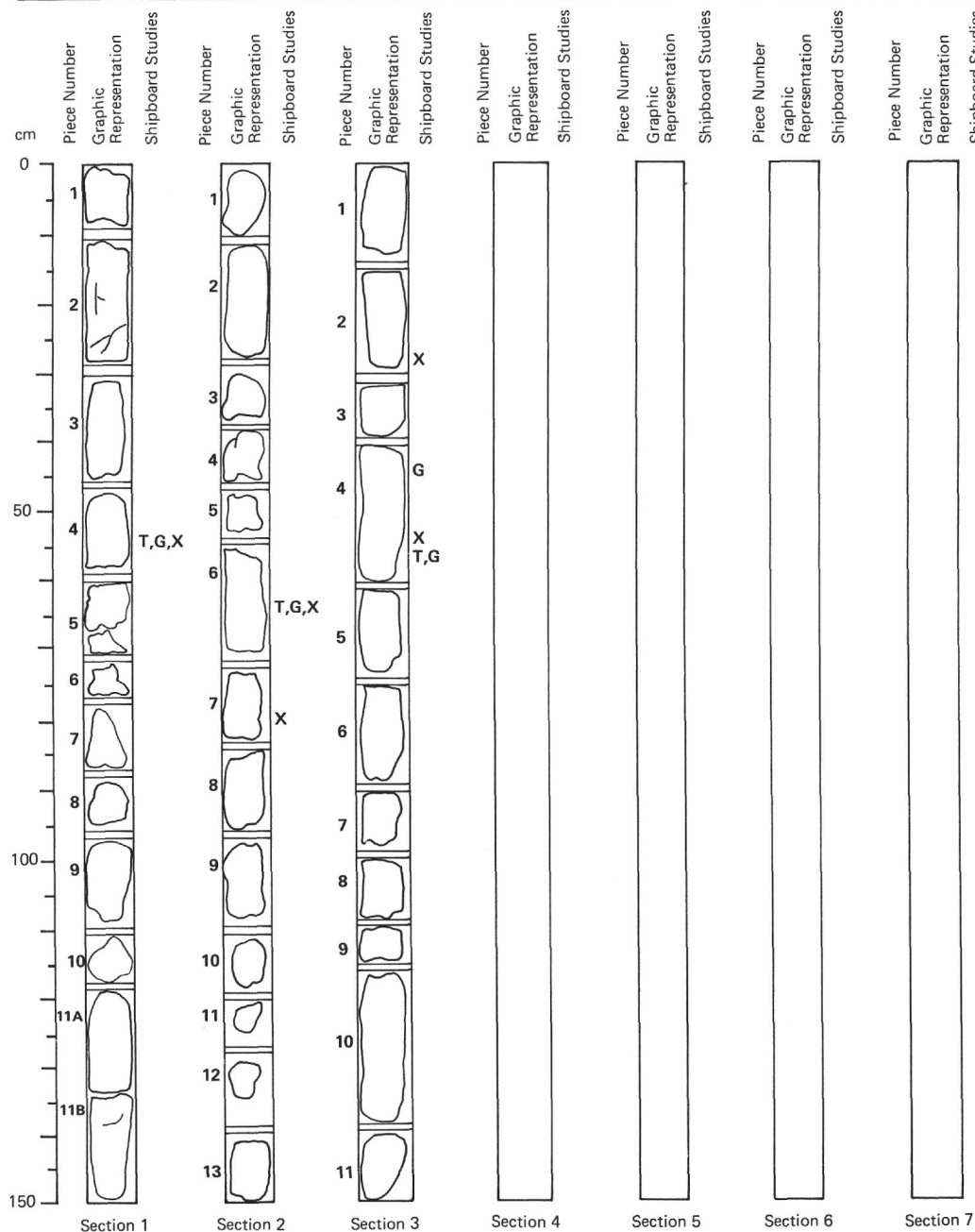


Original basalt recovery was 3.85 meters. Styrofoam spacers make the length shown here greater than the amount recovered.

Fine-grained holocrystalline aphyric basalt (2.5YR 5/0). Less than 1% vesicles (0.5-1.0 mm diameter). Some vesicles filled with secondary minerals. Fractures filled with carbonate, smectite and celadonite. Trace amounts of sulfide in Sections 1 and 2. Rare plagioclase microphenocrysts in Section 2. Petrography: sub-ophitic basalt; 2-3% plagioclase microphenocrysts. Normally zoned An_{80-70} , 45% groundmass plagioclase laths zones An_{60-50} with slightly resorbed margins. Thirty-five per cent groundmass clinopyroxene, 1% altered clinopyroxene microphenocrysts, 7-10% skeletal and barbed opaques, 5-10% secondary hematite and chlorite as vein fillings, 5-10% devitrified and recrystallized glass. Vesicles lined with fibrous chloritic material.

Shipboard Data

	Vp	NRM	Inc.
Sect. 1, 50 cm:	5.11	1501	-70°
Sect. 2, 30 cm:	—	2206	-55°
Sect. 2, 95 cm:	4.75	—	—
Sect. 3, 55 cm:	5.14	4058	-73°

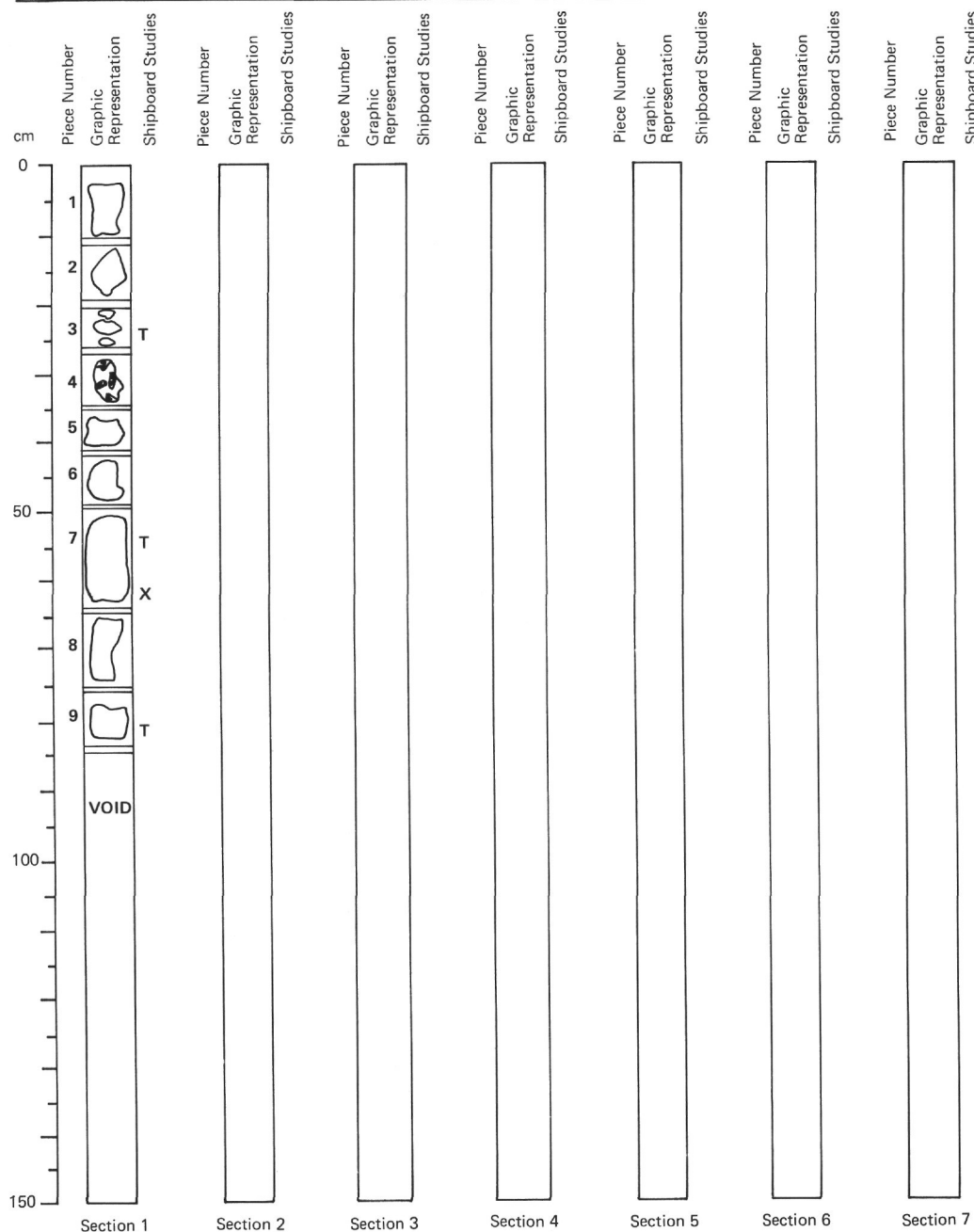


Original basalt recovery was 3.5 meters. Styrofoam spacers make the length shown here greater than the amount recovered.

Medium- to fine-grained aphyric basalt. Rare plagioclase phenocrysts (~An₇₀) 1-2 mm. Sub-ophitic groundmass of clinopyroxene and plagioclase with some glass. Estimated mode: plagioclase 40%, clinopyroxene 35%, glass 23%, opaques 2%. Much glass altered to smectite and chlorite. Scattered vesicles < 1 mm partly filled with secondary minerals. Steeply dipping veins (~2-3 mm) filled with smectite and chlorite. Trace of disseminated pyrite common.

Shipboard Data

	Vp	NRM	Inc.
Sect. 1, 50 cm:	5.62	2466	-76°
Sect. 2, 5 cm:	---	1026	-70°
Sect. 2, 65 cm:	4.96	---	---
Sect. 3, 30 cm:	5.18	2578	-78°
Sect. 3, 70 cm:	5.26	2055	-71°
Sect. 3, 145 cm:	---	---	Reversed

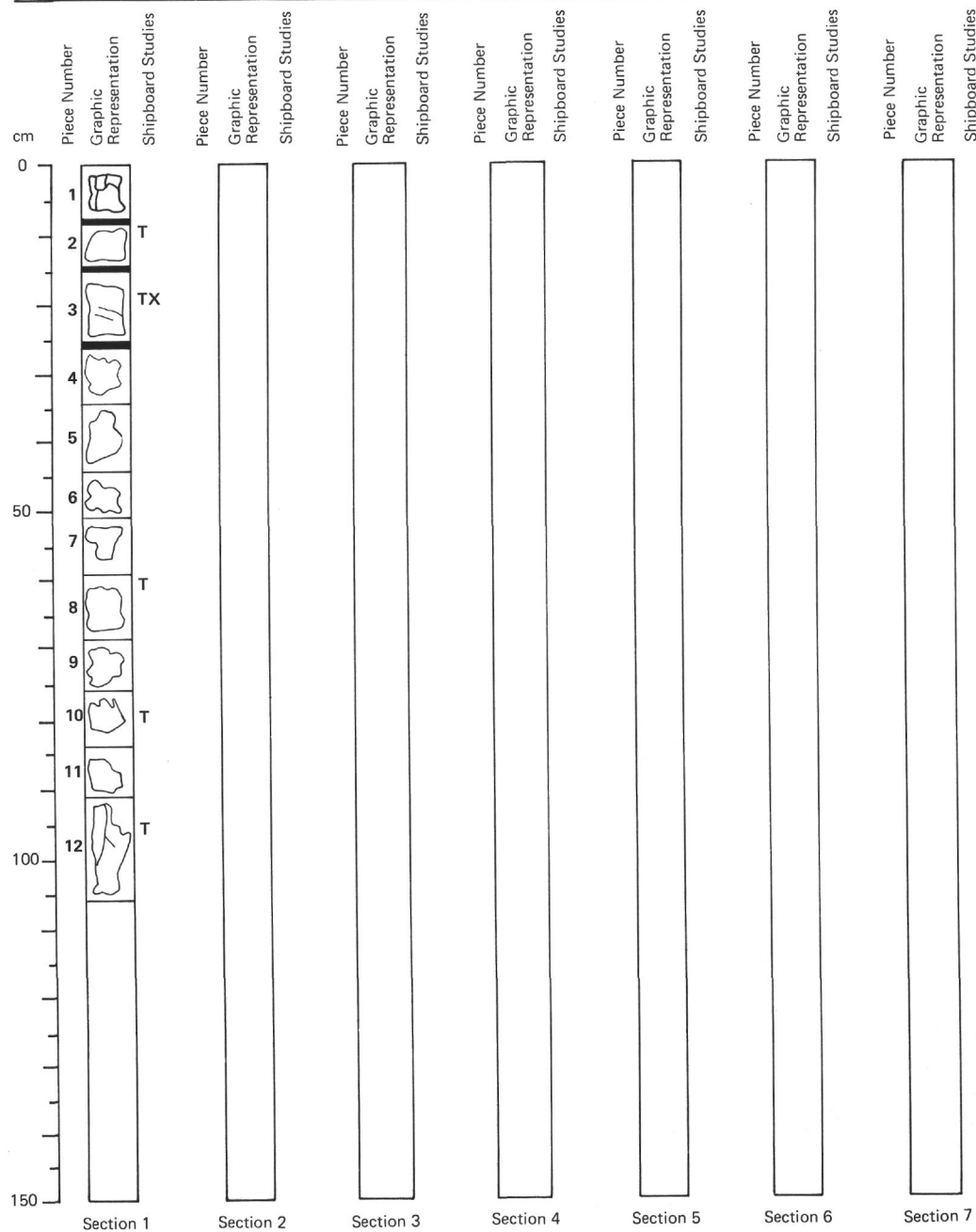


Original basalt recovery was 0.47 meters. Styrofoam spacers make the length shown here greater than the amount recovered.

Nonvesicular aphyric basalt with minor secondary alteration concentrated in the interval 50-85 cm. Breccia zone from 27-33 cm consists of angular basalt glass fragments embedded in carbonate matrix. Petrography: glomeroporphyritic-sub-ophitic. Two per cent plagioclase microphenocrysts (An_{52-56}), 25% groundmass plagioclase laths, 15% clinopyroxene groundmass, 3% clinopyroxene microphenocrysts with slight resorption. Opaque "dust" in groundmass. Rare olivine highly altered to smectite.

Shipboard Data

	Vp	NRM	Inc.
Sect. 1, 40 cm:	—	2805	-64°

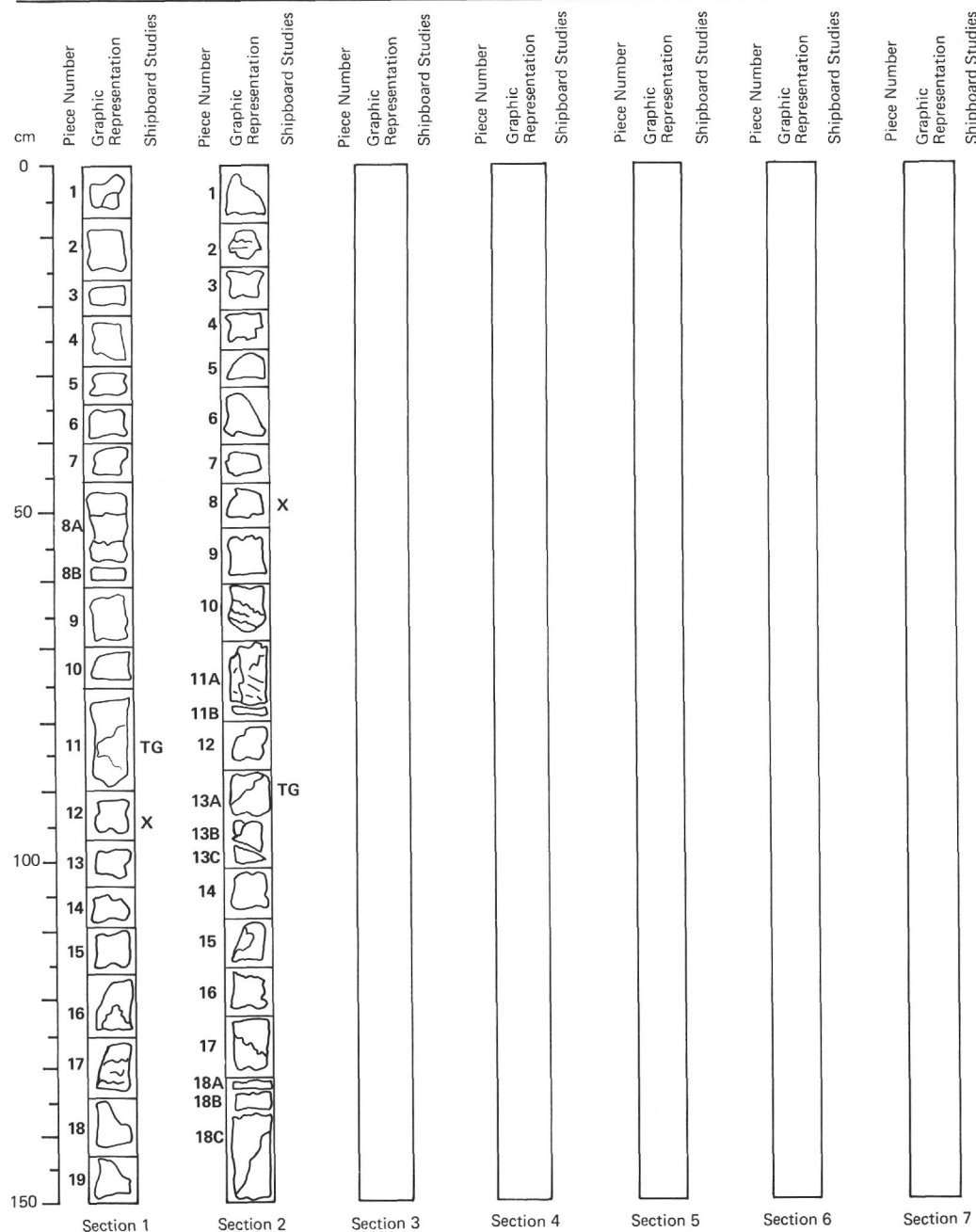


Original basalt recovery was 0.65 meters. Styrofoam spacers make the length shown here greater than the amount recovered.

Aphyric intergranular basalt (2.5YR 5/0) with 1% vesicles (0.5-1.0 mm). Fifty per cent vesicles filled with smectite or unknown clear white mineral. Fractures will with smectite, carbonate and/or Fe-oxides. Trace of sulfide at 50 cm. Breccia of angular black glass and carbonate at 0-8 cm. Petrography: sub-ophitic intergranular, hyalomicroporphyritic. Groundmass plagioclase 40%, microphenocrysts zoned An_{64-42} , 25% clinopyroxene groundmass, brown coloration; 5% groundmass olivine completely replaced by chlorite. Dendritic opaques, glass replaced by chlorite, glass fragments in breccia contain microphenocrysts of plagioclase 5%, clinopyroxene 3% and olivine 2%.

Shipboard Data

	Vp	NRM	Inc.
Sect. 1, 95 cm:	---	---	Reversed

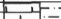



Original basalt recovery was 2.13 meters. Styrofoam spacers make the length shown here greater than the amount recovered.

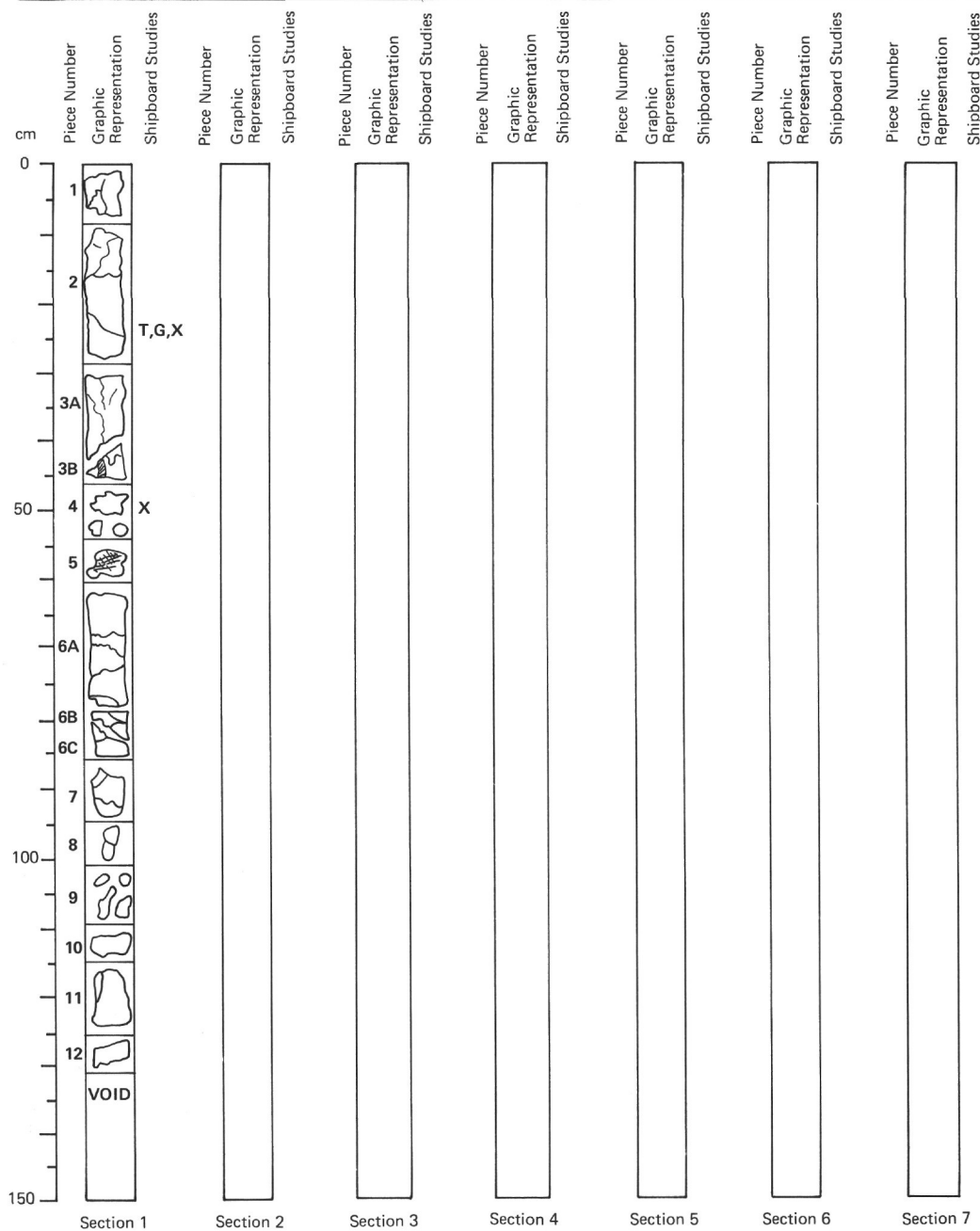
Aphyric basalt. Rare plagioclase microphenocrysts ~ 1 mm in an intersertal groundmass of plagioclase, clinopyroxene and glass. Estimated mode: plagioclase 40%, clinopyroxene 25%, olivine 5%, glass 25%, opaques 5%. Glass and olivine altered to smectite. Scattered vesicles < 1 mm mostly filled with smectite. Fractures filled with smectite and pyrite. Also some pyrite in vesicles and disseminated.

Shipboard Data

	Vp	NRM	Inc.
Sect. 1, 85 cm:	5.16	4773	-63°
Sect. 1, 115 cm:	4.13	2727	-67°
Sect. 2, 110 cm:	6.09	5281	-67°

SITE 407		HOLE		CORE 43		CORED INTERVAL: 405.0-424.0 m																																					
TIME-ROCK UNIT	BIOSTRAT ZONE	FOSSIL CHARACTER				SECTION	METERS	GRAPHIC LITHOLOGY	DRILLING LOG CORRELATION SEDIMENTARY STRUCTURES PALEONTOLOGIC SAMPLE	LITHOLOGIC DESCRIPTION																																	
		FORAMS	NANNOS	RADS																																							
Early Oligocene	NP20-NP21	Cg	Ag							dusky yellow green (5GY 5/2) streak at 5 cm is pale yellowish orange (10YR 8/6)																																	
						CC2																																					
P19-P20 NP22/NP23										<p><u>SANDY CALCAREOUS MUD</u> Dusky yellow green except for 2 cm-thick layer of pale yellowish orange calcareous zeolitic mud. CC1 is 4 remolded balls, CC2 is undeformed. High amount of clay (25-60%), few (5%-10%) heavy minerals and unspecified carbonate.</p> <p><u>Smear Slides</u></p> <table><thead><tr><th></th><th>CC2-4</th><th>CC2-6</th></tr></thead><tbody><tr><td>nannos</td><td>35</td><td>20</td></tr><tr><td>forams</td><td>Tr</td><td>Tr</td></tr><tr><td>zeolite</td><td>40</td><td>2</td></tr><tr><td>volc. glass</td><td>3</td><td>2</td></tr><tr><td>clay</td><td>25</td><td>60</td></tr><tr><td>qtz.</td><td>--</td><td>1</td></tr><tr><td>fspr.</td><td>--</td><td>Tr</td></tr><tr><td>H. mins.</td><td>--</td><td>5</td></tr><tr><td>palagonite</td><td>2</td><td>--</td></tr><tr><td>carb. unsp.</td><td>5</td><td>10</td></tr></tbody></table>		CC2-4	CC2-6	nannos	35	20	forams	Tr	Tr	zeolite	40	2	volc. glass	3	2	clay	25	60	qtz.	--	1	fspr.	--	Tr	H. mins.	--	5	palagonite	2	--	carb. unsp.	5	10
	CC2-4	CC2-6																																									
nannos	35	20																																									
forams	Tr	Tr																																									
zeolite	40	2																																									
volc. glass	3	2																																									
clay	25	60																																									
qtz.	--	1																																									
fspr.	--	Tr																																									
H. mins.	--	5																																									
palagonite	2	--																																									
carb. unsp.	5	10																																									

Explanatory notes in Chapter 1

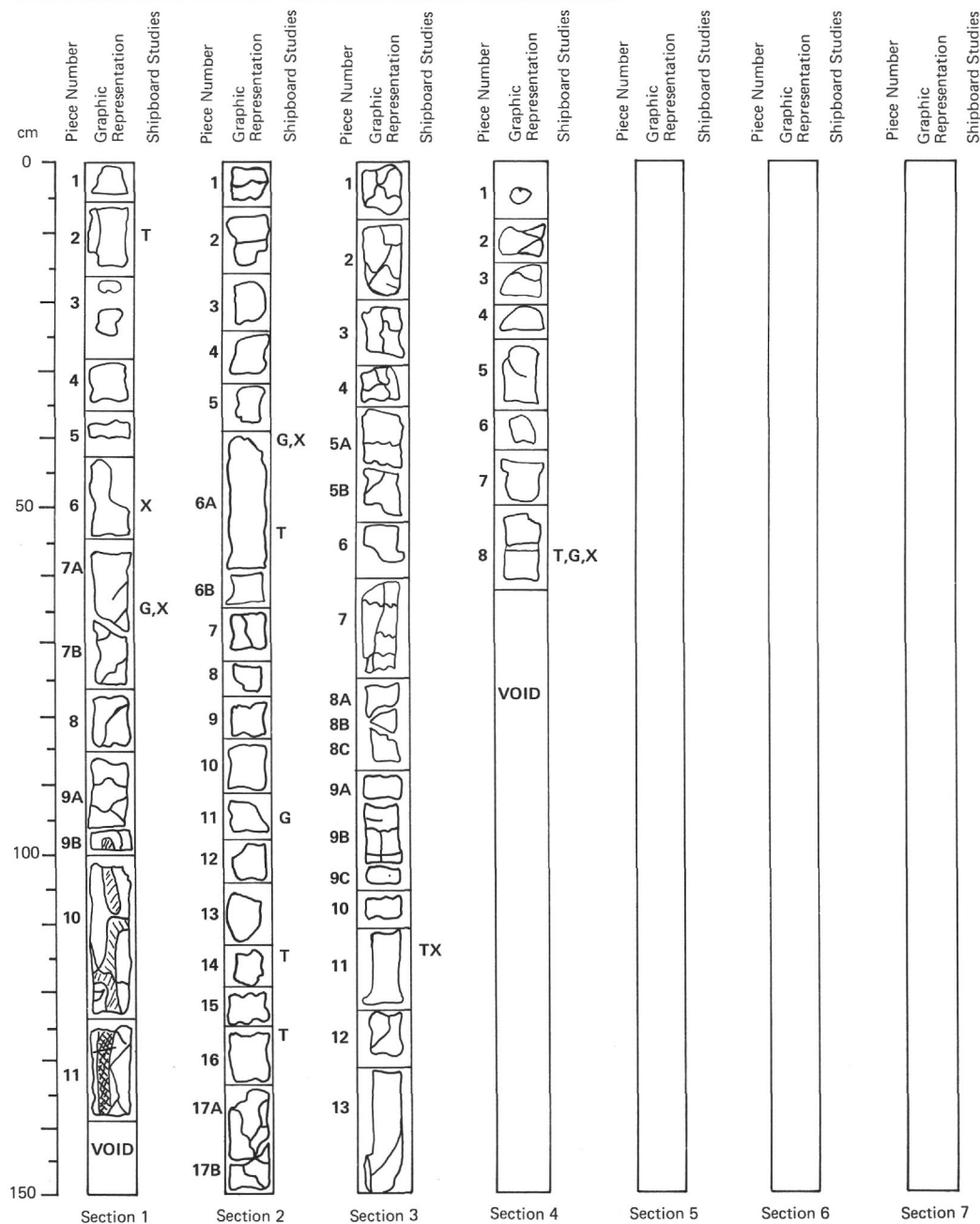


Original basalt recovery was 0.85 meters. Styrofoam spacers make the length shown here greater than the amount recovered.

Interval 0-130 cm, Sect. 1: aphyric basalt with rare phenocrysts of plagioclase and olivine. There are vesicles and veins (irregular). They are partly filled by smectite and sulfides (pyrite). There is smectite-carbonate mixture from 47 cm till 60 cm. Then there are zones of aphanitic basalt (43-46 cm) and of black glass (95-100 cm). It is probably pillow margin (2.5Y 5/0). Petrography: texture – sub-ophytic. Phenocrysts: plagioclase 5% (0.4-1.0 mm), olivine (altered to smectite and chlorite) 5% (0.4-1.0 mm). Groundmass: plagioclase 27%, clinopyroxene 20%, olivine (altered to smectite and chlorite) 15%, magnetite 4%, ilmenite 1% and glass 35%.

Shipboard Data

	Vp	NRM	Inc.
Sect. 1, 10 cm:	4.65	8158	-35°
Sect. 1, 70 cm:	—	—	Reversed

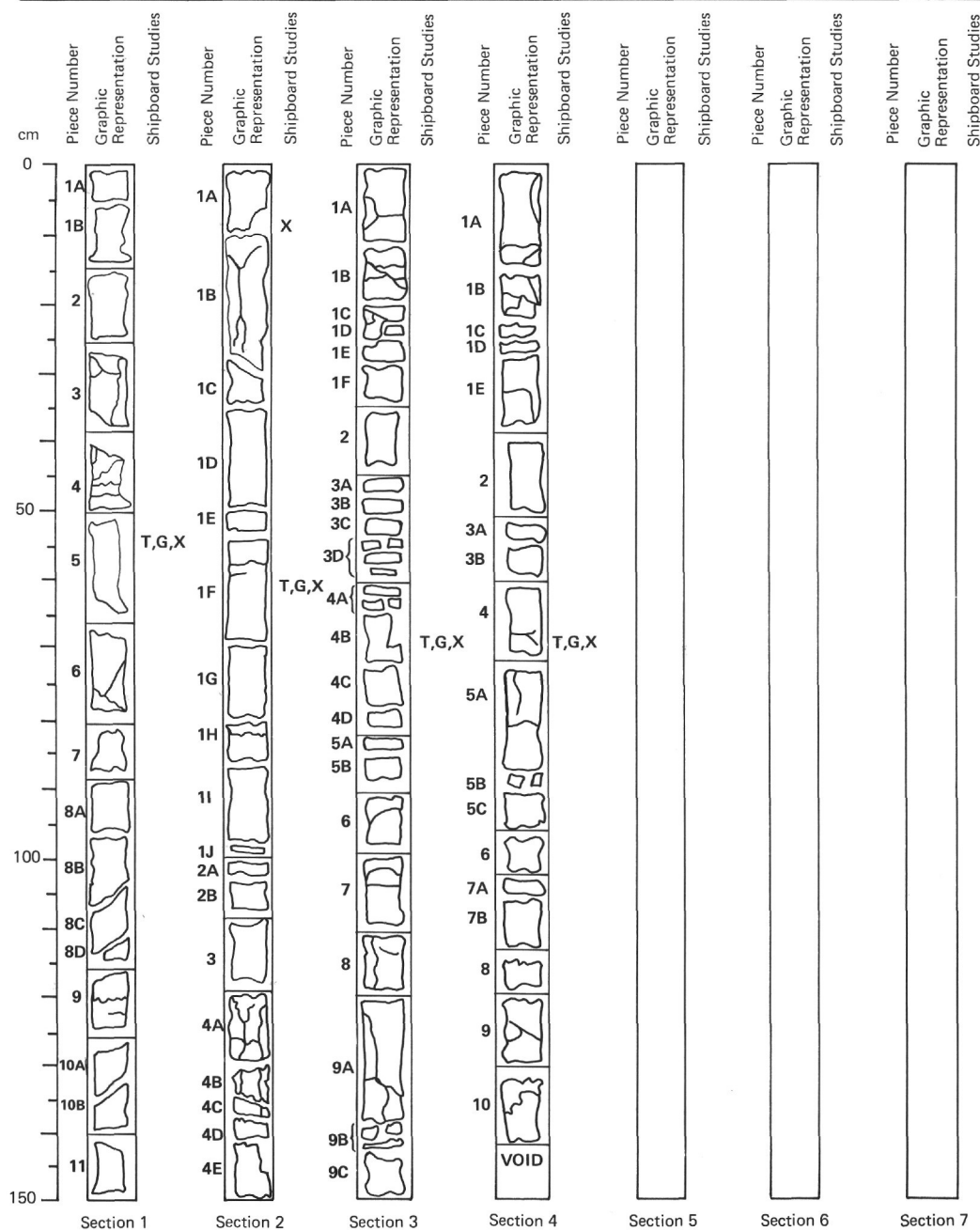


Original basalt recovery was 3.0 meters. Styrofoam spacers make the length shown here greater than the amount recovered.

Aphyric to sparsely phryic olivine basalt. Sparse vesicles (< 1%) about 1 mm in size partly filled with pyrite and other unidentified minerals. Some pipe vesicles near glass selvages. Average estimated mode: plagioclase 30%, clinopyroxene 15%, olivine 10%, glass 45%. Groundmass glass and mafics largely altered to smectite, chlorite and carbonate. Fragments with glass selvages common in Sections 2, 3, and 4, suggesting a succession of pillow lavas. Thin veins (< 4 mm) of smectite, carbonate, and other unidentified minerals common throughout core. Heavily oxidized zones present locally. Typically, glass selvage appears fresh but grades into highly oxidized and altered vesicular rock.

Shipboard Data

	Vp	NRM	Inc.
Sect. 1, 40 cm:	3.43	10548	-68°
Sect. 2, 30 cm:	4.22	1941	-36°
Sect. 3, 100 cm:	3.82	11439	-67°
Sect. 4, 20 cm:	2.95	14348	-50°
Sect. 4, 55 cm:	---	---	Reversed

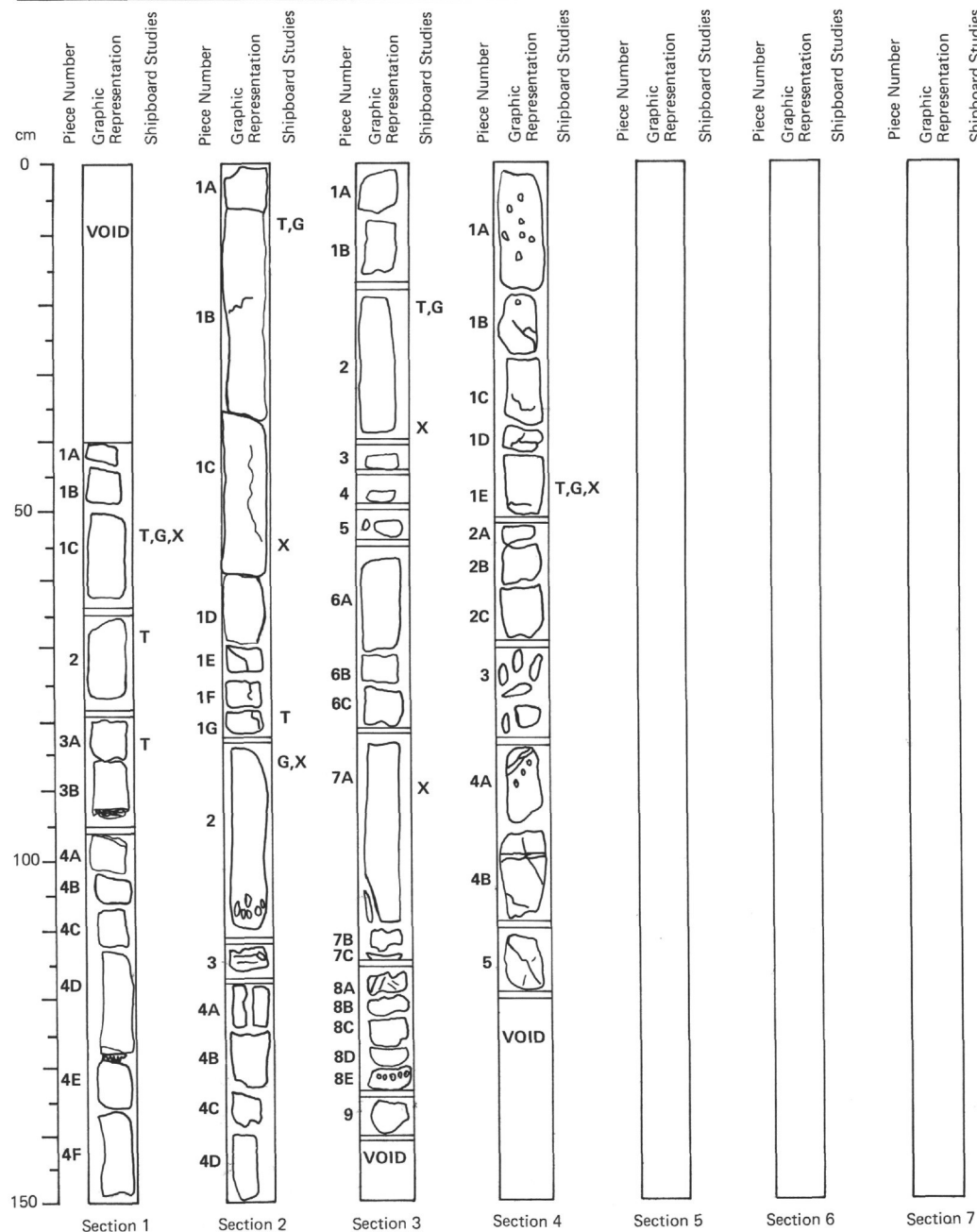


Original basalt recovery was 6.0 meters. Styrofoam spacers make the length shown here greater than the amount recovered.

Aphyric basalt with rare microphenocrysts of plagioclase, showing variable hydrothermal alteration and oxidation. Calcite filled amygdules and calcite veins common. Traces of pyrite in some veins. At 2.5 meters a glassy zone (flow surface) is veined by calcite. Grain size increases in basalt away from glass. Another glass occurs at 2.6 meters and many more in the lower 1.7 meters of the core. The rock is highly oxidized and amygdaloidal in the glassy zone. This is probably a succession of pillow lava.

Shipboard Data

	Vp	NRM	Inc.
Sect. 1, 10 cm:	—	—	Reversed
Sect. 1, 50 cm:	4.38	1787	-57°
Sect. 2, 50 cm:	4.19	6403	-68°
Sect. 3, 40 cm:	3.78	4754	-65°
Sect. 4, 50 cm:	4.82	2521	-54°



Original basalt recovery was 4.5 meters. Styrofoam spacers make the length shown here greater than the amount recovered.

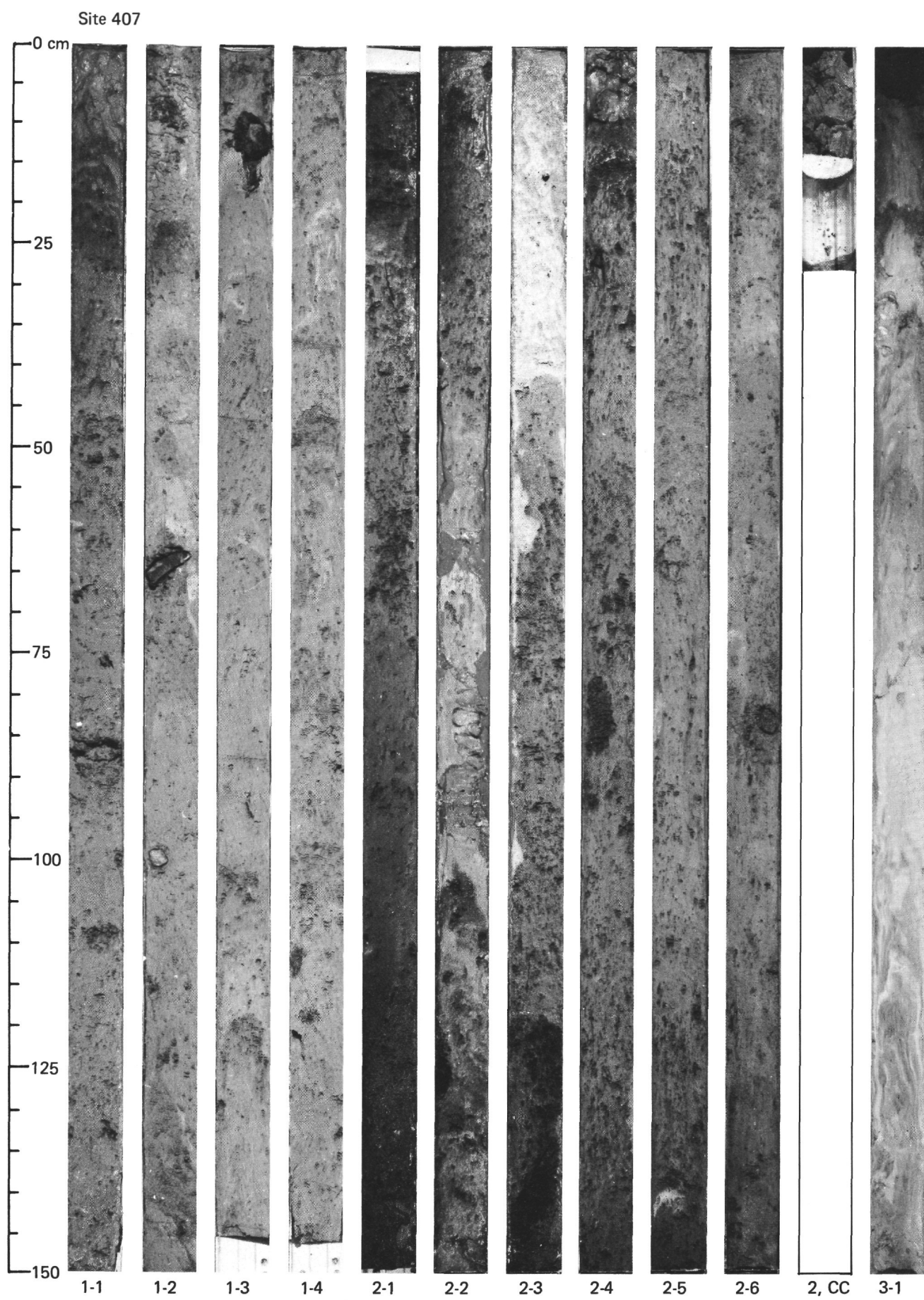
Section 1 - intergranular basalt (2.5YR 5/0) with up to 2% plagioclase microphenocrysts. Trace of sulphates, local vesicle concentration in 2-3 cm wide zones. Alteration varies from weak to moderate. Moderate oxidized zones contain up to 5% smectite amygdules and abundant carbonate veins. Altered olivine microphenocrysts (125-140 cm).

Section 2 (0-80 cm) - aphyric intergranular basalt with rare carbonate filled amygdules (3 mm). Weakly oxidized.

Section 2 (80-150 cm) and Sections 3-4 - pillow basalts, lithology varies (palagonitized black glass, vitrophyric, aphanitic, very fine-grained aphyric-aphyric intergranular) scattered local plagioclase and altered olivine microphenocrysts. Oxidation variable but generally strong. Calcite pipe vesicles to 5 mm adjacent to glass selvages. Smectite and carbonate veins and amygdules. Petrography: sub-ophitic, intersertal. Most sections have scattered fresh plagioclase and clinopyroxene (brown coloration) microphenocrysts. Olivine microphenocrysts (altered to chlorite, smectite and carbonate) are much less common. Glass replaced by chlorite and carbonate. Estimated mineral per cent: plagioclase 25-40, clinopyroxene 12-20, olivine 7-20, altered glass 25-40, opaques 1-6.

Shipboard Data

	Vp	NRM	Inc.
Sect. 1, 45 cm:	3.80	6453	-68°
Sect. 2, 10 cm:	4.71	1853	-59°
Sect. 2, 50 cm:	4.43	1336	-54°
Sect. 3, 10 cm:	4.11	2983	-59°
Sect. 4, 10 cm:	4.95	2301	-63°



Site 407

